DIFFUSION AND SOLUTION OF GASES IN PLASTICISED POLYMERS

by

Roger Mallinder

A thesis submitted for the degree of Doctor of Philosophy of the University of London

Chemistry Department,
Imperial College of Science and Technology,
LONDON, S.W.7.

January, 1966.

ABSTRACT

The diffusion and solution of hydrogen and neon have been measured in a series of polyvinyl chloride sheets containing various concentrations of plasticiser. Diffusion coefficients D_L and D_E were determined using the time-lag and 'early approximation' methods respectively, and permeability coefficients $\bar{P}$ from the steady-state permeation rate. Dynamic (σ_D,σ_E) and static (σ_S) solubility coefficients were respectively determined from permeation and equilibrium measurements.

Below the glass transition temperature of the unplasticised polymer, the behaviour of $\bar{P}$, D_L, D_E and σ_D was governed by history- and time-dependent effects. The permeation data were reproducible in the 'settled' state of the polymer, after 'annealing' above the glass transition temperature. The permeation data of the plasticised compositions were reproducible with no history-dependent effects. Logarithmic plots of $\bar{P}$, D_L and σ_D against reciprocal temperature for all gas-polymer systems showed inflections at temperatures T_l corresponding to the glass transition regions. The free volume theory has been used to correlate values of T_l. Polyvinyl chloride shows an improved selectivity towards permeation of gases in

comparison with other polymer systems but the absolute permeabilities are lower. The temperature coefficients of diffusion have been interpreted in terms of the transition state and zone theories.

Values of σ_s were significantly below those of σ_D and the temperature dependence of σ_D was anomalous. Non-uniform distribution of plasticiser is not the factor contributing to the discrepancy between σ_D and σ_s. The free energy, heat and entropy of solution were deduced from the σ_s data. Solution of gases in unplasticised polyvinyl chloride below its glass transition temperature is an exothermal process, in which gas molecules are accommodated in pre-existing 'holes'. Residence in these 'holes' constitutes an interstitial mechanism of solution. Gaseous solution in the plasticised polymer is endothermal, indicating that gas molecules dissolve by the normal substitutional mechanism.

ACKNOWLEDGEMENTS

I am deeply indebted to Professor R.M. Barrer, F.R.S., who patiently guided and encouraged me throughout the course of this work.

I acknowledge with gratitude the financial support of the Fibres Division of I.C.I. Ltd. (formerly British Nylon Spinners Ltd.) in the award of a bursary. Thanks are also due to the Plastics Division of I.C.I. Ltd. for the polymer samples.

I wish to thank the technical staff of the Chemistry Department, Imperial College, for their help in assembling some of the equipment. I wish also to thank my research colleagues for their interest and suggestions.

Finally, thanks are due to my wife and parents for their unfailing support.

CONTENTS

		Page
Abstract		2
Acknowledgements		4
Contents		5
PART 1.	INTRODUCTION AND LITERATURE SURVEY	
1.1	Introduction	10
1.2	Effect of Temperature	14
1.3	Effect of Size and Shape of Diffusing Molecule	17
1.4	Effect of Filler Particles	18
1.5	Effect of Cross Linking	19
1.6	Effect of Glass-Rubber Transition	20
1.7	Effect of Crystallinity	23
1.8	Experimental Measurement of Permeation	26
1.9	Polyvinyl chloride, Unplasticised and Plasticised	28
1.9.1	General	28
1.9.2	Determination of microstructure	30
1.9.3	Transitions in polyvinyl chloride.	34
1.9.4	Volatility and diffusion of plasticisers	38

Page

PART 2. THEORETICAL

2.1 Diffusion in a plane sheet..... 41

2.1.1 Laws of diffusion..... 41

2.1.2 Solutions of Diffusion Equations (for constant D only)..... 42

(a) Steady-state diffusion..... 43

(b) Transient state diffusion and the 'early approximation' method... 46

2.2 Significance of Diffusion Coefficients in a Binary Mixture..... 49

2.2.1 Intrinsic diffusion coefficients.. 49

2.2.2 Mutual diffusion coefficients..... 50

2.2.3 Self-diffusion coefficients..... 52

2.2.4 Diffusion coefficient relationships..... 52

2.2.5 Measurement of diffusion coefficients..... 55

2.3 Classification of Polymer-Penetrant Systems in Diffusion and Solution..... 57

2.4 Application of the Transition State Theory to Diffusion..... 60

2.5 Diffusion Coefficient according to the Kinetic Statistical Theory (Barrer's Theory of Zone of Activation)..... 63

2.6 Thermodynamics of Polymer Solutions... 67

2.6.1 Entropy of mixing (ΔS_m) and dilution (ΔS_1) according to the liquid lattice theory..... 69

Page

2.6.2 Free Energy and heat of mixing.... 71

2.6.3 Free energy and heat of dilution.. 74

2.6.4 Swelling of polymer networks..... 75

2.6.5 Limitations of the lattice treatment..... 77

2.7 Glass Transition Relationships for Polymer-Diluent Systems..... 79

PART 3. EXPERIMENTAL MATERIALS, APPARATUS AND EXPERIMENTAL TECHNIQUES

3.1 Polyvinyl Chloride Sheets..... 83

3.2 Gas Samples..... 85

3.3 General Description of Apparatus..... 85

3.3.1 The pumping system..... 85

3.3.2 The permeation system..... 87

(a) The membrane holder..... 87

(b) The diffusion cell..... 90

3.3.3 The solubility system..... 91

3.3.4 The McLeod gauge..... 93

3.3.5 Thermostat..... 94

3.4 Calibration of Apparatus..... 95

3.4.1 The permeation system: determination of V_o..... 95

3.4.2 The solubility system: determination of V_d..... 95

Page

3.5 Experimental Techniques..... 96

3.5.1 Permeation experiment..... 96

3.5.2 Equilibrium solubility measurement 98

3.6 Accuracy of Measurements..... 100

PART 4. RESULTS AND DISCUSSIONS

4.1 Permeability, Diffusion and Solubility Coefficients..... 103

4.1.1 Hydrogen data from permeation experiments..... 105

4.1.2 Neon data from permeation experiments..... 108

4.1.3 Hydrogen data from static solubility experiments..... 111

4.1.4 Neon data from static solubility experiments..... 113

4.2 Kinetic Phenomena..... 115

4.2.1 Permeability and diffusion coefficients..... 115

(a) Unplasticised polyvinyl chloride.. 119

(b) Plasticised polyvinyl chloride.... 129

4.2.2 Influence of plasticiser on the permeability and diffusion coefficients..... 134

4.2.3 Separation of gases..... 138

4.2.4 Intersection temperatures..... 140

4.2.5 Temperature coefficients of permeation and diffusion..... 145

Page

4.2.6 Interpretation of D_o..... 151

4.2.7 Functional relationships..... 159

4.3 Equilibrium Phenomena..... 164

4.3.1 The solubility coefficients..... 164

(a) Unplasticised polyvinyl chloride... 167

(b) Plasticised polyvinyl chloride..... 173

4.3.2 Influence of plasticiser on the steady state coefficients..... 179

4.3.3 Temperature dependence of the solubility coefficients..... 182

(a) Heat of solution..... 182

(b) Free energy and entropy of solution..... 185

4.3.4 Comparison between the theoretical and observed heats of dilution..... 189

4.3.5 Statistical treatment of the solubility of gases..... 192

REFERENCES..... 198

PART I

INTRODUCTION AND LITERATURE SURVEY

1.1 Introduction

Many studies[1-20] have been made of transport and solution equilibrium phenomena in high polymeric membranes, as it is possible to correlate the diffusion parameters with the known molecular structure parameters. From determinations of permeation, diffusion and solution of gases or vapours in high polymers, valuable knowledge may be gained on the microstructure of the polymer and the mechanism of the diffusion process. From these investigations it is also possible to characterise these membranes as barriers to gases or vapours.

Although Graham[21] did some early work on the flow of gas through natural rubber, the main systematic advances in the subject commenced with the work of Barrer[1] and of van Amerongen.[3] The concept of permeation of gas or vapour through a polymeric membrane is generally considered as taking place in the following sequence: (i) sorption of gas at one interface; (ii) solution of gas into, and diffusion in and through the membrane; and (iii) evaporation at the opposite interface. Normally

diffusion is the slowest process and thus constitutes the rate determining step.

Fick's law states that the rate of permeation per unit area is the product of the diffusion coefficient and the concentration gradient within the membrane. Thus the diffusion coefficient and the solubility of the penetrant will be affected by certain factors, which control the rate of permeation. The factors may include at least the temperature, the size and shape of the penetrant molecule, the crystallinity and glass transition of the polymer, the cross-linking of the polymer, the concentration of the penetrant molecule and sometimes the previous history of the polymer.

This project is an attempt to present systematic data of permeation, diffusion and solution of permanent and inert gases in polyvinyl chloride polymer, containing varying quantities of essentially involatile plasticiser. The gases are chosen to act as molecular probes in an attempt to elucidate further the mechanism of plasticiser action in polyvinyl chloride. The possibility of varying the selectivity towards permeation of gases in polyvinyl chloride, by using certain quantities of plasticiser, will also be considered.

Little systematic information of the diffusion and solution of gases and vapours in polyvinyl chloride (unplasticised or plasticised) has been published. In 1942 Muller[22] determined the permeability of unplasticised poly-vinyl chloride to the inert gases and water vapour at 20°C. Values of the permeability, diffusion and solubility coefficients of hydrogen in poly-vinyl chloride were also quoted by Reitlinger[25] at the same temperature. Most investigators[23,24,27-32] find that the rate of gas permeation is generally increased by addition of plasticisers to polymeric membranes although experimental evidence is limited in some cases.[28-32] Van Amerongen[4] and Morris[26] found, however, that small quantities of plasticisers and softening oils added to natural rubber had relatively little effect on the rate of gas permeation. Brubaker and Kammermeyer[23] measured the permeabilities of hydrogen and carbon dioxide in poly-vinyl chloride containing known amounts of dioctyl phthalate plasticiser. Permeability of carbon dioxide at a given temperature was found to increase uniformly with plasticiser content, although hydrogen showed a radically different behaviour as discontinuities appeared.

Diffusion and solution of water vapour[35-39] and n-butyl alcohol[40] in poly-vinyl chloride have been

investigated. The addition of tri-cresyl phosphate plasticiser to poly-vinyl chloride produced a lowering of the heat of solution of water vapour, as compared to the unplasticised polymer.[36] Kumins and Roteman[33] observed that the diffusion coefficients of water vapour in plasticised poly-vinyl chloride - poly-vinyl acetate co-polymer were greater than those through the unplasticised counterpart. The activation energies for diffusion above the second order transition temperatures appeared to be the same for both plasticised and unplasticised polymer. The effect of high molecular weight liquid plasticisers on the diffusion properties is, however, complicated by the plasticising action of the water vapour,[34] which may also facilitate rotation of adjacent chain segments. Kanamaru and Sigiura[40,41] have studied the temperature dependence of the diffusion coefficient D of some simple organic penetrants within several polymers by the rate of sorption method. Measurements were made in the temperature range around the glass transition temperatures Tg of the polymers. The system, n-butyl alcohol in poly-vinyl chloride, produced a log D vs. 1/T plot consisting of one intersection point and two linear branches. This was designated[40] as being typical of a system in

which neither the high polymer nor the solvent form hydrogen bonds. The poly-vinyl chloride was also considered as being lyophobic and only slight swelling occurred on sorption of the penetrant.

1.2 Effect of Temperature

The temperature coefficient of the permeation rate is found to be independent of the pressure difference and the thickness of the membrane. Barrer[1,42] has shown from correlation of extensive experimental data, that the diffusion-controlled permeability coefficient $\overline{P}$ over a moderate temperature range is given by

$$\overline{P} = P_o \exp(-\frac{E_p}{RT}) \qquad (1.1)$$

where P_o is a constant independent of temperature and E_p the apparent activation energy for permeation. $\overline{P}$ may also be resolved into the product of the diffusion coefficient D and the solubility coefficient σ_D, i.e.

$$\overline{P} = D\sigma_D \qquad (1.2)$$

A good proportion of polymer-penetrant systems produce satisfactory agreement between the values of σ_D or D calculated from (1.2) and values obtained experimentally.

D and σ were also shown by Barrer[1,2] to vary exponentially with temperature so that

$$D = D_o \exp(-\frac{E_D}{RT}) \qquad (1.3)$$

$$\sigma = \sigma_o \exp(-\frac{\Delta \bar{H}^o}{RT}) \qquad (1.4)$$

where D_o and σ_o are constants, E_D is the activation energy for diffusion and $\Delta \bar{H}^o$ is the heat of solution of gas in the membrane. By comparing equations (1.1) to (1.4) it is obvious that the three energy terms are related by

$$E_p = E_D + \Delta \bar{H}^o \qquad (1.5)$$

The temperature coefficient of $\bar{P}$ represented by (1.1) is, therefore, the direct outcome of the activated diffusion process according to (1.3), and the equilibrium property, solubility, following a similar law shown by (1.4).

The activation energy for diffusion E_D may be pictured as the energy required for completion of a unit diffusion process, and presumably it involves the work of separation of the polymer chains, whilst D_o, according to Barrer's zone theory,[45] is a measure of the zone size. Both E_D and D_o may therefore throw light upon the nature of the diffusion process.[1,3,5-8,43,45,49,50]

A plot of log D_o vs $\frac{E_D}{T}$ yields a functional relationship[1,3,5,6,43,49,56] of the type

$$\log D_o = A + B \frac{E_D}{T} \qquad (1.3a)$$

The relationship follows from the Arrhenius equation (1.3) in the form $\log D = \log D_o - 0.22 \frac{E_D}{T}$. If the range in values of log D is small compared with that of $0.22 \frac{E_D}{T}$ then to a first approximation log D is constant (= A). Thus:

$$\log D_o = A + 0.22 \frac{E_D}{T} \qquad (1.3b)$$

which has the form of (1.3a). In fact it is always found that the range in log D is less than that in $0.22 \frac{E_D}{T}$, either due to experimental limitations of the measurements, or because of a fundamental property of rate processes in condensed phases.

Although a linear relationship of log D vs $\frac{1}{T}$ is postulated by (1.3), a slight curvature is often perceptible over a wide range of temperature.[5,6,12,43,44] Thus both D_o and E_D can prove to be temperature dependent, the value of each decreasing for rising temperature. An interpretation of this situation can be made from the zone theory,[45] and also from Eyring's treatment of rate processes.[46]

1.3 Effect of size and shape of diffusing molecule

With increasing molecular size of the penetrant the majority of investigators[3-9,11,12,14,42,43] find that the diffusion coefficient decreases and the activation energy for diffusion increases. The size of the diffusing molecule tends to have a much smaller influence on the diffusion coefficient in elastomers,[6,19,42,48] than in the more rigid membranes such as poly-vinyl acetate[7-9] or silica glass.[49,50]

The shape of the penetrant molecule has also been found to have a marked effect on the diffusion properties.[44,47] Aitken and Barrer[44] and Prager et al.[47] postulated that diffusion occurs preferentially along the direction of greatest length of the diffusing molecule. This was concluded from the knowledge that addition of a CH_3 side chain to a diffusant reduces D by a larger amount than an increase of chain length by one carbon atom. Prager and Long[47] considered that for branched chain molecules the diffusion of the group with side chain is the main rate-controlling step. Molecules with the same degree of branching (except straight chain molecules) should, therefore, have similar diffusion coefficients provided that they do not differ too greatly in length.

This was generally found to be the case on comparing the D values for isobutane and iso-pentane.[44,47]

1.4 Effect of Filler Particles

The incorporation of filler particles into a polymer matrix creates a complex heterogeneous medium, which has the expected result of giving a permeability decrease for increasing concentration of filler.[19,20,51-53] Plate-like fillers such as mica or graphite have been found to produce large reductions in $\bar{P}$, especially if the orientation of their larger surface area is perpendicular to the gas stream.[52,53] Melikhova et al.[53] concluded that the permeability in such cases depends on the dimensions and orientation of the filler particles, the nature of bonding of rubber to filler and the extent to which the polymer wets the filler particles. Sorption of gas by the filler is also considered to take place by van Amerongen [52] from experiments with filled natural rubber.

An exact solution of the diffusion equation for heterogeneous membranes is difficult to achieve and so the corresponding equation for flow through a homogeneous medium is usually modified by introduction of a suitable structural parameter. Barrer et al.[19,20] discussed the experimental data for diffusion in filled rubbers in terms

of two reference models, the first in which the polymer and filler are considered as independent sorbents; and second the polymer completely wets the filler which acts as a non sorbent. Both models were found not fully to satisfy the results, although some aspects of filler behaviour were explained. The existence of complex surface and gas phase flows within filler particles was indicated by trends in the results. It has also been pointed out [48] that the role of filler particles in the diffusion and solution of gases may alter, if the polymer is allowed to crystallise from the amorphous state.

1.5 Effect of Cross-Linking

Experiments have been conducted in order to study the effect of systematic alterations in the amount of cross-linking of rubber on the diffusion and solution of homologous hydrocarbons.[43,44] Using rubber cross-linked by sulphur Barrer and Skirrow[43] found that $\bar{P}$ and, particularly, D of the paraffins were sensitive to the degree of cross-linking. For the smaller, less soluble paraffins the degree of vulcanisation had little influence upon the solubility, but for the higher members this influence became significant. In a similar way, Aitken and Barrer[44] observed that D became smaller as cross-linking increased, showing an approximately linear

dependence on the reciprocal of the molecular weight between cross-links.

1.6 Effect of the Glass-Rubber Transition

Direct information about segmental motions in the region of the glass temperature T_g may be obtained by studying the diffusion of gases in polymers. The free volume and segmental motions in polymers are not usually affected by the volume fraction of gas sorbed at any reasonable pressure. Water vapour at not too high relative humidities diffuses in the manner characteristic of a gas.

There have been relatively few investigations of gaseous diffusion in polymers in their transition region. Zhurkov and Ryskin[11] examined water and methyl alcohol vapours in polystyrene and polymethyl methacrylate. Their data were comparable with those obtained from permeation and sorption experiments in poly-vinyl acetate, in which seven gases[7-9] and water [11,55] have been examined over a temperature range extending about 20 deg.C on either side of T_g. D was found to be independent of concentrati and decreased greatly with increasing diameter of diffusate molecules.

Although many authors[33,54,64,65] represent log D against 1/T by two straight lines which intersect at T_g,

Meares[7,8] found that for poly-vinyl acetate there was an unmistakable slow variation of log D with 1/T over a ten degree range directly below T_g. This behaviour was explained[8] by regarding the polymer just below T_g as a system of two phases glass-like and liquid-like with different diffusion coefficients.

Generally it is found that activation energies for diffusion, calculated from log D against 1/T graphs, are smaller below T_g than above.[7,8,11,33,54] Brandt's approach[58] to this behaviour indicates that the change of activation energy found experimentally at T_g can be understood as a consequence of the change of thermal expansion coefficient at this point. Certain details of molecular structure such as the shape of the potential barrier of hindered rotation. and the number of the degrees of freedom per monomer unit are found to have only a small effect on the resultant diffusion properties. The application of Brandt's theory to Meares's data for poly-vinyl acetate yielded poor agreement, however, between experimental and predicted values of the activation energies.[59]

Meares[7,8] was able to obtain a linear relationship between the activation energies above and below T_g against the squares of the gas collision diameters. Kumins

et al.[54] were not able, however, to show a similar relationship for several gases and vapours diffusing in poly-vinyl chloride - poly-vinyl acetate copolymer. A zone theory[45,56,57] interpretation of the poly-vinyl acetate data[7,8] shows that above T_g, the diffusion of argon and larger molecules requires a much greater disturbance of the surrounding polymer chain segments than does that of hydrogen. Below T_g a large zone of activation is not involved as it appears that the diffusing molecule manages to force apart only short chain segments.

From static solubility measurements on poly-vinyl acetate, it was concluded that just below T_g there are regions of minimum density in the polymer, which constitute high affinity sorption sites or 'holes' into which gas molecules penetrate preferentially.[9,59] A comparison of the solubility data from diffusion and static methods showed agreement above T_g, but below T_g the values from the equilibrium experiments were greater than those from the diffusion method.[7,8,9] It was inferred that molecules sorbed into the less dense regions tend to become immobilised and contribute only a little to the diffusion flux below T_g. These regions of low density were not, however, large enough for gas molecules in them to be thermodynamically similar to molecules free in the gas phase.[9]

Although convective flow was not considered to occur just below T_g, there is evidence that this may have occurred in gas sorption experiments with polystyrene [60] at a temperature well below its glass temperature. The results were interpreted as if the sorption occurred by a two-stage mechanism. The first stage was considered as sorption into a low density capillary system, in which the diffusion coefficients were only slightly dependent on the nature of the gas. The second stage was explained as absorption by the dense regions of the polymer from the capillary system. A theoretical treatment developed by Frisch [61] considers permeation of a gas across a polymer membrane, in which part of the flux is carried by diffusion, and part by simultaneous convection through a capillary system.

1.7 Effect of Crystallinity

A partially crystalline polymer may be regarded as a large number of tiny crystalline regions, often spherulites, dispersed in an amorphous matrix. It has also become clear that films of crystallising polymers are usually less permeable than amorphous ones.[15-18,23,24,29,30] The crystallites are often considered to dissolve no gas and to be quite impermeable so that all transport takes

place in the amorphous phase.[15-18] It also appears that the relationships for the solubility, diffusion and permeability coefficients are valid in partially or wholly amorphous systems, and might be corrected for the fraction of the system existing as crystallites.

Both polyethylene[15,16] and polyethylene terephthalate[62] have been treated as a simple two-phase mixture of crystalline and amorphous material each with a characteristic specific volume. The solubility coefficients for a particular diffusant in samples with various degrees of crystallinity were observed to be proportional to the volume fraction of the amorphous phase.

As indicated in section 1.4, the exact calculation of the permeability of a heterogeneous substance, consisting of discrete bodies dispersed in a continuous medium, is a complex problem. Klute[63] suggested that experimental impedances, determined from electrical conductivity measurements in beds of small non-conducting spheres, might serve as a better approximation of resistance to flow encountered in these polymers. Jeschke and Stuart,[64,65] studying gaseous and water vapour diffusion in polyethylene terephthalate and polypropylene, observed that crystallinity reduced $\bar{P}$, D and σ in every case, but the fractional

lowering was different for each gas. It was found that the model proposed by Klute predicts impedances which are lower than those found experimentally. From analogous problems of gaseous diffusion in clays, Meares[59] has suggested modification of the Klute approach. This has been applied to the Terylene results[62,64,65] with somewhat greater success, by accounting for the increased tortuosity of the diffusion paths.

A further investigation of the sorption and diffusion of seven gases in crystalline Terylene, has been made by Michaels et al.[18] in the region of the glass transition. It was concluded that the centres which impeded the flux were the tiny individual crystallites, and not the spherulites which must allow gas to permeate through their amorphous regions. Although there was a change in the activation energy for diffusion above and below T_g, there was no conclusive evidence for a variation of activation energy with the degree of crystallinity.

Barrie and Platt[66] measured sorption and diffusion of C_3 and C_4 hydrocarbons in rubber samples stretched to different extents so as to induce different degrees of crystallinity. The permeability and solubility both decreased with increasing crystallinity, and a two phase

model was used to interpret the results. Measurements of gaseous diffusion in stretched polymer films have also shown that induced orientation of crystallites can affect the diffusion properties, even if the degree of crystallinity is unaffected by the drawing process.[13]

1.8 Experimental Measurement of Permeation

Convenient and accurate methods for measuring the permeability coefficients of membranes and polymer films to gases and vapours, especially water vapour, are important in the packaging and building industries. They have also a potential use in the separation of gases by selective permeation. A survey of the literature reveals that the three most important methods of measuring permeation can be classified as the variable concentration, the variable volume and the variable pressure methods.

The variable concentration method: Two different gases are brought into contact with opposite sides of a membrane, and measurements conducted under zero pressure differential. The gas composition is monitored as a function of time on either side of the membrane.[67] A possible method of measuring gas concentration might be to employ radioactive labelled molecules as tracers.

The variable volume method: A conveniently high pressure is applied to one side of the membrane, and the permeating gas is allowed to expand against some low constant pressure on the outgoing side. The change of volume with time is then measured on the outgoing side by following, for instance, the displacement of a short column of liquid in a capillary. Brubaker and Kammermeyer[23,24] and Stern et al.[70] have employed this method for their measurements.

The variable pressure method: A constant gas pressure is applied to one side of an outgassed membrane, and the increase of pressure of the permeating gas measured on the outgoing side. This method has been used frequently by investigators; Barrer[1] developed a research apparatus for the simultaneous determination of permeability, diffusion and solubility coefficients. Permeability cells have also been designed by other workers.[7,29,68]

Of the three methods described, the last two have proved to be the most popular, as costly analytical apparatus is not required. The variable pressure method was used for this work.

1.9 Polyvinyl Chloride, Unplasticised and Plasticised

1.9.1 General

Vinyl polymerisation is an example of a free radical reaction, where many thousands of monomer molecules may be caused to react for each initiating free radical introduced into the system. The monomer for the preparation of polyvinyl chloride (PVC) is vinyl chloride $CH_2{:}CHCl$ which on polymerisation forms chains that, apart from the initial and terminal groups, have the general formula $\left[CH_2 - CHCl \right]_n$.

During polymerisation it is usual to incorporate a catalyst, which breaks down into free radicals more readily than the vinyl chloride monomer. Frequently the catalysts are organic peroxides such as benzoyl or lauroyl peroxide. Polyvinyl chloride is insoluble in its monomer and most solvents, except for organic, high boiling solvents such as cyclohexanone and tetrahydrofuran. As homogeneous polymerisation requires such expensive solvents, polymerisation in an emulsion or suspension is favoured industrially.[75] Polymerisation of vinyl chloride on heterogeneous catalysts has become especially important, as the catalyst often exerts a precise steric control over the addition of the monomer units.[71]

The range over which any polymer shows rubber-like properties can be shifted to lower temperatures by incorporating into it a liquid plasticiser, which swells the network. The plasticiser is believed to operate by facilitating motions of the chain segments between different configurations.[59,74,82] If involatile liquids are used, these are retained by the network almost indefinitely and do not necessarily have to be thermodynamically compatible with the polymer.

A great number of plasticisers are used to lower the glass transition temperature of poly-vinyl chloride, common examples being the esters of phosphoric and phthalic acids.[73] Tricresyl phosphate plasticiser, incorporated in poly-vinyl chloride, displays the smallest loss due to migration and subsequent volatility at high temperatures.[74,103,104] The behaviour of a plasticiser is dependent upon its inherent physical and chemical properties, some of which are vapour pressure, viscosity, melting point, molecular structure or shape, molecular weight and finally the molecular aggregate it forms with the polymer. Some of the physical characteristics of plasticised poly-vinyl chloride compositions will be discussed in later sections.

Small quantities of stabilizers are usually incorporated in poly-vinyl chloride to prevent discolouration and evolution of HCl. When the polymer is heated above about 110° without sufficient stabiliser, and in an inert atmosphere, degradation commences with the evolution of HCl resulting in the formation of conjugated polymer, unsaturation and coloured polyene systems.[75,76] Although poly-vinyl chloride degradation appears to be negligible below 100°, the majority of stabilisers act by absorbing any free HCl evolved during processing and removing it as an insoluble product. A large group of stabilisers comprises the metallic soaps, of which lead, barium and calcium are the most common. Stabilisers do not increase the tensile strength of the polymers, like the action of fillers in elastomers, but may cause a slight deterioration in mechanical strength.

1.9.2 Determination of microstructure

The predominance of the head-to-tail chemical structure $\frac{1}{+}$ CH_2 - $CHCl$ $\frac{1}{+}_n$ has been established for poly-vinyl chloride from chemical evidence,[70] as well as from infrared studies.[72] Polyvinyl chloride, when stretched into a fibre, is found to crystallise, though only feebly owing to imperfections in the structure.[77,78] Early

X-ray work[77] had indicated that the chain configuration inside crystals might be syndiotactic, but this primarily depended on interpretation of the 5.1 Å fibre axis repeat. The remainder of the pattern was not, however, detailed enough to test this hypothesis adequately, so that this structure could not be considered to be firmly established. A more detailed X-ray diffraction study of poly-vinyl chloride, using oriented fibres prepared with the aid of free radical catalysts, confirmed the syndiotactic configuration within the small ordered regions of the chain. In a syndiotactic configuration the substituents alternate on either side of the place of the zig-zag carbon backbone. As D and L units occur in equal numbers in the chain, the structure is also optically inactive.

Extensive studies of the infrared spectrum of poly-vinyl chloride in various states (solution, powder and film) have been made by Krimm and co-workers.[80-83] The importance of understanding the origins of the bands has been emphasised; and the reasons why they differ in samples from different sources, or in different physical states, before reliable infrared measurements of tacticity may be made.[80] Besides using 'ordinary' poly-vinyl chloride samples polymerised at high temperatures, some interesting behaviour of the C-Cl stretching modes has

has been observed using samples polymerised at low temperatures, for example. -50°. The syndiotactic part of the polymer chains was observed to increase by lowering the polymerisation temperature. Assignment of the infrared spectra was facilitated by the use of deuterated polymers[80,83] and model compounds, appropriate low molecular weight analogues of the polymer.[82,83]

Krimm et al.[81] were able to identify, from frequencies of the several C-Cl stretching bands, the chain conformations which are associated with particular Cl pair configurations. It was established that changes in conformational structure accompanied certain changes in physical state of the polymer. These changes were brought about by solvent extraction, by heating and by stretching of pressed and cast films.

A spectroscopic study of the effect of plasticiser on the chain conformation of pressed poly-vinyl chloride films has been made.[82] Di-isobutyl adipate plasticiser was chosen for the investigation, in preference to other plasticisers, as it does not possess absorption bands which interfere with the C-Cl stretching modes of the polymer. It was concluded that the plasticiser decreases the crystallinity present and changes the chain conformation to a less favourable state.

The infrared spectra of poly-vinyl chloride in cyclohexanone and cycloheptanone solutions has also been investigated.[84,85] Assuming a Boltzmann distribution between the two possible syndiotactic conformations, the configuration of the chain, i.e. the syndiotacticity, was determined by measuring the temperature dependence of the intensity ratios of these two C-Cl stretching bands. Furthermore, the energy difference between the two syndiotactic conformations was obtained. Krimm[83] has, however, doubts about whether the critical assignments for the infrared bands obtained in the above investigations are correct.

Nuclear magnetic resonance spectroscopy of vinyl polymers in solution has proved to be an effective means for the determination of tacticity.[86-89] Vinyl polymers give complex NMR spectra on account of the coupling of the spins of the methylene protons with those of the neighbouring α-hydrogen atoms. The problem may be simplified by using polymers prepared from monomers deuterated on the α-carbon atom. Careful examination of the methylene spectrum of poly-vinyl chloride has been made. The interpretation suggested by Tincher [87] seems more satisfactory than that proposed earlier by Johnsen,[86]

and enables the tacticity to be analysed in terms of isotactic and syndiotactic diads.

The existence of some ordered or crystalline regions in poly-vinyl chloride has also been indicated by dilatometric[95] and calorimetric studies.[96] The dependence of the specific volume and specific heat, respectively, on temperature was measured in the region of 100°C.

The degree of branching of poly-vinyl chloride has been estimated by an infrared technique.[92,93] Polymer prepared at -40°C was found to be essentially linear, but samples obtained at +45°C had between one and two branches per hundred monomer units. Increases in the temperature of polymerisation are generally found to increase the degree of branching. The relatively high degree of branching in poly-vinyl chloride can be attributed to the ease with which chlorine atoms are removed by radical attack during polymerisation.

1.9.3 Transitions in poly-vinyl chloride

The thermodynamic melting point T_m of poly-vinyl chloride is difficult to measure experimentally by dilatometric and calorimetric methods. As already discussed in Section 1.9.1, degradation of the polymer occurs before the melting temperature is reached.[75,76]

Kockott,[97] however, regarded stereoregular poly-vinyl chloride as a copolymer of syndiotactic and isotactic parts only the former being able to crystallise. Following Flory's theory of copolymer crystallisation,[91] it is possible to determine the melting temperature T_m^o of completely crystallised syndiotactic poly-vinyl chloride, the enthalpy of fusion ΔH and the surface energy s from tacticity and degree of crystallinity of the samples as a function of temperature. Tacticity was known from NMR and infrared experiments and degree of crystallinity determined by X-ray diffraction. Kockott[97] obtained values of $T_m^o = 273^oC$, $\Delta H = 2.7$ k.cal.mole^{-1} and s = 16 erg cm.$^{-2}$. Nielsen[101] quotes values for poly-vinyl chloride of $T_m = 212^oC$ and $\Delta H = 3.04$ k.cal.mole^{-1}. A lower limit for the length of crystallised sequences was also calculated to be 12 monomer units, by application of Flory's theory[91] to experimental data.

The glass temperature T_g of a polymer represents fairly precisely the boundary between the glassy and rubbery states. When the temperature is lowered over the glass transition region, the segmental motions owing to thermal energy and existence of free volume are considered to 'freeze', and 'holes' present at the

glass temperature become immobilised.[59,99] Thus the distribution of chain segments and free volume at T_g, which represents an equilibrium liquid-like distribution at that temperature, is considered to be retained at all temperatures below T_g. The glass transition usually occurs over a narrow range of temperature, and no matter how carefully measurements are made it is not possible to specify a point at which the properties change discontinuously.

The glass transitions of poly-vinyl chloride, unplasticised and plasticised, have been studied by both dynamic and static measurements. The former include principally mechanical energy absorption and dielectric dispersion.[74,94,99-101] Both these methods reveal the existence of a number of transitions. Besides the true glass transition, effects are detected which may be connected with the motions of very short chain segments or undissolved plasticiser, if present. Taylor and Tobolsky[94] investigated the time dependent relaxation modulus of both unplasticised and plasticised poly-vinyl chloride samples over their glass transition regions. The general behaviour of the results suggested that poly-vinyl chloride is semicrystalline in nature, the crystallites being small enough to act as crosslinks. The

diethylhexyl phthalate plasticiser, whilst reducing the inflection and glass temperature of the polymer, was considered not to alter the microcrystalline structure. This was contrary to the conclusions drawn from infra-red measurements.[82]

One of the most accurate static methods is the dependence of specific volume on temperature over the glass transition region.[94.98,99] For reproducible results the temperature of the sample in a dilatometer must be changed very slowly, especially when going through the transition region. Heydemann et al.[98] determined the specific volume of unplasticised and plasticised poly-vinyl chloride as a function of temperature and hydrostatic pressure. Besides the glass transitions secondary transitions were observed which corresponded, however, to dynamic secondary dispersion ranges below the glass transition. All transition temperatures were shifted by increases of pressure, and addition of plasticiser to the polymer shifted the glass transition to lower and the secondary transition to higher temperatures.

The temperature of the glass transition can also be located by studying the shapes of NMR spectra. For poly-vinyl chloride the NMR transition at about 97°C occurs near the transformation observed by refractrometric

studies and by specific heat measurements.[102] However, this is higher than dilatometric and appropriate dynamic values of the glass transition temperature. These are usually quoted within the temperature range 70-85° for unplasticised poly-vinyl chloride, and correspondingly lower values for plasticised compositions.[40,94,98,99,101,124,137] The differences in the quoted T_g values are probably brought about by differences in microstructure and molecular weight, and the extent of chain branching and cross linking of the samples under test.

1.9.4 Volatility and diffusion of plasticisers

The loss of plasticisers from poly-vinyl chloride and vinyl polymers has been measured directly from experiments conducted in a stream of air[74] and under high vacuum.[103,104,107,108] The diffusion of plasticiser within poly-vinyl chloride samples has also been measured, with the sample exposed to high vacuum[107,108] or in direct contact with a second sample with a lower plasticiser concentration.[105,106,107] The time dependence of plasticiser concentration has been followed by techniques, such as the variation of refractive index of the compositions,[105-107] and the change in intensity of infrared absorption bands of plasticisers.[108] Hellwege et al.[107]

also measured the concentration gradient by splitting samples into layers 30-40 μ thick. The concentration of plasticiser was determined for each layer, enabling the concentration of plasticiser at the surface of the samples to be calculated by extrapolation.

The diffusion of plasticiser to the surface of the sample, and subsequent evaporation, show a dependence on the vapour pressure and viscosity of the plasticiser, although other factors are also relevant.[103,104] Heine et al.[106] studied the diffusion of diethylhexyl phthalate plasticiser between polyvinyl chloride samples. They came to the conclusion that at the interface there exists a time and temperature dependent jump in plasticiser concontration, which acts as contact resistance for the diffusing medium. An exact determination of the diffusion coefficient and the magnitude of the concentration jump can also be difficult, because of the constant shift of the interface owing to gelling and shrinkage of the two samples.

The plasticiser diffusion coefficient rises rapidly with increasing plasticiser concentration.[103,105-108] Because of this strong concentration dependence of the diffusion coefficient the material tends to seal itself

against further loss as plasticiser disappears. Although the concentration of diethylhexyl phthalate near the surfaces of poly-vinyl chloride samples decreased strongly during desorption, it was never found, however, to reach zero.[107] Thus the assumption of zero surface concentration put forward by earlier workers [103,104] for the calculation of the diffusion coefficients may need revision. Luther et al.[108] found that the diffusion coefficient is only a little concentration dependent above the glass transitions of plasticised compositions, but shows a large concentration dependence below the transition.

The energy of activation for diffusion of plasticiser in poly-vinyl chloride decreases with increasing concentration. For example, this energy decreases from 24 k.cal.mole^{-1} at 10% concentration of trioctyl phosphate to 6 k.cal.mole^{-1} at 80% concentration.[105]

PART 2

THEORETICAL

2.1 Diffusion in a Plane Sheet

Diffusion takes place as a result of the random Brownian jumps of the diffusate molecules, and matter is transferred from one part of a system to another. If there is a gradient of chemical potential of the diffusate, the frequencies of jumps in opposite directions across a plane at right angles to the gradient are not equal, and there is a net flux across the plane.

2.1.1 Laws of diffusion

The mathematical theory of diffusion in isotropic substances is based on the hypothesis that the isothermal rate of transfer of diffusing matter through a unit area of a section is proportional to the gradient of chemical potential measured normal to the section. The vector determining the diffusion rate can be chosen as the gradient of concentration instead of chemical potential,[115,120] so that

$$R = -D \frac{\partial C}{\partial x} \qquad (2.1)$$

where R is the isothermal rate of transfer per unit area

of section, C the concentration of diffusing substance, x the space co-ordinate measured normal to the section, and D is the diffusion coefficient. This coefficient is essential for describing diffusion phenomena, and gives information on the nature of the transport process and on the interaction of the molecules involved. If R and C are both expressed in terms of the same unit of quantity, then it is clear from (2.1) that D is independent of this unit and has dimensions $\text{length}^2\text{time}^{-1}$ e.g. $\text{cm}^2\text{sec}^{-1}$. The negative sign in equation (2.1) arises because diffusion occurs in the direction opposite to that of increasing concentration.

From (2.1) the condition of conservation of mass yields for constant D

$$\frac{\partial C}{\partial t} = D \frac{\partial^2 C}{\partial x^2} \qquad (2.2)$$

which is valid for one-dimensional diffusion. Expressions (2.1) and (2.2) are sometimes referred to as Fick's first and second laws of diffusion respectively.

2.1.2 Solutions of diffusion equations (for constant D)

In this section only the one dimensional problem in a medium, bounded by two parallel planes at $x = 0$ and $x = \ell$,

will be considered for constant D. The solutions apply to diffusion in a plane sheet membrane so thin that all the diffusing substance enters through the membrane surface, and a negligible amount through the edges.

The general boundary conditions for diffusion in a membrane with thickness, ℓ , are:

$C = 0$ at $0 < x < \ell$ for $t = 0$

$C = C_1$ at $x = 0$ for $t \geq 0$

$C = C_2$ at $x = \ell$ for $t \geq 0$

The relevant boundary conditions for the experimental arrangements used here are obtained by putting $C = C_1 = 0$ or rather $C_2 >> C_1$.

(a) Steady-state diffusion

For steady-state flow, $\frac{\partial C}{\partial t} = 0$, as the concentration remains constant at all points of the membrane. Equation (2.2) then reduces to

$$D \frac{\partial^2 C}{\partial x^2} = 0 \qquad (2.3)$$

On integrating (2.3) twice with respect to x, and introducing the boundary conditions at $x = 0$ and $x = \ell$, we have

$$C = C_1 + (C_2 - C_1) \frac{x}{\ell} \qquad (2.4)$$

The rate, R, at which gas emerges from a unit area of the face x = 0 of the membrane is $-D(\frac{\partial C}{\partial x})_{x=0}$ as defined by (2.1), so that from (2.4)

$$R = -D(\frac{\partial C}{\partial x})_{x=0} = D(\frac{C_2 - C_1}{\ell}) \qquad (2.5)$$

(2.4) and (2.5) imply that the concentration of the penetrant changes linearly from C_2 to C_1 through the sheet, as required for constant D.

In this practical arrangement, surface concentrations C_2 and C_1 are not determined, but the ingoing (p_2) and the outgoing (p_1) gas pressures respectively. The rate of transfer of diffusate per unit area in the steady state can then be written as:

$$R = \overline{P}\ (\frac{p_2 - p_1}{\ell}) \qquad (2.6)$$

where $\overline{P}$ is the permeability coefficient expressed as the volume (cm^3) of gas at N.T.P. passing per second through a unit area (cm^2) of the surface of a membrane 1 cm thick, when the pressure difference across the membrane is 1 cm Hg. In practice, $p_2 >> p_1$, so that

$$\overline{P} = R\,\frac{\ell}{p_2} \qquad (2.7)$$

If D is constant, and the sorption isotherm is linear in that Henry's law is obeyed, then (2.5) and (2.6) are

equivalent under these circumstances. The linear isotherm may be expressed as

$$C = \sigma p \qquad (2.8)$$

where the gas concentration C within the membrane is in equilibrium with a gas pressure p, and σ is Henry's law solubility coefficient. Since C_1, p_1 and C_2, p_2 in (2.5) and (2.6) are connected by (2.8) it follows that:

$$\bar{P} = D\sigma \qquad (2.9)$$

where D is expressed in $cm^2 sec^{-1}$ and σ in cm^3 N.T.P. per cm^3 of membrane for a pressure of 1 cm Hg.

Expressing the flow rate, R, per unit area in terms of $\frac{V_o}{A} \cdot \frac{dp_1}{dt}$ where V_o is the outgoing gas volume, A the membrane area, and p_1 the outgoing pressure, (2.7) becomes:

$$\bar{P} = \frac{V_o}{p_2 A} \cdot \frac{273.16}{273.16 + T_R} \cdot \ell \frac{dp_1}{dt} \qquad (2.7a)$$

where T_R is the room temperature, and V_o is expressed in cm^3 at N.T.P.

The steady state diffusion coefficient D_S can be calculated from (2.9), by measurement of $\bar{P}$ from the steady state flow using (2.7a), and by determination of the static solubility coefficient σ_s from an equilibrium (static) technique.

(b) Transient state diffusion and the 'early approximation' method

If one face of a gas-free membrane is brought into contact with penetrant, it will take some time before the penetrant has crossed the membrane to reach the other face, and even more time before steady-state flow is established. Whereas steady-state flow is used for measuring $\bar{P}$, the time lag before the steady state is reached is a convenient measure of the diffusion coefficient.

An equation was found relating the extrapolated time-lage L, after which steady-state permeation starts, with the diffusion coefficient D_L and the thickness, ℓ, of the membrane by solving the general equation for uni-dimensional diffusion.[109] For the appropriate boundary conditions the equation reads:

$$D_L = \frac{\ell^2}{6L} \qquad (2.10)$$

where L, the time lag is the intercept on the time axis of the linear extrapolation of the line of outgoing pressure versus time representing steady-state flow.

Barrer,[1] in particular, has promoted the use of this equation for calculating the diffusion coefficient D_L of gases. Since $\bar{P}$ can be calculated from steady-state flow using (2.7a), the solubility coefficient is easily

deduced from (2.9). Solubility coefficients determined by this means are dynamic solubility coefficients, denoted by σ_D.

Although D_L, $\overline{P}$ and σ_D can be determined simultaneously by the above method, the time lag does not depend on the precise form of the permeation curve during the transient period. A procedure has been developed for the determination of the diffusion and solubility coefficients directly from transient state data, by using the 'early approximation' method.[110-112]

A convenient solution of the diffusion equation, which gives the rate of permeation during the transient period, was obtained by Holstein[110] as a transformation of the expression:

$$\frac{dp_1}{dt} = \left(\frac{A\sigma p_2 D}{V_o \ell}\right)\left[1 + \sum_{m=1}^{\infty} 2 \cos \pi m \exp \left\{-\frac{m^2\pi^2 Dt}{2}\right\}\right] \qquad (2.11)$$

Holstein's solution when D is constant is:

$$\frac{dp_1}{dt} = \left(\frac{2A\sigma p_2}{V_o}\right)\left(\frac{D}{\pi t}\right)^{\frac{1}{2}} \sum_{m=0}^{\infty} \exp \left\{-\left(\frac{\ell^2}{4Dt}\right)(2m+1)^2\right\} \qquad (2.12)$$

where $\frac{dp_1}{dt}$ is the rate of increase of outgoing pressure, and the remaining symbols have the same significance as before.

As t becomes larger the series in (2.11) tends towards zero. This is the form of equation which is used to relate the time lag to D. In equation (2.12) the dimensionless quantity Dt/ℓ^2 is inverted in the exponent, so that the series tends towards zero as t tends towards zero. For sufficiently short times, (2.12) may be approximated by neglecting all but the leading term in the series of exponentials. It is convenient to multiply by $t^{\frac{1}{2}}$, and take logarithms on both sides, so that (2.12) is converted into:

$$\ln\left(t^{\frac{1}{2}} \frac{dp_1}{dt}\right) = \ln\left[\left(\frac{2A\sigma p_2}{V_o}\right)\left(\frac{D}{\pi}\right)^{\frac{1}{2}}\right] - \left(\frac{\ell^2}{4Dt}\right) \qquad (2.13)$$

Equation (2.13) is usually referred to as the early approximation.

By plotting the quantity on the left hand side of (2.13) against reciprocal time, a straight line should be obtained. From the slope of this line, the diffusion coefficient, designated as D_E, can be obtained according to the relation:

$$\text{slope} = -\frac{\ell^2}{4D_E} \qquad (2.14)$$

After D_E has been determined from (2.14), the solubility coefficient σ_E can be obtained from the intercept on the $\ln\left(t^{\frac{1}{2}} \frac{dp_1}{dt}\right)$ axis which is given by:

$$\text{Intercept} = \ln\left[(2A\sigma_E p_2)\left\{\frac{76(273.16 + T_R)}{273.16\ V_o}\right\}\left(\frac{D_E}{\pi}\right)^{\frac{1}{2}}\right] \quad (2.15)$$

where the volume of gas is expressed in cm^3 at N.T.P.

To obtain the true value of D_E from the plot of (2.13), it is necessary to obtain experimental data at values of t which are sufficiently small, and not greater than 2.7 times the time lag L.[110] This method has been used to obtain D_E values for gaseous diffusion in glass.[110-112] It was more convenient than the time lag determination, as long periods of time were required before steady state flow was established.

2.2 Significance of Diffusion Coefficients in a Binary Mixture

A binary mixture of species 1 and 2 (gas, liquid or solid) can be characterised by five diffusion coefficients depending on the frame of reference. These are namely, two intrinsic diffusion coefficients D_1 and D_2, one mutual diffusion coefficient D_{12} ($\equiv D_{21}$), and two self-diffusion coefficients D_1^* and D_2^*. The physical significance of these diffusion coefficients has been discussed in some detail.[113-115]

2.2.1 Intrinsic diffusion coefficients

Intrinsic diffusion coefficients, D_1 and D_2, are defined in terms of the rate of transfer of species 1

and 2 across a section fixed so that no mass flow occurs through it. Such a section may be impossible to determine in practice as the coefficients refer to pure diffusion. Considering pure diffusion of species 1 and 2 along the x-coordinate, the origin of the x-coordinate is in a plane normal to the flow. This section must follow the mass flow, although this flow is not normally directly observable. The flow densities R_1 and R_2 of species 1 and 2, respectively, in the x-direction normal to the section are:

$$R_1 = -D_1 \frac{\partial C_1}{\partial x} \quad \text{and} \quad R_2 = -D_2 \frac{\partial C_2}{\partial x} \qquad (2.16)$$

where D_1, D_2, C_1 and C_2 are respectively the intrinsic diffusion coefficients and concentrations of species 1 and 2, in moles per unit volume.

2.2.2 Mutual diffusion coefficients

These coefficients D_{12} and D_{21} are expressed in terms of the rate of transfer of species across a section so defined that the total volume on either side of it remains constant as diffusion proceeds. In the particular case under consideration it is therefore fixed with respect to the closed containing vessel. We assume that there is no overall change of volume of two species 1 and 2 on mixing at constant pressure. If transport takes place through a unit area of the section normal to the

x-coordinate, a compensating mass flow must occur to maintain uniform pressure since the flow rates of species 1 and 2 are usually not equal. The volume transfer of species 1 and 2 per unit time across a unit area of the section defined is therefore:

$$R_1' = -D_{12}V_1 \frac{\partial C_1}{\partial x} \quad \text{and} \quad R_2' = -D_{21}V_2 \frac{\partial C_2}{\partial x} \qquad (2.17)$$

where V_1 and V_2 are the ~~specific~~ molar. volumes of species 1 and 2 respectively. As there is no net transfer of volume across the section, we have:

$$D_{12}V_1 \frac{\partial C_1}{\partial x} + D_{21}V_2 \frac{\partial C_2}{\partial x} = 0 \qquad (2.18)$$

For a unit volume of solution:

$$V_1C_1 + V_2C_2 = 1 \qquad (2.19)$$

which, following differentiation w.r.t.x., becomes:

$$V_1 \frac{\partial C_1}{\partial x} + V_2 \frac{\partial C_2}{\partial x} = 0 \qquad (2.20)$$

V_1 and V_2 are usually not equal to zero. Therefore, in order to satisfy (2.18) and (2.20) it follows that $D_{12} \equiv D_{21}$. A combination of mass flow and pure diffusion can, therefore, be described by one mutual diffusion coefficient.

2.2.3 Self-diffusion coefficients

By using radioactively-labelled molecules it is possible to observe the rate of diffusion of one component in a two-component system. If we consider a mixture of $(n_1 + n_1^*)$ molecules of species 1 (n_1^* are labelled molecules), and n_2 molecules of species 2, in solution we have

$$\frac{dn_2}{dx} = 0 \quad \text{and} \quad d\left(\frac{n_1 + n_1^*}{dx}\right) = 0 \ .$$

On condition that $\frac{dn_1^*}{dx}$ and $\frac{dn_1}{dx}$ are not zero, the pure diffusion flux R_1^* can be determined from $R_1^* = -D_1^* \frac{\partial C_1^*}{\partial x}$ and D_1^* evaluated. It follows that D_2^* may be determined in a similar manner.

2.2.4 Diffusion coefficient relationships

Relationships have been derived between the five diffusion coefficients described above, on condition that there is no overall volume change on mixing species 1 and 2.[2,114,115] The mutual and intrinsic diffusion coefficients are related in the following way.

On one side of a section fixed so that no mass flow occurs through it, there is a rate of accumulation of volume $\partial V/\partial t$ which, according to (2.16) since $R_1 \neq R_2$, is:

$$\frac{\partial V}{\partial t} = D_1 V_1 \frac{\partial C_1}{\partial x} + D_2 V_2 \frac{\partial C_2}{\partial x} \qquad (2.21)$$

As thus defined, $\frac{\partial V}{\partial t}$ is actually the rate of increase of volume on the side of smaller x, and this must be equal to the rate of transfer of total volume by mass flow through a fixed cross-section. Accordingly the rate of transfer of species 1 by mass flow is $(\partial V/\partial t)C_1$, and the total rate of transfer of species 1 is:

$$-D_{12} \frac{\partial C_1}{\partial x} = -D_1 \frac{\partial C_1}{\partial x} + \frac{\partial V}{\partial t} C_1 \qquad (2.22)$$

by equating two expressions for the net rate of transfer of species 1 through the fixed cross-section. On substituting for $\frac{\partial V}{\partial t}$ from (2.21) and using (2.19) and (2.20) we have:

$$D_{12} = V_1 C_1 D_2 + V_2 C_2 D_1 \qquad (2.23)$$

and when $V_1 = V_2$

$$D_{12} = N_1 D_2 + N_2 D_1 \qquad (2.24)$$

where N_1 and N_2 are mole fractions of species 1 and 2, respectively.

The relation between D_1 and D_1^{*} is derived as follows. The driving force causing diffusion of species 1 is usually assumed proportional to $-\partial\mu_1/\partial x$ where μ_1 is its chemical potential. The total force on all molecules of species 1 at a point x is then proportional to

$-C_1(\partial\mu_1/\partial x)$ and the flux R_1 through a unit area is therefore:

$$R_1 = -B_1 C_1 \frac{\partial \mu_1}{\partial x} \qquad (2.25)$$

As $d\mu_1 = RT\ d\ln a_1$ substitution in (2.25) gives:

$$R_1 = -RTB_1 \frac{d \ln a_1}{d \ln C_1} \times \frac{\partial C_1}{\partial x} \qquad (2.26)$$

where B_1 is the intrinsic mobility of species 1, and a_1 denotes its activity. Comparing (2.16) and (2.26) we then have:

$$D_1 = RTB_1 \frac{d \ln a_1}{d \ln C_1} \qquad (2.27)$$

On applying the same treatment to the diffusion of labelled molecules we obtain:

$$D_1^{*} = RTB_1 \frac{d \ln a_1^{*}}{d \ln C_1^{*}} \qquad (2.28)$$

The intrinsic mobility B_1 is the same for both labelled and unlabelled molecules of species 1. Since

$$\frac{d(n_1 + n_1^{*})}{dx} = 0 = \frac{dn_2}{dx}$$

we must have

$$\frac{d \ln a_1^{*}}{d \ln C_1^{*}} = 1$$

so that

$$D_1^{\ast} = RTB_1 \qquad (2.29)$$

A comparison of (2.29) and (2.27) then shows that

$$D_1 = D_1^{\ast} \frac{d \ln a_1}{d \ln C_1} \quad \text{and also} \quad D_2 = D_2^{\ast} \frac{d \ln a_2}{d \ln C_2} \qquad (2.30)$$

which are the desired relations between the intrinsic and self-diffusion coefficients.

It is now possible to derive a relationship between D_{12} and $D_1^{\ast}$, $D_2^{\ast}$. The Duhem-Margules relationship gives:

$$\frac{\partial \ln a_1}{\partial \ln N_1} = \frac{\partial \ln a_2}{\partial \ln N_2} \qquad (2.31)$$

Also, $C_1 = N_1/(V_1N_1 + V_2N_2)$; $C_2 = N_2/(V_1N_1 + V_2N_2)$

so that

$$\frac{d \ln a_1}{d \ln C_1} = \frac{d \ln a_1}{d \ln N_1} \frac{N_1V_1 + N_2V_2}{V_2} \qquad (2.32)$$

with an analogous expression for species 2. Substitution of (2.30), (2.31) and (2.32) in (2.23) then gives:

$$D_{12} = [N_2D_1^{\ast} + N_1D_2^{\ast}] \frac{d \ln a_1}{d \ln N_1} \qquad (2.33)$$

2.2.5 Measurement of diffusion coefficients

For liquid, gas or vapour diffusion in a polymer (species 2, say), D_2 may be considered to be negligible, so that, over nearly all the composition range, (2.23)

reduces to:

$$D_1 = \frac{D_{12}}{V_2 C_2} \tag{2.34}$$

The steady state permeation rate R_1 through a membrane of unswollen thickness ℓ can be shown[113] to be:

$$R_1 = \frac{1}{\ell} \int_0^{C_1} D_1 (V_2 C_2)^3 \, dC_1 \tag{2.35}$$

and

$$\ell \frac{dR_1}{dC_1} = D_1 (V_2 C_2)^3 = D_{12} (V_2 C_2)^2 \tag{2.36}$$

on substituting for D_1 by means of (2.34). D_1 can thus be measured from the slope of a plot of R_1 vs. C_1. The self-diffusion coefficient D_1^* has also been determined for several polymers.[6]

Methods of measurement of diffusion coefficients under different conditions have been reviewed by Crank and co-workers.[113,115] For diffusion between two liquids, the mutual and self-diffusion coefficients D_{12}, D_1^* and D_2^*, respectively, can be obtained by direct measurement. Intrinsic diffusion coefficients D_1 and D_2 can, however, be calculated from a knowledge of the quantities in (2.30), as an experimental method of separating intrinsic diffusion rate and mass flow has not been devised.

The existence of mass flow accompanying diffusion has been demonstrated in systems of two metals e.g. Ag-Au by the insertion of marker particles, whose movement can be observed. Indeed determination of all five diffusion coefficients has been possible in such systems.

2.3 Classification of Polymer-penetrant Systems in Diffusion and Solution

Barrer[2] was able to classify many polymer-penetrant systems, from the standpoint of diffusion and solution, into four main categories, as follows:

(1) $\frac{\partial C_1}{\partial t} = D_{12} \frac{\partial^2 C_1}{\partial x^2}$; $C_1 = \sigma p_1$ (Henry's law obeyed).

Into this category fall the diffusion and solution of permanent and inert gases in rubber, synthetic elastomers and often in harder polymers at temperatures just below the glass transition Tg. Since the volume fraction of polymer $V_2 C_2$ is approximately unity, and $D_2 << D_1$, it is clear from (2.23) that all measurements of D_{12} are in fact measurements of the intrinsic diffusion coefficient D_1. Also, at equilibrium $\frac{d \ln a_1}{d \ln C_1} = \frac{d \ln p_1}{d \ln C_1} = 1$, and so $D_1 = D_1^{*}$ from (2.30).

(2) $\frac{\partial C_1}{\partial t} = \frac{\partial}{\partial x}(D_{12} \frac{\partial C_1}{\partial x})$; $D_{12} = f(C_1)$; $C_1 = \sigma p_1$

This category is well represented by C_4 and C_5 paraffins diffusing and dissolving in rubber.[44] D_{12} is no longer independent of C_1, but Henry's law is still valid, so that $D_{12} = V_2 C_2 D_1$ and $D_1 = D_1^{\infty}$.

(3) $\frac{\partial C_1}{\partial t} = \frac{\partial}{\partial x}(D_{12} \frac{\partial C_1}{\partial x})$; $D_{12} = f(C_1)$; $C_1 = F(p_1)$

For penetrant-polymer systems in this category, typified by the sorption and diffusion of heavier hydrocarbon vapours or chloroform in rubber,[59,116] we no longer have a linear isotherm. Often the isotherm contours can be represented, over a substantial range of concentrations, by expressions based on the lattice theory of polymer-penetrant mixtures. Normally $D_2 << D_1$ and so from (2.23) the relationship $D_{12} \simeq V_2 C_2 D_1$ still holds. Experiments of this type are, therefore, conducted above Tg of the polymer, where there is high chain mobility and short relaxation times.

(4) $\frac{\partial C_1}{\partial t} = \frac{\partial}{\partial x}(D_{12} \frac{\partial C_1}{\partial x})$; $D_{12} = f(t, C_1)$ or $D_{12} = f_1(t) \times f_2(C_1)$; $C_1 = F(p_1)$

D_{12} is not only a function of concentration, but also time dependent; and Henry's law is not obeyed. This type of polymer-penetrant system involves the more

rigid and internally viscous polymers with long relaxation times.[10,59,116] Examples of this are given by the diffusion and solution of methylene chloride in polystyrene, and cellulose acetate; acetone and allyl chloride in polyvinyl acetate. The process of sorption on occasions takes place in two distinct stages in which swelling of the polymer occurs. Taken as a whole, it is possible for the two stage process to be represented as a diffusion with a complex time and concentration dependence of D_{12} ($D_{12} = f(t,C_1)$). Slow relaxation could also take place as a result of past treatments of the polymer which may be largely independent of the penetrant, such that $D_{12} = f_1(t) \times f_2(C_1)$.

The four categories of polymer-penetrant mixture already referred to are not the only possible cases. Where there is a steady thermal gradient across a membrane (as in thermo-osmosis[6,120]) or where a membrane consists of laminae of different polymers, the following cases may be concerned:

$$(5) \quad \frac{\partial C_1}{\partial t} = \frac{\partial}{\partial x}\left(D_{12} \frac{\partial C_1}{\partial x}\right); \quad D_{12} = f(x); \quad C_1 = \sigma p_1$$

$$(6) \quad \frac{\partial C_1}{\partial t} = \frac{\partial}{\partial x}\left(D_{12} \frac{\partial C_1}{\partial x}\right); \quad D_{12} = f(x,C_1); \quad C_1 = F(p_1)$$

Moreover, when thermal transients are combined with material diffusion, D_{12} in (5) and (6) may also be time

dependent. Diffusion and solution of penetrants in laminates have been investigated both theoretically and experimentally.[42,115,117-119] The behaviour of partially oxidised rubber to the diffusion of propane could be more closely approximated to a three layer composite, of which the surface layers are the more heavily reacted, than to a single layer.[117] Crank[115] has also discussed the effect of surface skins, which form a resistance to entry or exit from the polymer, on the sorption-desorption kinetics of vapour-polymer systems.

2.4 Application of the Transition State Theory to Diffusion

Since diffusion is a rate process, it is amenable to treatment by the transition state theory, also known as the theory of absolute reaction rates.[46,121] The theory is based on the assumption that the reactants approach one another to form an activated complex, which is regarded as being situated at the top of a potential energy barrier lying between the initial and final states. The rate of reaction is determined by the rate at which these complexes travel over the top of the barrier. This activated complex was considered by Eyring as an ordinary molecule possessing all the normal thermodynamic

properties, and it is assumed to be in equilibrium with the reactants, even when the reactants and products are not.

An expression for the rate constant k' of any process was derived[121] in terms of the equilibrium constant $K^{\ddagger}$ between the activated complex and the reactants, such that

$$k' = \frac{kT}{h} K^{\ddagger} \qquad (2.37)$$

where k and h are the Boltzman and Planck constants. If $\Delta G^{\ddagger}$, $\Delta H^{\ddagger}$ and $\Delta S^{\ddagger}$ refer to the free energy, heat content and entropy of activation, respectively, with reactants and activated complexes in their standard states, then:

$$\Delta G^{\ddagger} = -RT \ln K^{\ddagger} \quad \text{and} \quad \Delta G^{\ddagger} = \Delta H^{\ddagger} - T\Delta S^{\ddagger} \qquad (2.38)$$

Substitution of (2.38) in (2.37) then gives

$$k' = \frac{kT}{h} \exp(-\frac{\Delta G^{\ddagger}}{RT}) \qquad (2.39)$$

and

$$k' = \frac{kT}{h} \exp(\frac{\Delta S^{\ddagger}}{R}) \exp(-\frac{\Delta H^{\ddagger}}{RT}) \qquad (2.40)$$

If λ is the jump distance between successive equilibrium positions of the diffusing molecule, then it has been shown[121] that the diffusion coefficient D is given by:

$$D^{\ddagger} = \lambda^2 k' \tag{2.41}$$

Therefore combination of (2.40) and (2.41) gives an expression for D which is:

$$D = \lambda^2 \frac{kT}{h} \exp\left(\frac{\Delta S^{\ddagger}}{R}\right) \exp\left(-\frac{\Delta H^{\ddagger}}{RT}\right) \tag{2.42}$$

Taking logarithms and differentiating w.r.t.T, (2.42) becomes

$$\frac{d \ln D}{dT} = \frac{1}{T} + \frac{\Delta H^{\ddagger}}{RT^2} \tag{2.43}$$

Similarly from the Arrhenius equation (1.3)

$$\frac{d \ln D}{dT} = \frac{E_D}{RT^2} \tag{2.44}$$

Therefore comparing (2.43) and (2.44) we have

$$E_D = RT + \Delta H^{\ddagger} \tag{2.45}$$

which is the relationship between the energy of activation E_D and the heat of activation $\Delta H^{\ddagger}$. By equating (1.3) and (2.42) and substituting (2.45) we obtain:

$$D_o = e \frac{kT}{h} \lambda^2 \exp\left(\frac{\Delta S^{\ddagger}}{R}\right) \tag{2.46}$$

From the experimentally determined quantities E_D and D_o it has therefore been possible to calculate $\Delta S^{\ddagger}$, $\Delta H^{\ddagger}$ and $\Delta G^{\ddagger}$, assuming suitable values of the jump distance λ.[5,43,48] Values of $\Delta S^{\ddagger}$ determined in this way for polymer-penetrant systems are usually large and positive.[5,43,44,50,122]

These high values are attributed by Glasstone et al.[121] to the severing of bonds in the diffusion process. Barrer[50] suggested an alternative explanation in that this phenomenon is due to a considerable disturbance of the polymer matrix adjacent to the penetrant in the formation of the transition state. This led to Barrer's postulation of the Kinetic Statistical theory, also known as the theory of Zone of Activation.

2.5 Diffusion Coefficient according to the Kinetic Statistical theory (Barrer's Theory of Zone of Activation)

Barrer[45,56,57] postulated that for a unit diffusion process to take place in any region of the polymer, an activation energy must first appear in that region as a result of thermal energy fluctuations. The chance that there is a total energy $\geq E$ in a small region or zone surrounding the solute molecule and which, including the solute molecule, contains n degrees of freedom is

$$P = \sum_{f=1}^{f=n} \left(\frac{E}{RT}\right)^{f-1} \frac{1}{(f-1)!} \exp\left(-\frac{E}{RT}\right)$$

$$= \sum_{f=1}^{f=n} P_f \exp\left(-\frac{E}{RT}\right) \qquad (2.47)$$

where $P_f = \left(\frac{E}{RT}\right)^{f-1} \frac{1}{(f-1)!}$

Internal vibrational degrees of freedom normally need not be considered, because energies of activation are too small to excite them. If P_f is plotted against f, for any value of E/RT, a family of curves with maxima is obtained.[57] Representing $\bar{U}$ as the average energy in the chosen f degrees of freedom, the locus of the maxima corresponds to $E = \bar{U} = fRT$. This most probable distribution is not the one of importance in diffusion because the rate process would then occur with zero value of E_D, since $E_D = E - \bar{U} = 0$ which is not found. Thus the value of n in the region need not exceed f_{max} to include all energy distributions likely to contribute to a successful unit process, for all 'colder' than average distributions may be excluded.

If only 'hot' distributions ($E > \bar{U}$; $E_D > 0$) are considered, the important distributions are decided by two balancing factors: (1) $E_D = E - \bar{U}$ must be as concentrated as possible to give the most energised zone compatible with (2) below; (2) there must be an 'a priori' probability P_f which is as large as possible, bearing (1) in mind. This means that the optimum zone of activation will have values of f lying between 1 and f_{max} ($f_{max} = \frac{E}{RT}$). In addition there will normally be need for synchronisation between segmental rotations and intermolecular vibrations

within the activated zone, if a successful unit transport process is to occur within the lifetime of the important energy fluctuations defined by conditions (1) and (2). For example, the probability of each of p groups moving simultaneously in one of m directions is $(\frac{1}{m})^p$. Since various cooperations may be successful, the total probability of all individual possible chances of co-operation is the sum of all individual chances p_f. p_f will be expected to depend on f, and is < 1.

In general, for different values of f, a spectrum of terms p_f may contribute to the probability of a successful unit transport process. Therefore the expression for the diffusion coefficient[3,5,45,50,56,57] is:

$$D = \nu\lambda^2 \sum_{f=1}^{n} p_f \left(\frac{E}{RT}\right)^{f-1} \frac{1}{(f-1)!} \exp\left(-\frac{E}{RT}\right) \qquad (2.48)$$

where f is the number of degrees of freedom over which the total energy of activation E is divided in any zone, the summation being taken up to n. n is the number of degrees of freedom in the largest i.e. the most diffuse zone of activation contributing appreciably to D; λ is the mean distance moved in a unit diffusion step; ν is the mean vibration frequency of the diffusing molecule; and p_f has the form $\sum (\frac{1}{m})^p$ as explained previously. If only one term of the summation in (2.48) is assumed to be important

(most applicable when $E >> (f-1)RT$), then (2.48) becomes

$$D = p_f \nu \lambda^2 \left(\frac{E}{RT}\right)^{f-1} \frac{1}{(f-1)!} \exp\left(-\frac{E}{RT}\right) \qquad (2.49)$$

If f for the dominant term is independent of temperature, one finds on equating (2.49) to the Arrhenius equation $D = D_o \exp\left(-\frac{E_D}{RT}\right)$, and using Stirling's approximation for the factorial, that

$$E_D = E - (f-1)RT \qquad (2.50)$$

and therefore

$$D_o = p_f \nu \lambda^2 \left(\frac{E}{RT}\right)^{f-1} \frac{1}{(f-1)!} \exp(1-f) \qquad (2.51)$$

or

$$\ln D_o = \ln(p_f \nu \lambda^2) + (f-1) \ln \left[\frac{E_D + (f-1)RT}{RT}\right]$$

$$-(f-1)\ln(f-1) - \tfrac{1}{2} \ln \left[2\pi(f-1)\right] \qquad (2.52)$$

Equation (2.52) was used by Barrer and Skirrow[43] to measure f. By plotting the right hand side of (2.52) against f for different values of f, one may then read off from the curve the value of f required to give any experimental value of $\ln D_o$, assuming appropriate values for p_f, ν and λ.

A second approach to the value of f follows from (2.50), which shows that

$$\frac{dE_D}{dT} = -(f-1)R \qquad (2.53)$$

provided that f is independent of temperature T. E has been regarded as the effective activation energy at absolute zero temperature and assumed to be independent of T, but either D_o or E_D or both may be temperature dependent. Equation (2.53) provides a means of measuring f, as has been done by Barrer and co-workers[43,44] and by Van Amerongen.[5] The measurements of f so deduced correspond to an upper limit only.

According to (2.53) E_D has a negative temperature coefficient, although from the transition state theory using (2.45) we have:

$$\frac{dE_D}{dT} = R + \Delta C_V^{\ddagger} \qquad (2.45a)$$

where $\Delta C_V^{\ddagger} = \frac{\partial \Delta H^{\ddagger}}{\partial T}$ is the change of specific heat in passing to the transition state. Therefore it can be seen from (2.45a) that a positive temperature coefficient is predicted for E_D whenever $\Delta S^{\ddagger}$ is positive.

2.6 Thermodynamics of Polymer Solutions

The ideal solution law, as embodied in Raoult's law (i.e. the activity a_1 of solvent in the solution is equal to its mole fraction N_1) provides the basis for the treatment of small molecules. Although such solutions seldom behave ideally over a wide concentration range, the correlation is usually adequate to justify adoption of the

classical ideal solution as a standard for comparison. Solutions in which the solute is a high molecular weight polymer exhibit very large deviations from ideality, and some other relationship is therefore needed.

Considering the isothermal transfer of one mole of liquid from a mass of pure solvent of vapour pressure p_1^o to an infinite amount of solution, where the vapour pressure of the solvent is p_1, the resultant changes in the Gibbs free energy, heat content and entropy are signified as the Gibbs free energy of dilution ($\Delta \bar{G}_1$), the heat of dilution ($\Delta \bar{H}_1$) and the entropy of dilution ($\Delta \bar{S}_1$). If one is justified in ignoring gas imperfections:

$$\Delta \bar{G}_1 = RT \ln \frac{p_1}{p_1^o} \qquad (2.54)$$

and since $\Delta \bar{G}_1 = \Delta \bar{H}_1 - T\Delta \bar{S}_1$ we can also obtain

$$\Delta \bar{H}_1 = \left[\frac{\partial(\frac{\Delta \bar{G}_1}{T})}{\partial \frac{1}{T}}\right] \equiv - T^2\left[\frac{\partial}{\partial T}(\frac{\Delta \bar{G}_1}{T})\right] \qquad (2.55)$$

and

$$\Delta \bar{S}_1 = -\left[\frac{\partial \Delta \bar{G}_1}{\partial T}\right] \qquad (2.56)$$

Therefore $\Delta \bar{G}_1$, $\Delta \bar{H}_1$ and $\Delta \bar{S}_1$ may be determined from the variation with temperature of the vapour pressures of polymer-penetrant mixtures.

For solutions of polymers in non-polar liquids, values of $\Delta \bar{S}_1$ are positive but abnormally large whilst $\Delta \bar{H}_1$ values are usually small and positive. The conditions for ideal solution behaviour are therefore not fulfilled, and it is now accepted that the deviation is largely due to the entropy change rather than to the occurrence of a non-zero heat of dilution.

2.6.1 Entropy of mixing (ΔS_m) and dilution (ΔS_1) according to the liquid lattice theory

Meyer[125] suggested that the large entropy of mixing for athermal polymer solutions was a consequence of the great number of configurations available to a long flexible molecule in solution. On the basis of this suggestion, Flory[123,124] and Huggins[126-128] developed independently the first statistical treatment of the entropy of long chain molecules. They calculated the number of possible configurations for a mixture of solvent molecules and polymer molecules arranged in a lattice, each cell of which was able to accommodate one solvent molecule, or one segment of the polymer molecule having a size approximately equal to that of the solvent molecule. The expression for the entropy of mixing n_1 solvent molecules with n_2 randomly coiled polymer molecules was found by Flory to be:

$$\Delta S_m = -k(n_1 \ln \frac{n_1}{n_1 + xn_2} + n_2 \ln \frac{xn_2}{n_1 + xn_2}) \qquad (2.57)$$

or

$$\Delta S_m = -k[n_1 \ln v_1 + n_2 \ln v_2] \qquad (2.58)$$

where x is the number of segments per polymer molecule, or the ratio of molar volumes of polymer and solvent, V_2 and V_1 respectively. v_1 and v_2 are the volume fractions of solvent and polymer respectively.

By differentiating (2.57) with respect to n_1 and multiplying by Avogadro's number N, the expression for the partial molar entropy of dilution is given by

$$\Delta \bar{S}_1 = -R[\ln(1-v_2) + (1- \tfrac{1}{x})v_2] \qquad (2.59)$$

The result of the more precise treatment of the lattice model given by Huggins[128] is:

$$\Delta \bar{S}_1 = -R[\ln(1-v_2) - \tfrac{Z}{2}(1 - \tfrac{1}{x})\ln(1 - \tfrac{2v_2}{Z})] \qquad (2.60)$$

where Z is the lattice coordination number. Miller[129] has also applied a rigorous treatment to the lattice model, and arrived at a similar expression to (2.60). When x is large, equation (2.59), reduces to:

$$\Delta \bar{S}_1 = -R[\ln(1-v_2) + v_2] \qquad (2.61)$$

which is free from any molecular parameter. Therefore

according to this theory, the entropy of dilution of any polymer by any liquid should depend only on its volume fraction.

2.6.2 Free energy and heat of mixing

The heat of mixing can be considered to originate in the replacement of some of the contacts between like species in the pure liquids with contacts between unlike species in the solution. According to the lattice model, three types of first neighbour contacts, represented by the self-explanatory symbols, [1,1], [2,2], and [1,2] will occur. The formation of the solution may be likened to a chemical reaction signified by the stoichiometric equation:

$$\tfrac{1}{2}[1,1] + \tfrac{1}{2}[2,2] = [1,2] \qquad (2.62)$$

The change in energy for the formation of an unlike contact pair according to (2.62) is:

$$\Delta w_{12} = w_{12} - \tfrac{1}{2}(w_{11} + w_{22}) \qquad (2.63)$$

where w_{11}, w_{22} and w_{12} are the energies associated with respective contact pairs. The heat of mixing the two components is found to be given by:[124]

$$\Delta H_m = kT\chi_1 n_1 v_2 \qquad (2.64)$$

where

$$\chi_1 = \frac{z\Delta w_{12} x_1}{kT} \qquad (2.65)$$

if the solvent molecule contains x_1 segments instead of only one. The interaction parameter χ_1 is a dimensionless quantity characterising the interaction energy per solvent molecule divided by kT. The quantity $kT\chi_1$ represents the difference in energy of a solvent molecule immersed in the pure polymer ($v_2 \cong 1$) compared with one surrounded by molecules of its own kind, i.e. in the pure solvent.

The free energy of mixing, ΔG_m is obtained by combining (2.58) and (2.64) in:

$$\Delta G_m = \Delta H_m - T\Delta S_m^{Total} = \Delta H_m - T\Delta S_m$$

$$= kT[n_1 \ln v_1 + n_2 \ln v_2 + \chi_1 n_1 v_2] \qquad (2.66)$$

The effect of accepting the configurational entropy of mixing ΔS_m as being equal to the total, or effective, entropy of mixing ΔS_m^{Total} is to neglect possible contributions which may arise from specific interactions between neighbouring components of the solution. (It may also be noted[124] that the solvent molecule may consist of a number of segments, x_1, without altering the form of equation (2.58)).

In the above treatment the interactions have been considered to lead solely to a heat of mixing, but Guggenheim[130] emphasised that there is no justification

in not considering a contribution to the entropy from first neighbour interactions. Δw_{12} of equations (2.63) and (2.65) may be represented as:

$$\Delta w_{12} = \Delta w_h - T\Delta w_s \qquad (2.67)$$

where Δw_{12} acquires the character of a standard state free energy change, and Δw_h and Δw_s represent the changes in heat content and entropy for the process (2.62). Consequently χ_1 defined by (2.65) will contain an entropy contribution (divided by k) in addition to a heat of mixing term (divided by kT), and the quantity $kT\chi_1 n_1 v_2$ in (2.64) should be regarded as the standard state free energy change rather than the heat of mixing only. The form of the free energy function as expressed by (2.66) is unaltered by these considerations, but the revised expressions for the heat and entropy of mixing are:

$$\Delta H_m = -T^2\left[\frac{\partial\left(\frac{\Delta G_m}{T}\right)}{\partial T}\right] = -kT^2\left(\frac{\partial\chi_1}{\partial T}\right)n_1 v_2 \qquad (2.68)$$

and

$$\Delta S_m^{Total} = -\left[\frac{\partial \Delta G_m}{\partial T}\right] = -k\left[n_1 \ln v_1 + n_2 \ln v_2 + \frac{\partial(\chi_1 T)}{\partial T} n_1 v_2\right] \qquad (2.69)$$

If Δw_{12} is independent of T, i.e. if Δw_{12} contains no entropy contribution, χ_1 as given by (2.65) will be inversely proportional to T. The third term in (2.69) is

then zero, and $\Delta S_m^{Total} = \Delta S_m$; also $\chi_1 = -T(\frac{\partial \chi_1}{\partial T})$ and ΔH_m in (2.68) reduces to the previous expression (2.64).

2.6.3 Free energy and heat of dilution

Differentiation of (2.66) for ΔG_m with respect to n_1 and multiplication of the result by Avogadro's number, gives an expression for the free energy of dilution $\Delta \bar{G}_1$:

$$\Delta \bar{G}_1 = RT[\ln(1-v_2) + (1-\frac{1}{x})v_2 + \chi_1 v_2^2] \qquad (2.70)$$

If χ_1 varies inversely with T (i.e. if the interaction contributes an energy only), the first two terms in (2.70) represent the entropy of dilution $\Delta \bar{S}_1$ from (2.59). Since $\Delta \bar{G}_1 = -T\Delta \bar{S}_1 + \Delta \bar{H}_1$, the last term in (2.70) then gives an expression for the heat of dilution $\Delta \bar{H}_1$:

$$\Delta \bar{H}_1 = RTv_2^2\chi_1 \qquad (2.71)$$

If χ_1 contains an entropy contribution, the form of $\Delta \bar{G}_1$ is unaltered as given by (2.70), but its resolution into the heat and entropy of dilution is carried out by differentiating (2.68) and (2.69) w.r.t.n_1 and multiplying by Avogadro's number, so that

$$\Delta \bar{H}_1 = -RT^2(\frac{\partial \chi_1}{\partial T})v_2^2 \qquad (2.72)$$

and $$\Delta \bar{S}_1 = -R[\ln(1-v_2) + (1-\frac{1}{x})v_2 + \frac{\partial(\chi_1 T)}{\partial T} v_2^2] \qquad (2.73)$$

For the case where only dispersion forces are significant, Hildebrand et al.[131] expressed the heat of dilution $\Delta \bar{H}_1$ in terms of the cohesive energy densities $(\frac{E}{V})$ of the components as:

$$\Delta \bar{H}_1 = [(\frac{E_1}{V_1})^{\frac{1}{2}} - (\frac{E_2}{V_2})^{\frac{1}{2}}]^2 V_1 v_2^2 \qquad (2.74)$$

where V_1 is the molar volume of component 1 (solvent). The cohesive energy density (C.E.D.) is defined as the ratio of the molar energy of vaporisation to its molar volume, and is a measure of the cohesion per unit volume. Its square root $(\frac{E}{V})^{\frac{1}{2}}$ is called the solubility parameter, δ.

Hildebrand et al.[131] have shown that the solubility of many non-polar solutes in non-polar solvents can be satisfactorily accounted for by this method. The C.E.D. of a polymer can also be estimated by determining the equilibrium swelling of a slightly cross-linked analogue (such as lightly vulcanised rubber) in various solvents and correlating with the C.E.D. of the solvent.[132] In general, polymer-liquid systems do not follow (2.74) quantitatively, in which case it has simply been assumed that $\Delta \bar{H}_1 \propto v_2^2$, v_2 being the volume fraction of polymer.

2.6.4 Swelling of polymer networks

A cross-linked polymer placed in a non-polar liquid may absorb a large quantity of the liquid, but constraints

of the three dimensional network of chains prevent miscibility in all proportions. Therefore, only limited swelling will occur. The relationship of the equilibrium swelling to the χ_1 value for this system has been developed by Flory et al.[133,134] When it is considered that the network swells until the partial molar free energy of elastic stretching is equal to the free energy of dilution by (2.70) assuming an infinite value of x, it is clear that at equilibrium one needs only to equate the expression for these two quantities. The mathematical formulation of this reasoning leads to the following equation:[134]

$$-[\ln(1-v_{2m}) + v_{2m} + \chi_1 v_{2m}^2] = (\frac{v_1}{\bar{v}M_c})(1 - \frac{2M_c}{M})(v_{2m}^{\frac{1}{3}} - \tfrac{1}{2}v_{2m}) \quad (2.75)$$

where v_{2m} is the volume fraction of polymer at swelling equilibrium; $\bar{v}$ is the specific volume of pure polymer; M_c is the average molecular weight between cross links; M is the primary molecular weight. The factor $(1 - \frac{2M_c}{M})$ expresses the correction for network imperfections resulting from chain ends. For a perfect network ($M = \infty$) it reduces to unity. The left-hand side of (2.75) represents the lowering of the partial molar free energy owing to dilution of polymer by the solvent; that on the right gives the increase from the elastic reaction of the network.

For networks of very low degrees of cross linking in good solvents, (2.75) can be approximated and rearranged to give:[133,134]

$$\ln(1-v_{2m}) + v_{2m} + \chi_1 v_{2m}^2 + \frac{v_1 v_{2m}^{\frac{1}{3}}}{\bar{v} M_c} = 0 \qquad (2.76)$$

Direct determination of M_c in (2.76) is usually not possible, but it may be determined approximately from swelling measurements in a liquid whose χ_1 value with the non-cross-linked polymer is known from osmotic pressure measurements. If it is assumed that χ_1 is the same in both polymer systems, M_c can then be determined. Swelling measurements in other liquids with the cross-linked polymer, thus calibrated, leads at once to the approximate χ_1 values for these systems. This method has been used for various liquids, including plasticisers, with slightly cross-linked polyvinyl chloride[135] and polystyrene.[136]

2.6.5 Limitations of the lattice treatment

The acceptance of a single lattice to characterise both solvent and polymer and all intermediate compositions is seldom justified by the spatial requirements of the species involved. Compared with the physical unrealities of the model, mathematical approximations for simplifying

the treatment appear to be of little significance.[124] Derivation of ΔS_m in (2.57) assumes random mixing, although this cannot be strictly so, unless $\Delta H_m = 0$ with no specific attractions between unlike species. Owing to the discontinuous nature of very dilute polymer solutions the thermodynamic expressions for ΔH_m and ΔS_m are inapplicable in principle at high dilutions, apart from the question of the validity of the lattice model. These relations are appropriate in general only at concentrations where the randomly coiled molecules overlap one another extensively. For crystalline polymers the free energy change involved in dissolution of the crystals by the solvent must be taken into account. Often crystalline polymers are appreciably soluble (much below their melting points) only in solvents which have some specific interaction with them, other than dispersion forces. Equation (2.70) predicts that the parameter χ_1 is independent of concentration, but this is usually found not to be the case except for the rubber-benzene system.[124] The quantity $\frac{\Delta \bar{H}_1}{v_2^2}$ according to (2.74) should also be constant, but generally it increases with increasing v_2.

Deviations of $\Delta \bar{H}_1$ and $\Delta \bar{S}_1$ from theory are to some extent mutually compensating, so that the expression

for $\Delta\bar{G}_1$ often affords a considerably better working approximation than either (2.59) for $\Delta\bar{S}_1$ or (2.71) for $\Delta\bar{H}_1$. Only approximate values of χ_1 can be determined by the convenient swelling method described in section 2.6.4, owing to limitations of the theory and the calibration technique. However there is little doubt that various solvents can be classified in order of solvent power with respect to a given polymer by this means.

2.7 Glass Transition Relationships for Polymer-diluent Systems

At the glass temperature chain segments of polymer molecules begin to participate more, as units, in the general kinetic agitation. The coefficient of thermal expansion α also increases sharply at T_g. These two facts taken together suggest a close connection between the glass transition and the free volume of polymer. It is clear that any factor which controls the free volume of a polymer at constant temperature affects the value of T_g.

According to Meares,[59] the addition of even a small amount of liquid to a polymer has a large effect on the total free volume in the polymer phase and T_g is considerably reduced. Jenckel and Heusch[140] examined the

transition behaviour of polystyrene and polymethyl methacrylate mixed with varying proportions of a wide range of liquids. When the diluent itself formed a glass at a temperature T_{g_1}, the mixtures were studied over the whole range of composition from pure polymer to pure diluent. In such cases T_g of the mixture can be expressed as:

$$T_g = w_2 T_{g_2} + w_1 T_{g_1} + w_2 w_1 b(T_{g_2} - T_{g_1}) \qquad (2.77)$$

where w_1 and w_2 are the weight fractions of diluent and polymer respectively, T_{g_2} the glass temperature of pure polymer and b an empirical parameter for each system.

By postulating that the free volumes of the separated polymer and diluent are additive in the mixture, and that the free volume fraction has a critical value ϕ_g which is the same for the pure polymer, the diluent and their mixtures at their respective glass temperatures, Kelley and Bueche[139] derived a relation between T_g and composition. The latter is most conveniently expressed in terms of the volume fractions of polymer v_2 and diluent v_1.

The free volume fraction $\phi(T)$ in a polymer at a temperature T, above T_{g_2}, has been expressed in a linear form[59,141]:

$$\phi(T) = \phi_g + \Delta\alpha_2(T - T_{g_2}) \qquad (2.78)$$

where ϕ_g is the free volume fraction at the glass transition. $\Delta\alpha_2$ is the difference between the coefficients of thermal expansion above and below T_g. ϕ_g has been thought to have the universal value 0.025 for all polymers.[141] According to eq.(2.78) the free volume ϕ_2 associated with $v_2 cm^3$ of polymer at the glass temperature T_g of the mixture of polymer and diluent is[139]:

$$\phi_2 = v_2[\phi_g + \Delta\alpha_2(T_g - T_{g_2})] \qquad (2.79)$$

Similarly for $v_1 cm^3$ of the diluent the free volume ϕ_1 is:

$$\phi_1 = v_1[\phi_g + \alpha_1(T_g - T_{g_1})] \qquad (2.80)$$

since for a simple liquid the whole of the thermal expansion α_1 may to a first approximation be regarded as contributing extra free volume. Thus for 1 cm^3 of the mixture the free volume fraction at T_g i.e. ϕ_g is given by $(\phi_1 + \phi_2)$. Hence, by adding eqs.(2.79) and (2.80) and rearranging one obtains:

$$T_g = \frac{v_2 T_{g_2} \Delta\alpha_2 + v_1 T_{g_1} \alpha_1}{v_2 \Delta\alpha_2 + v_1 \alpha_1} \qquad (2.81)$$

By substituting suitable values of the quantities $\Delta\alpha_2, \alpha_1$

and T_{g_1}, Kelley and Bueche[139] showed that eq.(2.81) gave a good representation of the variation of T_g with composition of the systems polystyrene + diethyl benzene and polymethyl methacrylate + diethyl phthalate.

PART 3

EXPERIMENTAL

MATERIALS, APPARATUS AND EXPERIMENTAL TECHNIQUES

3.1 Polyvinyl Chloride sheets

Polyvinyl chloride sheets of known plasticiser content were supplied by the Plastics Division of I.C.I. Ltd. All sheets were prepared from the same polymer Corvic D65/6 which was obtained by suspension polymerisation using peroxides as free radical catalysts. The polymer, in the form of powder, was reported to have a purity of at least 99% after the polymerisation process. The powdered polymer was well mixed with appropriate amounts of stabilisers (cadmium stearate and stearic acid) and plasticiser (tricresyl phosphate), and the sheets were prepared in their final form by calendering at about 120°C.

Information supplied by I.C.I. concerning the formulation of the sheets and other details which were measured or calculated are:

Constituents	Parts by weight
Corvic D65/6 polymer	100
Cadmium stearate	2
Stearic acid	0.2
Tricresyl phosphate	variable as below

Permeation Membranes

Polyvinyl chloride sheet	Parts by weight of tricresyl phosphate	Volume fraction v_1 of tricresyl phosphate	Average thickness (cm x 10^2)
J1	0	0.0	3.3_6
J2	0	0.0	3.4_4
H	10	0.107	8.5_7
G	20	0.194	3.2
F	40	0.325	7.9_5
E	60	0.419	7.6

average density of unplasticised polyvinyl chloride membrane: 1.40 (g/cc)

average density of tricresyl phosphate plasticiser at 20°C: 1.16 (g/cc)

3.2 Gas Samples

Hydrogen, nitrogen, helium and neon were used for permeation, solubility and calibration work. Each gas was supplied in a litre glass cylinder with a break-seal from the British Oxygen Co. Ltd. Hydrogen and nitrogen were reported to be pure and helium and neon spectrally pure.

3.3 General description of apparatus

The apparatus for permeation and for direct solubility measurements, shown diagramatically in Fig.3-1, consists of three main sections, namely, the pumping system, the permeation system and the solubility system. Pyrex glass was used in its construction and all taps were lubricated with Apiezon N high vacuum grease.

3.3.1 The pumping system

The pumping system is shown in the left hand side of Fig.3-1. The apparatus was evacuated to better than 10^{-6} cm of Hg by means of a two-stage mercury diffusion pump backed with an Edward's Speedivac rotary oil pump. Wherever practicable, large bore tubing was used in this section in order to facilitate out-gassing of the permeation and solubility systems. In case of a power failure, oil sucked into the system from the rotary pump was contained

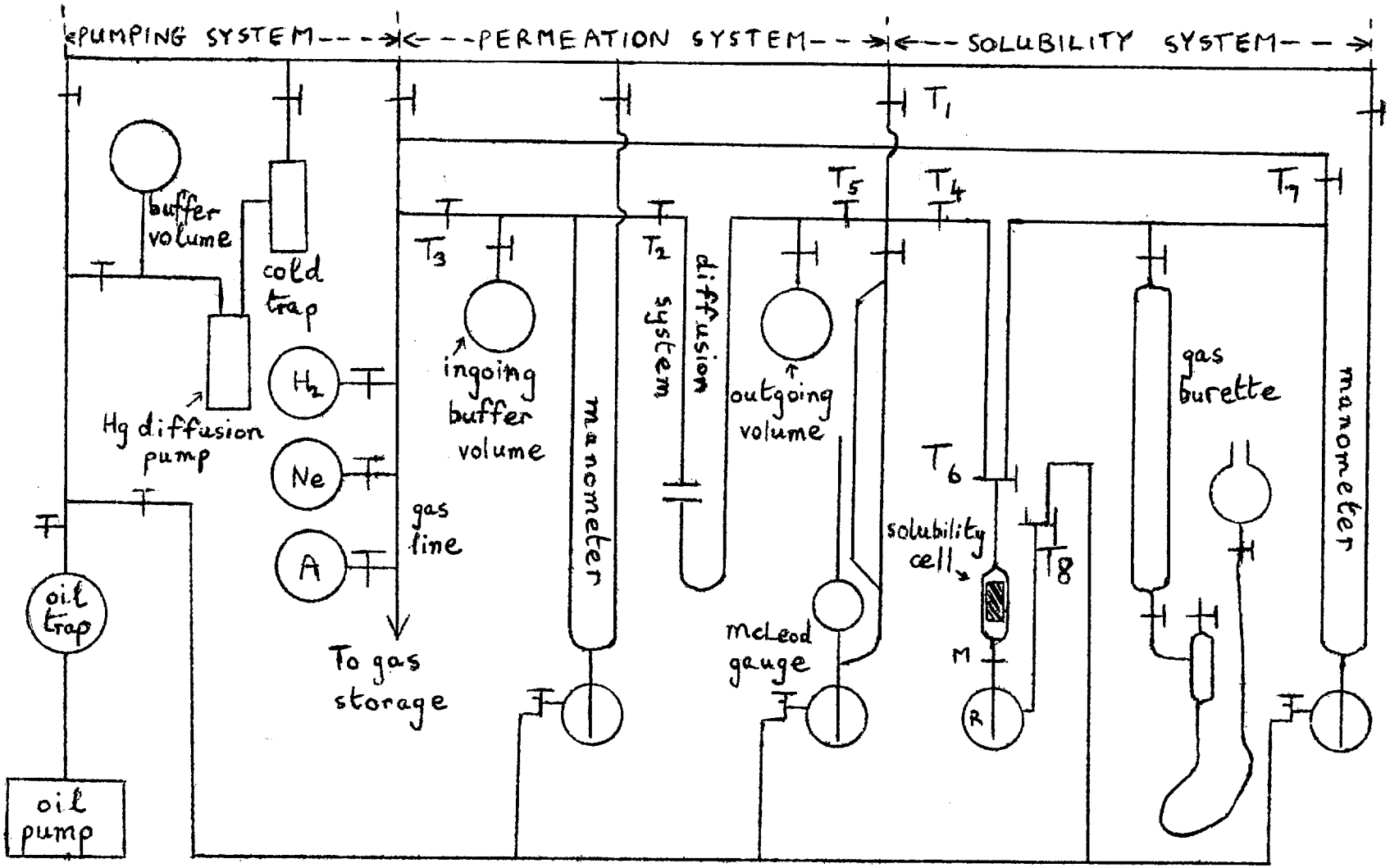


Fig. 3-1 The pumping, permeation and solubility systems

in the oil trap. The cold trap, partially immersed in liquid nitrogen, served to prevent any condensable vapours from contaminating the pumps; and also to prevent uncondensed mercury vapour from the mercury diffusion pump entering other parts of the system. A by-pass enabled air or other gases to be admitted to the main system without involving the mercury diffusion pump. The buffer volume between the oil pump and mercury diffusion pump enabled the latter to operate if the oil pump was otherwise engaged.

3.3.2 The permeation system

The permeation system, shown in the central part of Fig.3-1, consists of an ingoing buffer volume of 1-litre capacity, a manometer, a diffusion cell (containing the membrane) immersed in a thermostat, a McLeod gauge and a variable outgoing volume. The stainless steel diffusion cell (see Fig.3-2) is circular in cross section and contains the plane sheet membrane clamped in a holder shown in Fig.3-3. A similar arrangement was used by Barrer[1] and later by other workers in this field.

(a) The membrane holder

The membrane holder and the manner in which the membrane M was held is shown in Fig.3-3. The holder consists of two circular steel plates, P_1, P_2, which were

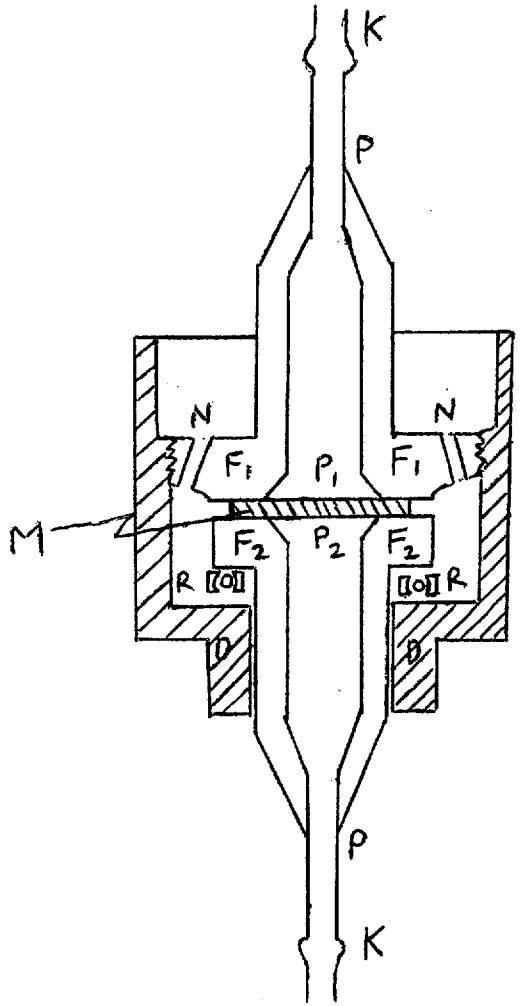


Fig. 3-2
Diffusion cell

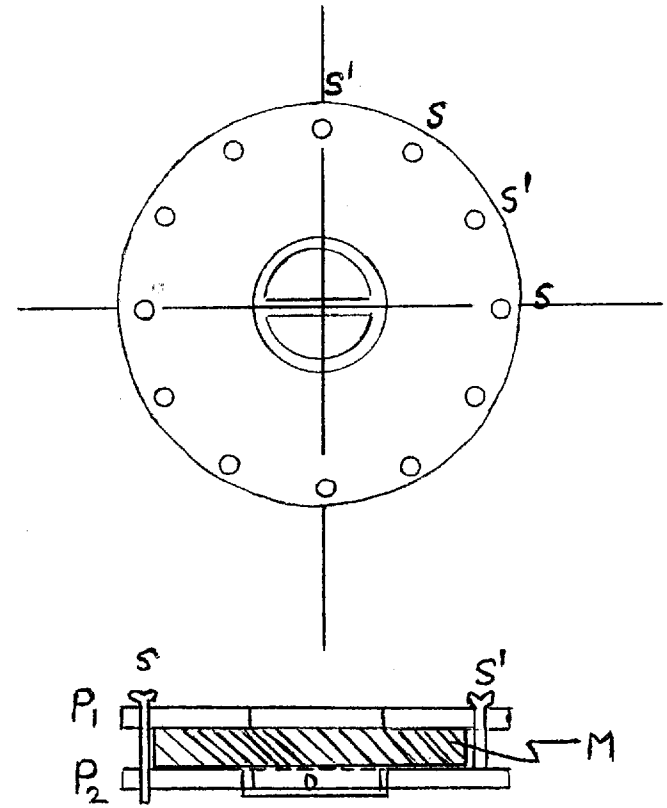


Fig. 3-3
Membrane holder

joined together by a series of screws S with the membrane clamped between them. The screws S were tightened as much as possible without causing the membrane to distort in the central hole. With the rigid membranes (generally, the lower plasticiser contents) it was not possible to clamp them directly between the plates as a good vacuum seal was not attainable. Natural rubber O-rings whose central hole was the same as that of plates P_1, P_2 were prepared, extracted with acetone for several hours and thoroughly out-gassed under high vacuum. The O-rings were then positioned on each side of the membrane and the central holes in both the O-rings and plates P_1, P_2 were made to coincide before clamping together the arrangement. With the membrane in position, the second series of screws S^1 was screwed through the top plate P_1 until they lightly touched the bottom plate P_2; thus ensuring that the distance of separation of the plates remained constant once the membrane had been clamped. To minimise distortion by the high ingoing pressure, the membrane was supported on the outgoing side by a copper gauze (lower side in Fig.3-3) held horizontally by a steel disc D. The area of the membrane into which the gas diffused was determined by measuring the diameter of the aperture of the plates P_1, P_2 or rubber O-rings by means of a travelling microscope.

(b) The diffusion cell

The cell consists of four parts, namely, the outer cup D, the flanged parts F_1 and F_2 between which the plates P_1, P_2 were held, and a set of steel ball bearings R fixed loosely on a steel ring (see Fig.3-2). Neoprene O-rings were extracted with acetone, out-gassed and mounted between the holder P_1, P_2 and flanges F_1, F_2 of the diffusion cell to ensure a mercury tight seal. With the holder P_1, P_2 and flanges F_1, F_2 aligned the cell was assembled by screwing the outer casing D until it was sufficiently tight. Mercury poured into the holes N in flange F_1 occupied the annular space below F_1 as well as the cup above the holes, thus creating a gas-tight seal. The entire cell was lowered into a cylindrical glass vessel and allowed to rest firmly on a support made from cork rings. The glass cylinder was immersed in a water thermostat and the connection to the permeation apparatus was made through Kovar-pyrex glass seals K, the Kovar alloy being silver soldered to the cell at P. To eliminate any small leakage of gas through the above seals, the adhesive 'Araldite' was applied at these positions. The space between the diffusion cell and the end of the glass cylinder was loosely packed with cotton wool to minimise convection currents.

3.3.3 The solubility system

Since the solubility of permanent and inert gases in rigid polymers is frequently small it is impracticable to measure volumetrically the gas sorbed by a small polymer sample. The basis of the experimental method was to establish equilibrium between the polymer sample at a known temperature and a gas phase of known pressure, to sweep away the gas phase by surrounding the sample with mercury and finally to desorb the gas from the sample into a known volume and determine its pressure and temperature.

The solubility system is similar to that used by Meares[9] and Stuart et al.[65] and is shown on the right hand side of Fig.3-1. The solubility cell is shown in detail in Fig.3-4., and is connected to the McLeod gauge, manometer and gas burette by a 2-way right angled tap, T_6. T_6 enables the polymer sample to be connected to either the McLeod gauge or the manometer but not both at the same time. The polymer sample consisted of one or two polymer sheets of approximate dimensions 2.5 cm by 6 cm. Its volume was accurately determined from its weight and density. The sheets were suspended on a glass rod framework and tightly positioned between glass hooks to prevent movement. The framework was placed inside the cell which was then immersed in the thermostat as far as the cone

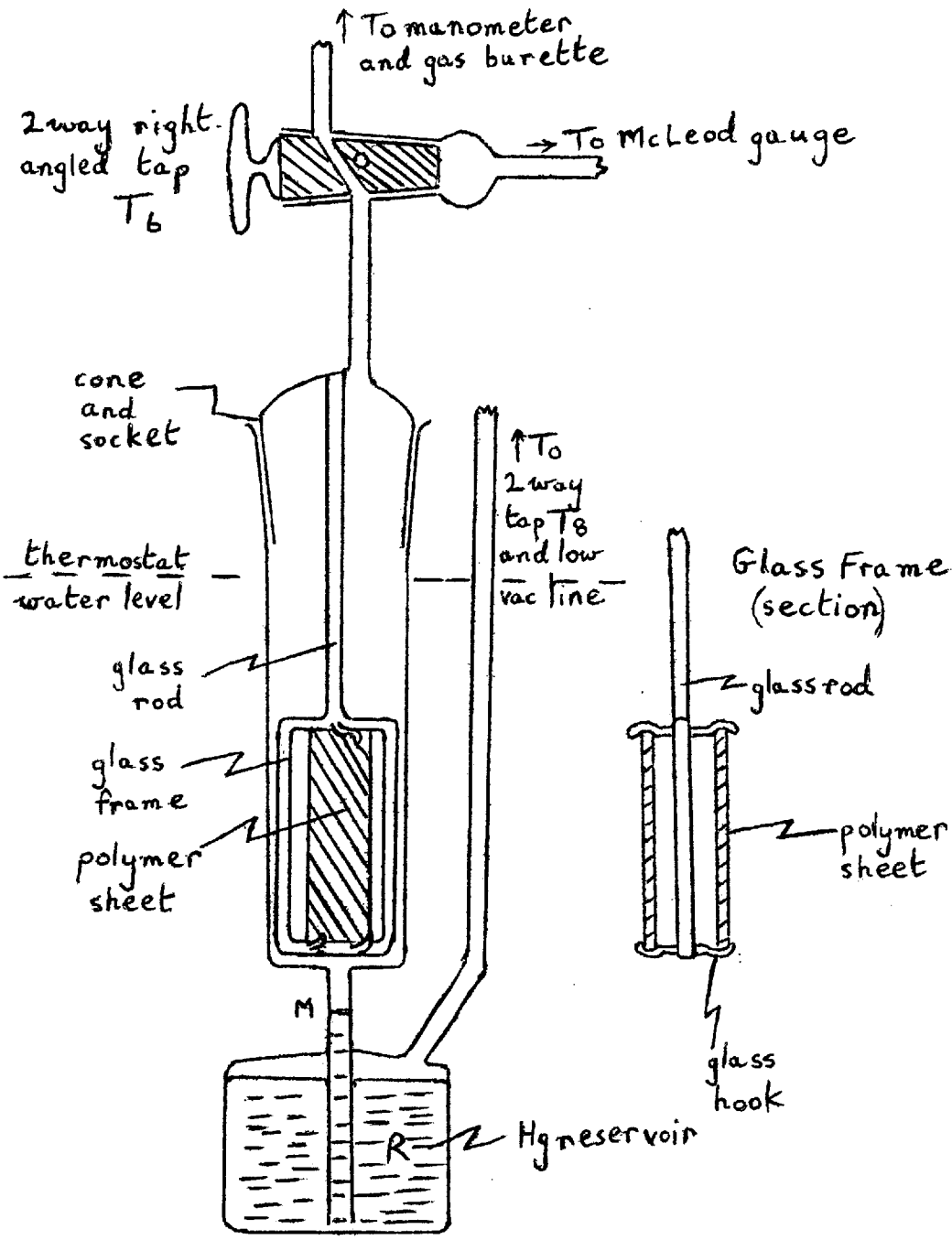


Fig. 3-4 The solubility cell for plane sheet

and socket joint. The mercury reservoir R (Fig.3-4) enables the polymer sample to be immersed in mercury at will.

3.3.4 The McLeod gauge

The McLeod gauge used in measuring the outgoing pressure of the diffusion system and the desorption pressure of the solubility system has a pressure range of 10^{-6} cm Hg to about 2×10^{-1} cm Hg. In the actual experiments the upper limit of pressure was normally not greater than 10^{-2} cm.Hg. The capillary stems of the gauge were made from Veridia tubings of 2 mm. diameter. The closed stem was so constructed that the end was at right angles to the length of the bore.

The determination of the cross sectional area, a, of the bore throughout the length of the closed stem was achieved by measurement with a cathetometer of lengths of known weights of mercury. A reference mark corresponding to the top of the closed stem was etched on the other capillary. The outgoing pressure was measured by raising the mercury meniscus to the fixed reference mark and measuring the difference in mercury heights in the two capillary stems i.e. the length of the enclosed gas column l. Since the bore of the closed stem was sufficiently uniform, it is then possible to apply a square root relationship

such that the outgoing pressure p_1 is given by:

$$p_1 = \frac{a}{V} \ell^2$$

where V is the total volume of the gauge and equal to 266.5 cm^3. The ratio $\frac{a}{V}$ was found to be equal to 1.184×10^{-4} cm^{-1}.

3.3.5 Thermostat

The water thermostat was employed for work requiring controlled temperatures between 0°C and 85°C. The bath consisted of a large cylindrical Dewar vessel ($7\frac{3}{4}$ inch diameter and $14\frac{1}{2}$ inch height) with unsilvered strips on opposite sides to facilitate observation of objects in the bath. Temperature control was maintained by means of a 100 W heater operated by a 'Sunvic' relay, keeping bath temperatures to $\pm$ 0.05°C. Efficient stirring was always maintained to ensure an even temperature throughout the bath.

Between 0°C and room temperature cold water was circulated through a copper coil immersed in the bath contents and temperature control was maintained as before. For a temperature of 0°C the Dewar was partially filled with small pieces of ice. The stirrer was enclosed in a metal gauze which ensured a continuous circulation of the water present. The water was maintained at constant temperature by the ice and no other form of temperature control was necessary.

3.4 Calibration of Apparatus

3.4.1 The permeation system: determination of V_o

The outgoing volume, V_o, on the low pressure side of the apparatus is defined in Fig.3-1 by the volume enclosed between the tap T_1 and the diffusion cell with tap T_4 closed. V_o was capable of variation from 0.5 to 1.5 litres as determined by the flow rate. V_o was calibrated by pressure drop on expansion measurements against the standard volume of the McLeod gauge using nitrogen gas. Permeation through the membrane in the short period between successive pressure readings was considered negligible. The error caused by the thermostat temperature varying the 'effective volume' of the outgoing system was also not significant.

3.4.2 The solubility system: determination of V_d

It is necessary to determine the volume, V_d, of the desorption system as defined in Fig.3-1 by the volume enclosed between tap T_1 and the etched mark M of the solubility cell (see Fig.3-4) with tap T_5 closed. Tap T_6 was turned to connect the McLeod gauge and the solubility cell and before calibration mercury from R was raised to the reference mark M. The volume V_d was determined in a similar manner to that of V_o from the standard volume of the McLeod gauge by expansion measurements using helium

gas. As the pressure of the helium did not exceed 10^{-2} cm Hg, a negligible amount of gas was sorbed by the polymer in the short time it was exposed between two successive pressure readings.

3.5 Experimental Techniques

3.5.1 Permeation experiment

Before each permeation run the membrane was maintained at the experimental temperature for not less than 12 hours. Normally out-gassing was carried out at this temperature although effected more easily at a higher temperature. The membranes were also not subjected to a rate of temperature change of greater than 1.0^{o}C/hour. Complete out-gassing of the membranes with the lower plasticiser contents was of the order of weeks, so that the out-gassing rate sometimes became significant when measuring a low gas permeation rate. The outgassing rate was normally measured on the outgoing side by the McLeod gauge (with T_1 and T_4 closed) before commencing an experiment. This pressure rise with time did not exceed one tenth of the steady-state rate of increase of outgoing pressure $\frac{dp_1}{dt}$ of permeating gas during an experiment, but warranted a correction being applied for it.

With T_2 closed (see Fig.3-1) a charge of gas was

introduced via T_3 into the ingoing side of the permeation system. The 1 litre buffer volume served to avoid fluctuations in the ingoing pressure p_2. T_1 was then closed and almost immediatly afterwards the permeation experiment was started by opening T_2, using a stop watch to record the time. Outgoing pressure p_1 measurements were made at suitable time intervals using the McLeod gauge. The average values of the ingoing pressure p_2 and the room temperature T_R in ^oC were determined over a regular time interval during the permeation experiment. A plot of outgoing pressure p_1 vs time t gave, as explained in sections 2.1.2(a) and (b), the time lag L and the steady-state rate of increase of outgoing pressure $\frac{dp_1}{dt}$. L and $\frac{dp_1}{dt}$ can be obtained by application of the method of least squares to the p_1 vs. t data. It was then possible to determine the permeability coefficient $\bar{P}$, the transient-state diffusion coefficient D_L and the dynamic solubility coefficient σ_D from one and the same experiment using equations (2.7a), (2.10) and (2.9) respectively.

The transient state data of outgoing pressure p_1 vs. time t could be treated by the early approximation method provided that sufficient data was obtained in this region of diffusion. As explained in section 2.1.2(b), following eq.(2.13) a plot of log $(t^{\frac{1}{2}} \frac{dp_1}{dt})$ against $\frac{1}{t}$ gave

a straight line from whose slope and intercept, as given by eq.(2.14) and (2.15) respectively, D_E and σ_E were deduced. Values of $\frac{dp_1}{dt}$ were obtained from tangents drawn to the p_1 vs. t curve at appropriately small t values.

3.5.2 Equilibrium solubility measurement

After the whole apparatus had been thoroughly outgassed by prolonged pumping, T_6 was connected to the appropriate gas supply (see Fig.3-1) and equilibrium established between the polymer and gas at a pressure p_s, measured by observing the manometer with T_7 closed. By operating T_8 mercury in R was raised until its height above the sample was greater than the equilibrating pressure p_s to prevent loss of sorbed gas under vacuo (applied later). With T_8 and T_5 closed, T_6 was turned to connect the cell with the McLeod gauge and the pumps through T_1 and the excess gas was pumped away. At high equilibrating pressures tiny gas bubbles were sometimes trapped between the mercury and the walls of the glass cell and possibly also between the mercury and polymer although these were not visible. To remove this trapped gas before commencing desorption the following procedure was adopted. By operating tap T_8 as rapidly as possible, the mercury was lowered below the mark M and raised again until it was at its former height above the sample.

A stop watch was started when the mercury was half way down the polymer sample and stopped when it was half way up again. This gave the mean time for which the specimen was uncovered during this re-sweeping procedure and the time varied between 4 and 5 seconds.

The apparatus was then set for desorption by closing T_1 and the mercury was lowered through the cell to the mark M. The dissolved gas was allowed to desorb from the polymer into the McLeod gauge. The rate of desorption with time was recorded together with the room temperature $T_R(^oC)$ until the final pressure p_d was attained. The amount of gas remaining in the polymer was negligible.

The volume (NTP) V_s of gas desorbed at thermostat temperature is given by

$$V_s = \frac{273.16\ p_d V_d}{76(273.16 + T_R)}$$

This can be corrected for the amount of gas lost from the specimen during the re-sweeping procedure by appropriate solution of the diffusion equation given by Jost[144] and applied to this situation by Meares.[9] Treating the polymer sample approximately as an infinite slab and, if δ_q is the difference between unity and the ratio of the amount desorbed at time t, Q_t, to that at infinite

time , Q_o , then[144]:

$$(1 - \frac{Q_t}{Q_o}) = \delta q = \frac{8}{\pi^2} \sum_{n=0}^{\infty} \frac{1}{(2n+1)^2} \exp[- \left\{\frac{(2n+1)\pi}{\ell}\right\}^2 Dt]$$

where ℓ is the thickness of the sample. For short times ~~the above~~ an alternative equation reduces to[144]:

$$\frac{Q_t}{Q_o} = (1 - \delta q) = \frac{4}{\ell}(\frac{Dt}{\pi})^{\frac{1}{2}}$$

Using an appropriate value of the transient state diffusion coefficient D_L, it is therefore possible to estimate the loss of sorbed gas during the re-sweeping period t.

The static solubility coefficient σ_s is given by $\sigma_s = \frac{V_s}{p_s V}$ where V is the volume of the sample. At a given thermostat temperature a series of V_s and p_s measurements was obtained and from the isotherm of $\frac{V_s}{V}$ vs. p_s the average static solubility coefficient σ_s was deduced from the slope. This procedure was repeated to obtain σ_s at various temperatures of the polymer.

3.6 Accuracy of Measurements

In order to compute the permeability, diffusion and solubility coefficients, it is necessary to measure the following basic variables with the accuracy stated. Absolute accuracy is, however, difficult to determine.

(1) Dimensions of the polymer sheet.

The thickness was measured with a micro-meter screw gauge reading to 0.001 cm. The mean value used in the calculation was for at least 20 measurements and was found to have a maximum spread of $\pm$ 2%. The area of the permeation membrane was assumed to be the same as that of the opening of the membrane holder. A cathetometer was used to measure the diameter of the opening. The error in the area of the membrane was estimated to be about 1%.

(2) McLeod gauge.

The spread of points giving the pressure p_1 in the plots of pressure vs. time was reasonably good.

(3) Volumes V_o and V_d

These were determined from the known cut-off volume of the McLeod gauge by expansion measurements. The reproducibility was about $\pm$ 1%. Variation of the 'effective volume' with the thermostat temperature was too small to be significant.

(4) Pressures p_2 and p_s

These were recorded to 0.02 cm by reading on a glass scale the height of the mercury meniscus in a wide bore manometer. The maximum variation of the pressure was less than 1% and average values were used.

(5) Room temperature T_R.

The average value over the time of the experiment was used and the temperature did not fluctuate by more than 2%.

(6) Thermostat temperature.

The required temperature was maintained within $\pm$ 0.05°C during an experiment.

The correction for the sorbed gas lost from the polymer during the re-sweeping procedure (solubility apparatus) was probably accurate to about $\pm$ 10%, and the uncertainty created in the final solubility was about $\pm$ 2%. No account has been taken of the coefficient of thermal expansion of the polymer. It may be stated, in conclusion, that the accuracy of the reported data is of the order of $\pm$ 5%.

PART 4

RESULTS AND DISCUSSION

4.1 Permeability, Diffusion and Solubility Coefficients

The experimental data for permeation, diffusion and solution are tabulated and presented in this section (4.1). The section is further subdivided into four, the first two being concerned with data from permeation experiments and the remaining two with the static solubility data. An explanation of the symbols used is as follows:

T = temperature (^{o}C) of permeation experiment.

p_2 = ingoing pressure (cm Hg).

L = time lag (minutes).

D_L = transient-state diffusion coefficient ($cm^2 sec^{-1}$) deduced by the time lag method.

D_E = transient-state diffusion coefficient ($cm^2 sec^{-1}$) deduced by the early approximation method.

D_S = steady-state diffusion coefficient ($cm^2 sec^{-1}$).

$\overline{P}$ = permeability coefficient in cc NTP/sec/cm^2 area/cm thickness/cm Hg.

σ_D = dynamic solubility coefficient (cm^3 NTP/cm^3 of polymer/cm Hg gas pressure).

$$(\sigma_D = \frac{\overline{P}}{D_L})$$

σ_E = dynamic solubility coefficient deduced by the early approximation method (in same units as σ_D)

σ_s = static solubility coefficient (in same units as σ_D and σ_E).

T_s = temperature (^oC) of static solubility experiment.

p_s = equilibrium pressure (cm Hg) of gas in static experiments.

$\frac{V_s}{V}$ = volume (NTP) of gas desorbed per unit volume of polymer after application of equilibrium pressure p_s

Polyvinyl chloride sheet	J	H	G	F	E
Volume fraction plasticiser V_1	0.0	0.107	0.194	0.325	0.419

4.1.1 Hydrogen data from permeation experiments

TABLE 4-1 Sheet J1

Run No.	T	p_2	L	$\bar{P}x10^{10}$	$D_L x10^7$	$D_E x10^7$	$\sigma_D x10^3$	$\sigma_E x10^3$
1	0.0	34.51	53.4	0.710	0.587		1.21	
2	14.0	28.95	46.9	1.27	0.669	0.681	1.89	1.58
3	24.0	24.34	42.3	1.83	0.741		2.47	
4	34.0	18.69	38.9	2.57	0.806		3.19	
5	34.0	18.26	36.0	2.53	0.871	0.905	2.90	2.30
6	44.0	15.51	27.5	3.41	1.14		2.99	
7	54.0	14.01	17.4	4.13	1.80	1.60	2.29	2.35
8	64.0	12.64	14.5	5.38	2.16	2.08	2.49	2.37
9	74.0	11.52	10.5	7.20	2.99	2.76	2.41	2.33
10	84.2	10.51	7.4	9.83	4.24		2.32	
11	54.0	13.53	17.0	3.85	1.85		2.09	
12	44.1	16.82	20.6	2.74	1.52		1.80	
13	34.1	25.06	23.3	2.06	1.35	1.23	1.53	1.49
14	24.1	30.62	26.3	1.40	1.19	1.12	1.17	1.13
15	54.0	16.57	17.9	3.79	1.75	1.65	2.17	2.08
16	64.0	14.51	15.5	5.01	2.02	1.91	2.48	2.48
17	69.0	13.26	14.4	5.79	2.18		2.66	
18	74.2	12.07	11.5	6.61	2.73		2.43	
19	78.8	10.98	9.5	7.60	3.30		2.30	
20	84.0	11.27	7.4	9.32	4.24		2.20	

N.B. Runs 1-10 are for increasing temperature from 0°C.

The sheet was annealed at 87°C and runs 11-20 were performed.

TABLE 4-2 Sheet H

T	p_2	L	$\bar{P}x10^{10}$	$D_L x10^7$	$D_E x10^7$	$\sigma_D x10^3$	$\sigma_E x10^3$
23.0	32.80	86.7	1.96	2.35	2.07	0.834	0.899
28.0	29.67	80.5	2.35	2.53		0.927	
32.0	26.85	76.1	2.69	2.68	2.38	1.00	1.04
37.0	21.82	73.9	3.17	2.76		1.15	
37.0	24.20	72.5	3.30	2.82	2.56	1.17	1.12
42.0	19.56	68.8	3.73	2.97	2.74	1.26	1.27
47.0	16.33	64.1	4.35	3.18	3.14	1.37	1.25
53.0	14.76	58.5	5.63	3.49	3.76	1.61	1.32
58.0	13.31	46.4	6.62	4.40		1.51	
63.0	12.07	36.9	7.84	5.53	5.05	1.42	1.37
68.0	10.92	29.6	9.30	6.89	6.12	1.35	1.36
72.0	10.43	25.4	9.78	8.03	7.07	1.22	1.36

TABLE 4-3 Sheet F1

T	p_2	L	$\bar{P}x10^{10}$	$D_L x10^6$	$\sigma_D x10^4$
20.0	16.07	21.6	3.76	0.803	4.68
24.0	4.16	19	4.66	0.912	5.10
24.0	16.60	19.5	4.51	0.889	5.16
24.0	17.02	19.8	4.52	0.876	5.16
28.0	16.43	17.5	5.72	0.991	5.77
32.0	13.70	15.8	6.62	1.10	6.04
37.0	11.37	11.9	8.04	1.46	5.52
41.0	14.84	9.7	9.37	1.79	5.24
45.0	11.23	8.2	10.3	2.11	4.89
49.0	10.60	6.8	11.9	2.55	4.65
53.0	10.90	5.5	13.5	3.15	4.28

TABLE 4-4 Sheet E

T	p_2	L	$\bar{P}x10^{10}$	$D_L x10^6$	$D_E x10^6$	$\sigma_D x10^4$	$\sigma_E x10^4$
0.0	32.90	40.7	1.79	0.394	0.330	4.55	4.96
6.1	31.78	29.4	2.94	0.546		5.40	
7.5	26.46	27.4	3.42	0.586	0.554	5.83	5.12
11.0	24.21	21.5	4.28	0.746	0.667	5.74	5.92
12.0	23.80	19.5	4.11	0.823	0.717	5.00	5.20
14.0	20.49	15.3	4.96	1.05	0.858	4.73	5.44
17.0	18.67	11.6	5.72	1.38	1.00	4.13	5.69
20.0	15.24	9.5	6.36	1.69		3.77	
20.0*	18.66	9.8	6.01	1.65		3.66	
23.0	16.92	7.5	7.07	2.14		3.30	
26.0	15.38	5.9	7.98	2.72		2.93	

4.1.2 Neon data from permeation experiments

TABLE 4-5 Sheet J1

Run No.	T	p_2	L	$\bar{P}x10^{11}$	$D_L x10^8$	$\sigma_D x10^4$
1	34.0	34.87	49.0	3.87	6.40	6.05
2	41.0	31.45	45.8	5.27	6.85	7.69
3	47.9	33.91	42.0	7.00	7.47	9.38
4	54.0	30.43	38.8	8.78	8.08	10.9
5	62.2	27.47	25.4	10.8	12.4	8.73
6	67.0	27.97	19.7	12.0	15.9	7.54
7	71.9	26.49	17.7	12.2	17.7	6.91
8	75.9	27.88	16.8	13.4	18.7	7.18
9	79.7	25.24	16.1	16.0	19.5	8.22
10	83.9	22.93	15.2	19.1	20.6	9.25
11	66.8	29.54	19.7	10.5	15.9	6.62
12	60.0	26.68	25.9	8.91	12.1	7.36
13	54.0	31.04	35.5	7.46	8.83	8.44
14	48.0	28.09	37.2	6.24	8.43	7.40
15	41.0	29.94	39.0	4.92	8.04	6.12
16	34.0	34.79	40.9	3.86	7.67	5.03
17	34.1	31.46	40.9	3.79	7.67	4.95
18	51.0	28.27	36.6	6.70	8.57	7.82
19	63.0	25.76	23.2	9.71	13.5	7.18
20	72.0	25.68	17.7	12.3	17.7	6.92
21	80.0	23.26	16.0	16.3	19.6	8.31

N.B. Runs 1-10 are for increasing temperature from 34°C. The sheet was annealed at 85°C and runs 11-21 were performed.

TABLE 4-6 Sheet J2

Run No.	T	p_2	L	$\bar{P}x10^{11}$	$D_L x10^8$	$\sigma_D x10^4$
1	34.1	34.88	42.3	3.90	7.77	5.02
2	43.0	31.53	40.0	5.40	8.22	6.57
3	52.2	28.50	37.9	7.19	8.67	8.29
4	57.0	25.77	31.8	8.62	10.3	8.34
5	62.1	27.85	25.0	9.81	13.2	7.46
6	67.0	25.30	20.3	11.2	16.2	6.90
7	72.2	28.16	18.6	13.0	17.7	7.37
8	77.1	25.48	17.2	15.5	19.1	8.09
9	82.0	23.17	16.3	19.2	20.2	9.52

N.B. Temperature increased from 34.1°C after annealing at 86°C.

TABLE 4-7 Sheet G

T	p_2	L	$\bar{P}x10^{11}$	$D_L x10^7$	$D_E x10^7$	$\sigma_D x10^4$	$\sigma_E x10^4$
18.0	31.09	14.2	3.46	2.00		1.73	
18.1	25.30	15.0	3.24	1.90	1.94	1.71	1.64
22.1	28.11	12.9	4.12	2.21	2.12	1.87	1.90
27.0	25.59	11.0	5.26	2.59	2.49	2.03	2.05
32.0	23.16	9.3	6.92	3.06	3.06	2.26	2.16
37.1	21.04	7.8	9.01	3.65	3.68	2.47	2.42
42.0	19.16	5.7	11.7	4.99	4.67	2.35	2.29
46.1	16.75	4.3	14.4	6.62	6.22	2.18	2.14
49.8	15.87	3.2	18.0	8.89		2.03	

TABLE 4-8 Sheet F1

T	p_2	L	$\bar{F}x10^{10}$	$D_L x10^7$	$D_E x10^7$	$\sigma_D x10^4$	$\sigma_E x10^4$
14.0	31.82	48.9	0.650	3.64	4.00	1.78	1.58
16.2	25.55	46.4	0.753	3.84	4.21	1.96	1.72
19.1	26.44	41.2	0.953	4.33	4.23	2.20	2.19
24.0	21.24	34.3	1.36	5.20	4.89	2.61	2.85
28.0	23.98	28.3	1.72	6.30	6.59	2.73	2.41
32.1	21.65	20.8	2.06	8.57	8.51	2.40	2.36
36.1	19.53	16.0	2.28	11.1	11.0	2.05	2.03
40.0	17.74	11.9	2.77	15.0		1.85	
44.1	16.10	8.7	3.34	20.5		1.63	

TABLE 4-9 Sheet E

T	p_2	L	$\bar{F}x10^{10}$	$D_L x10^7$	$\sigma_D x10^4$
0.0	30.32	48	0.483	3.34	1.45
6.0	33.63	41.2	0.743	3.93	1.89
8.0	27.33	36.9	0.901	4.35	2.07
10.6	24.74	27.4	1.06	5.86	1.82
14.1	23.19	19.4	1.38	8.27	1.67
17.0	25.64	14.4	1.53	11.1	1.37
21.1	20.85	9.4	2.13	17.1	1.25
24.9	18.96	6.3	2.52	25.5	0.990

4.1.3 Hydrogen data from static solubility experiments

TABLE 4-10 Sheet J3

T_s = 26.0°C	p_s	2.53	4.01	5.14	7.46
	$V_s/VX10^3$	1.18	1.80	2.39	3.38
T_s = 36.1°C	p_s	2.47	3.71	5.56	8.31
	$V_s/VX10^3$	1.11	1.61	2.47	3.62
T_s = 46.0°C	p_s	3.39	5.43	7.01	10.57
	$V_s/VX10^3$	1.37	2.16	2.86	4.21
T_s = 56.0°C	p_s	3.25	4.78	6.53	8.36
	$V_s/VX10^3$	1.24	1.81	2.49	3.17
T_s = 66.0°C	p_s	2.97	3.88	5.66	7.94
	$V_s/VX10^3$	1.09	1.42	2.10	2.88

TABLE 4-10A Sheet J3

T_s(°C)	26.0	36.1	46.0	56.0	66.0
$\sigma_s x10^4$	4.60	4.42	4.04	3.84	3.70
$D_s x10^7$	3.30	4.99	7.30	10.4	14.3
$\sigma_D x10^3$(J1)	1.29	1.56	1.86	2.19	2.55
$D_L x10^7$(J1)	1.19	1.39	1.60	1.83	2.08

TABLE 4-11 Sheet F2

T_s = 10.1°C	p_s	1.89	2.90	4.35
	$V_s/VX10^4$	5.24	7.96	12.3
T_s = 17.9°C	p_s	2.50	3.94	4.94
	$V_s/VX10^4$	7.45	11.9	14.8
T_s = 23.9°C	p_s	2.85	4.28	5.26
	$V_s/VX10^4$	9.16	13.5	16.9
T_s = 29.0°C	p_s	1.74	2.61	3.93
	$V_s/VX10^4$	5.75	8.67	12.9
T_s = 33.9°C	p_s	1.77	3.44	4.67
	$V_s/VX10^4$	6.05	11.8	15.7
T_s = 39.1°C	p_s	1.50	2.16	3.13
	$V_s/VX10^4$	5.19	7.65	10.8

TABLE 4-11A Sheet F2

T_s(°C)	10.1	17.9	23.9	29.0	33.9	39.1
σ_s x10^4	2.77	3.02	3.18	3.29	3.38	3.50
D_Sx10^6	0.769	1.11	1.46	1.83	2.14	2.48
σ_Dx10^4(F1)	3.52	4.41	5.20	5.94	5.83	5.37
D_Lx10^6(F1)	0.614	0.762	0.893	1.02	1.25	1.62

4.1.4 Neon data from static solubility experiments

TABLE 4-12 Sheet J3

T_s = 26.1°C	p_s	3.00	4.56	5.42	6.58
	$V_s/VX10^4$	6.65	10.1	12.2	14.8
T_s = 36.1°C	p_s	2.96	4.42	4.98	5.99
	$V_s/VX10^4$	6.30	9.45	10.7	12.8
T_s = 46.0°C	p_s	3.31	4.04	4.81	5.74
	$V_s/VX10^4$	6.55	8.06	9.55	11.7
T_s = 56.0°C	p_s	2.86	3.71	5.46	
	$V_s/VX10^4$	5.26	6.74	10.3	
T_s = 66.1°C	p_s	3.03	3.47	5.19	
	$V_s/VX10^4$	5.39	6.43	9.25	

TABLE 4-12A Sheet J3

T_s(°C)	26.1	36.1	46.0	56.0	66.1
$\sigma_s \times 10^4$	2.23	2.13	2.02	1.87	1.82
$D_s \times 10^7$	1.29	1.95	2.90	4.20	5.81
$\sigma_D x10^4$(J1,J2)	4.00	5.33	7.05	8.28	6.84
$D_L x10^7$(J1,J2)	0.733	0.783	0.836	0.980	1.55

TABLE 4-13 Sheet F2

T_s = 10.0°C	p_s	1.99	3.26	4.96
	$V_s/VX10^4$	2.29	3.76	5.91
T_s = 18.0°C	p_s	2.31	3.19	4.86
	$V_s/VX10^4$	3.22	4.65	6.84
T_s = 23.8°C	p_s	2.14	3.43	4.65
	$V_s/VX10^4$	3.39	5.31	7.13
T_s = 28.7°C	p_s	2.05	3.48	5.22
	$V_s/VX10^4$	3.41	5.76	8.57
T_s = 33.9°C	p_s	1.94	3.21	4.79
	$V_s/VX10^4$	3.45	5.82	8.45
T_s = 40.0°C	p_s	2.15	3.08	4.37
	$V_s/VX10^4$	4.18	5.79	8.38

TABLE 4-13A Sheet F2

T_s(°C)	10.0	18.0	23.8	28.7	33.9	40.0
$\sigma_s \times 10^4$	1.18	1.43	1.55	1.66	1.79	1.91
$D_s \times 10^7$	3.96	6.22	8.71	10.7	12.5	14.8
$\sigma_D x10^4$(F1)	1.54	2.10	2.61	2.64	2.21	1.83
$D_L x10^7$(F1)	3.11	4.21	5.18	6.67	9.95	15.4

4.2 Kinetic Phenomena

4.2.1 Permeability and diffusion coefficients

The permeability coefficients $\bar{P}$ and the transient-state diffusion coefficients D_L and D_E for the unplasticised and plasticised membranes have been measured at an appropriate number of temperatures within the range $0^{\circ}C$ to $84.2^{\circ}C$. The permeation data for hydrogen are presented in section 4.1.1 (Tables 4-1 to 4-4) and that for neon presented in section 4.1.2 (Tables 4-5 to 4-9). When sufficient data of the outgoing pressure p_1 were obtained during the transient state of the diffusion process, analysis by the early approximation method became more appropriate. Therefore the transient-state diffusion coefficients D_E determined by the early approximation method are given in Tables 4-1, 4-2 and 4-4 for hydrogen and Tables 4-7 and 4-8 for neon.

Typical plots from which D_E was deduced are shown in Figs.4-1 to 4-3. As explained previously, data of $\frac{dp_1}{dt}$ were obtained by drawing tangents at various times, t, to the curve of outgoing pressure p_1 vs. time. Despite the obvious errors introduced by such a technique, the agreement between D_E and D_L was reasonable in the cases considered. The D_E determination was facilitated by high flow rates, which lend themselves to accurate measurement,

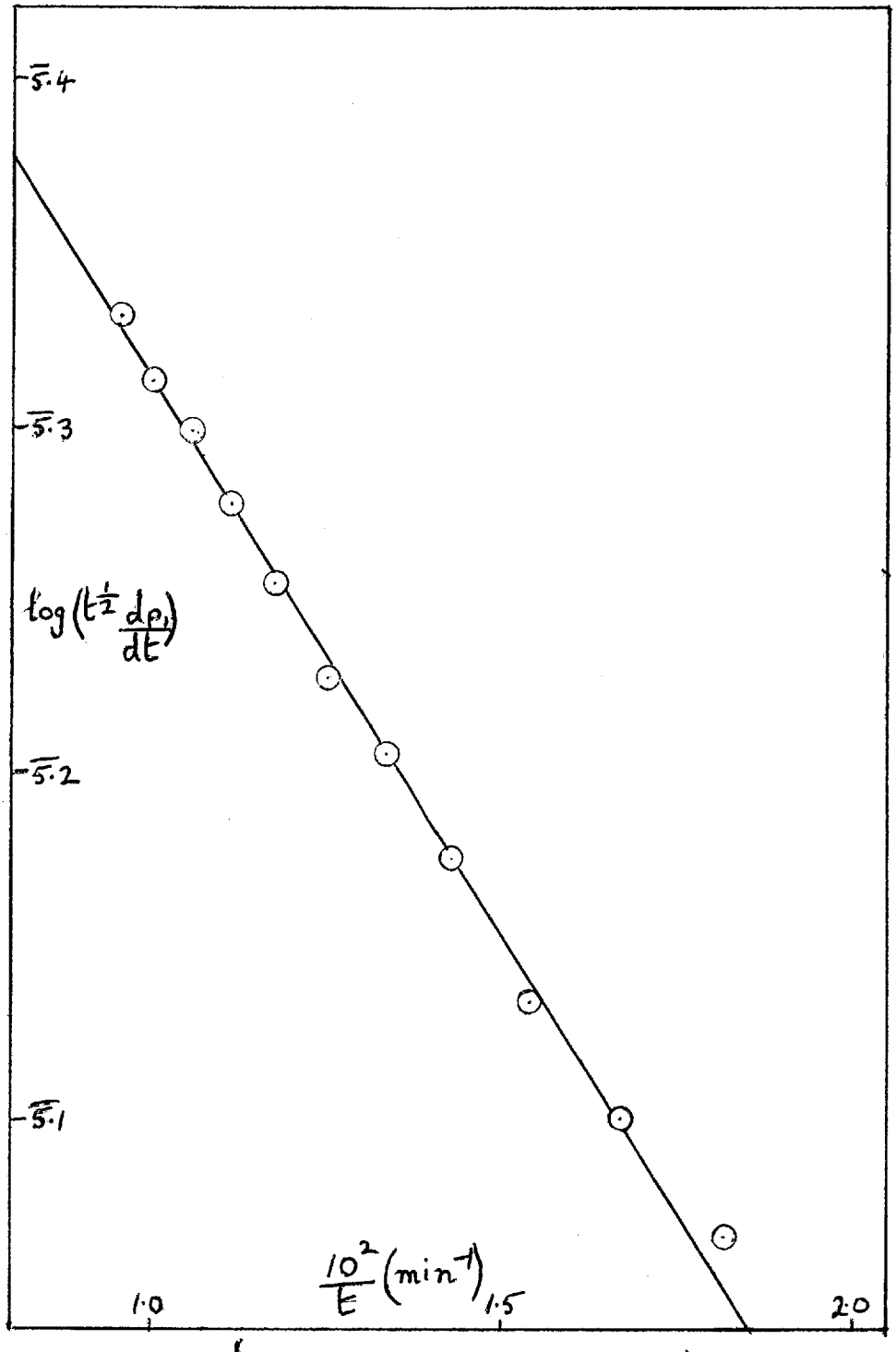


Fig 4-1 'Early Approximation' analysis for E: H_2 at 0.0°C

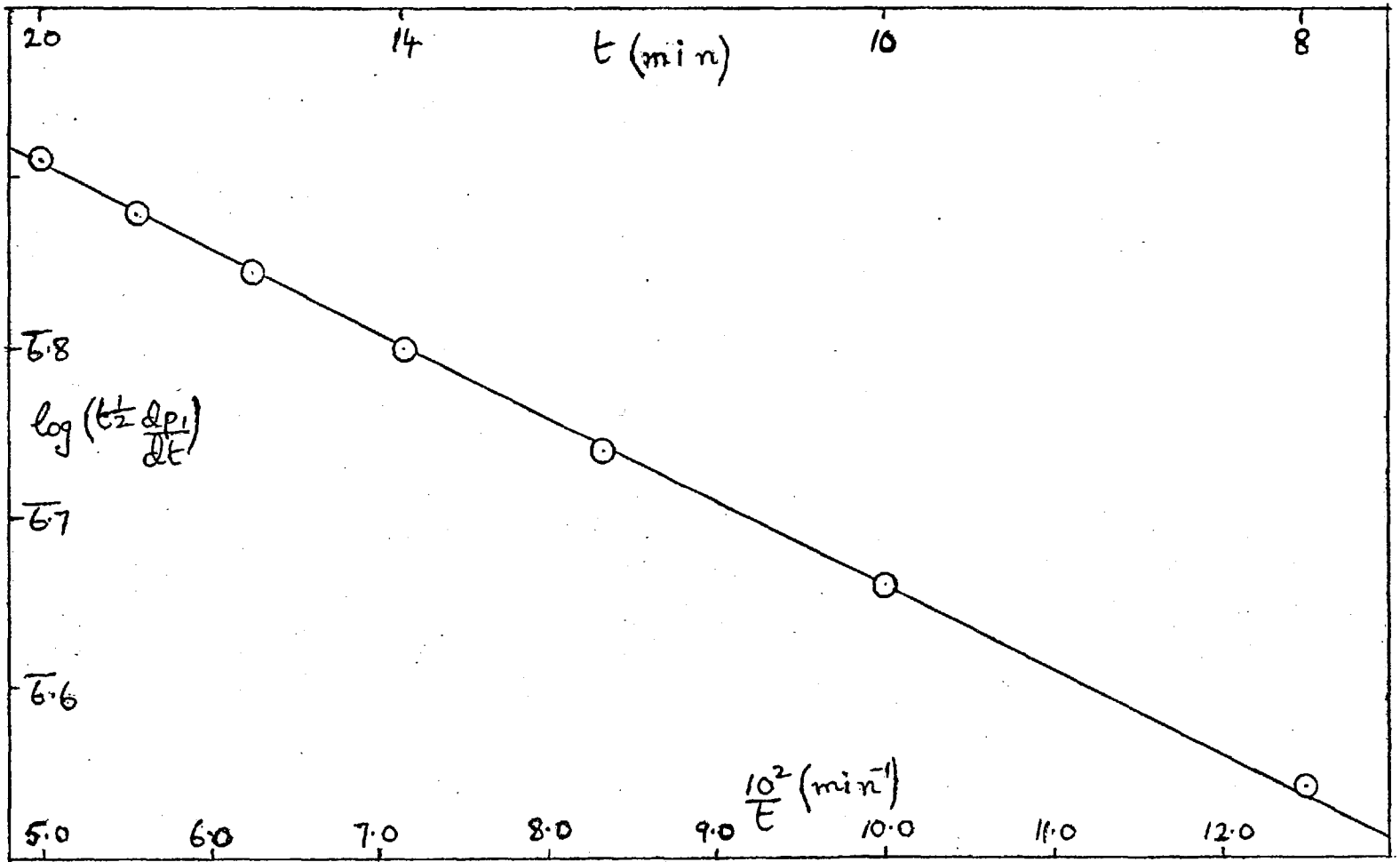


Fig. 4-2 : 'Early approximation' analysis for G : Ne at 37·1°C

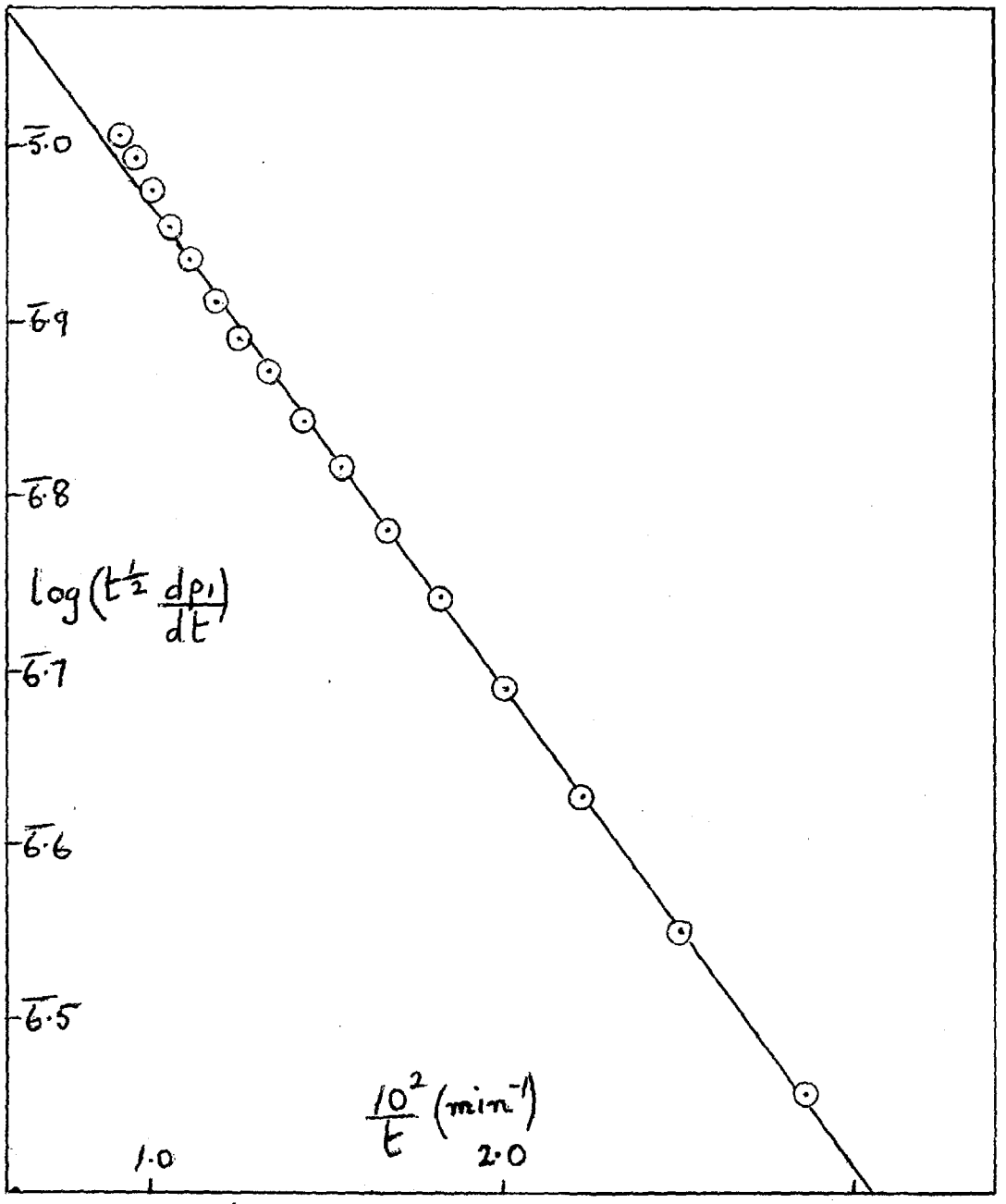


Fig. 4-3 'Early approximation' analysis for F1: Ne at 19.1°C

and long time lags which allow a sufficient number of pressure readings at relatively short intervals of time. As indicated in section 2.1.2b, the early approximation analysis is not applicable beyond a time corresponding to about 2.7 times the time lag. This is apparent in Fig.4-3 where the higher values of log $(t^{\frac{1}{2}} \frac{dp_1}{dt})$ begin to deviate above the line.

(a) Unplasticised polyvinyl chloride

It became apparent during the permeation and diffusion of hydrogen and neon that the unplasticised polymer was exhibiting a history dependence which necessitated careful study, the more so because such behaviour must be eliminated or minimised for a quantitative understanding of the diffusion processes. For hydrogen permeation in sheet J1 the values of $\bar{P}$ and D are tabulated in Table 4-1 and are plotted in Fig.4-4 and 4.5. The numbers associated with the experimental runs, performed on the unplasticised polymer J1, represent the order in which they were determined. The polymer was maintained at the appropriate temperature for not less than 12 hours before commencing an experiment. The main points of interest are:

(1) The initial values of $\bar{P}$ and D from 0° to $54^{\circ}C$ corresponding to runs 1-7 were not subsequently reproduced.

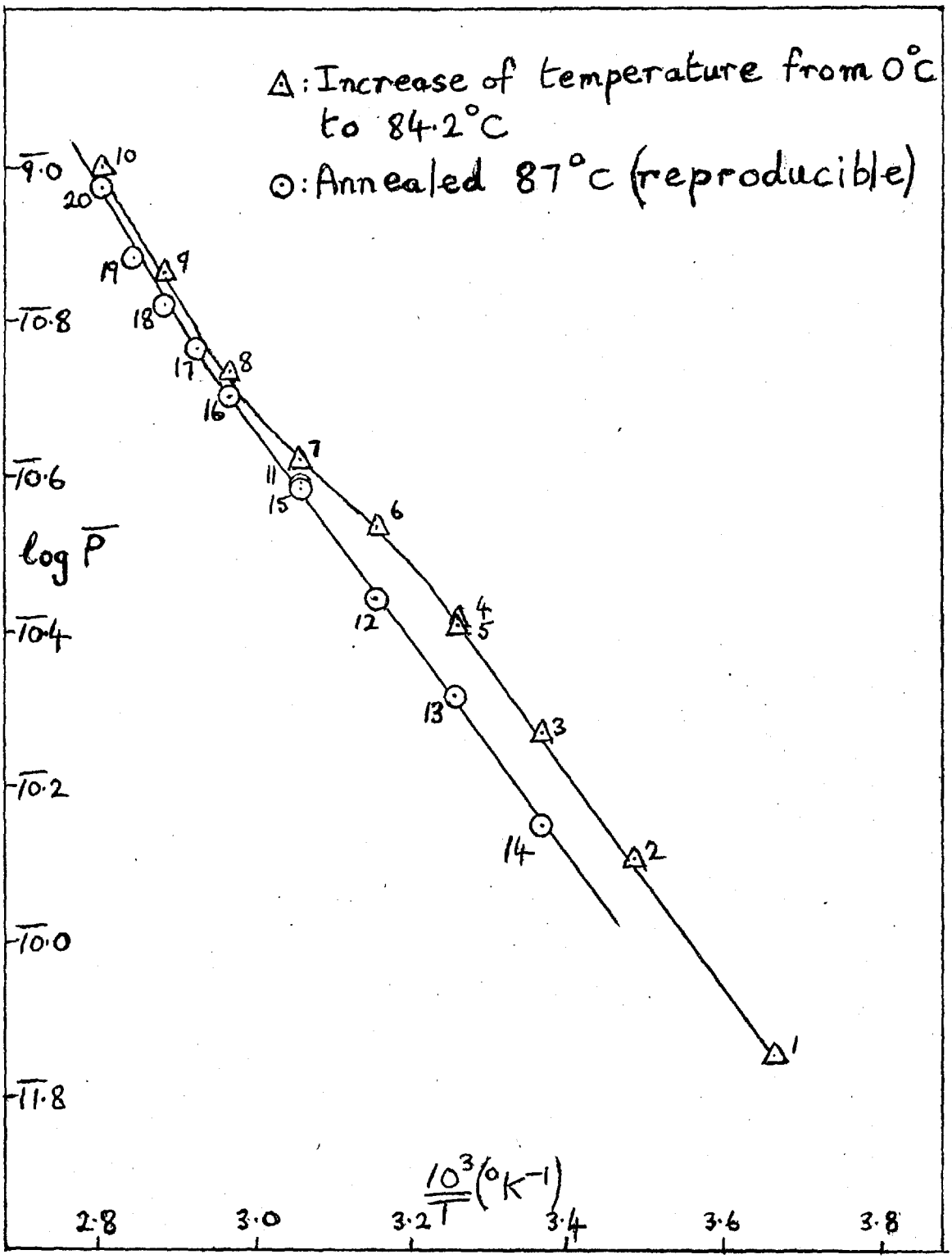


Fig. 4-4 Log. $\bar{P}$ vs. $\frac{1}{T}(^\circ K^{-1})$ for J1 : H_2

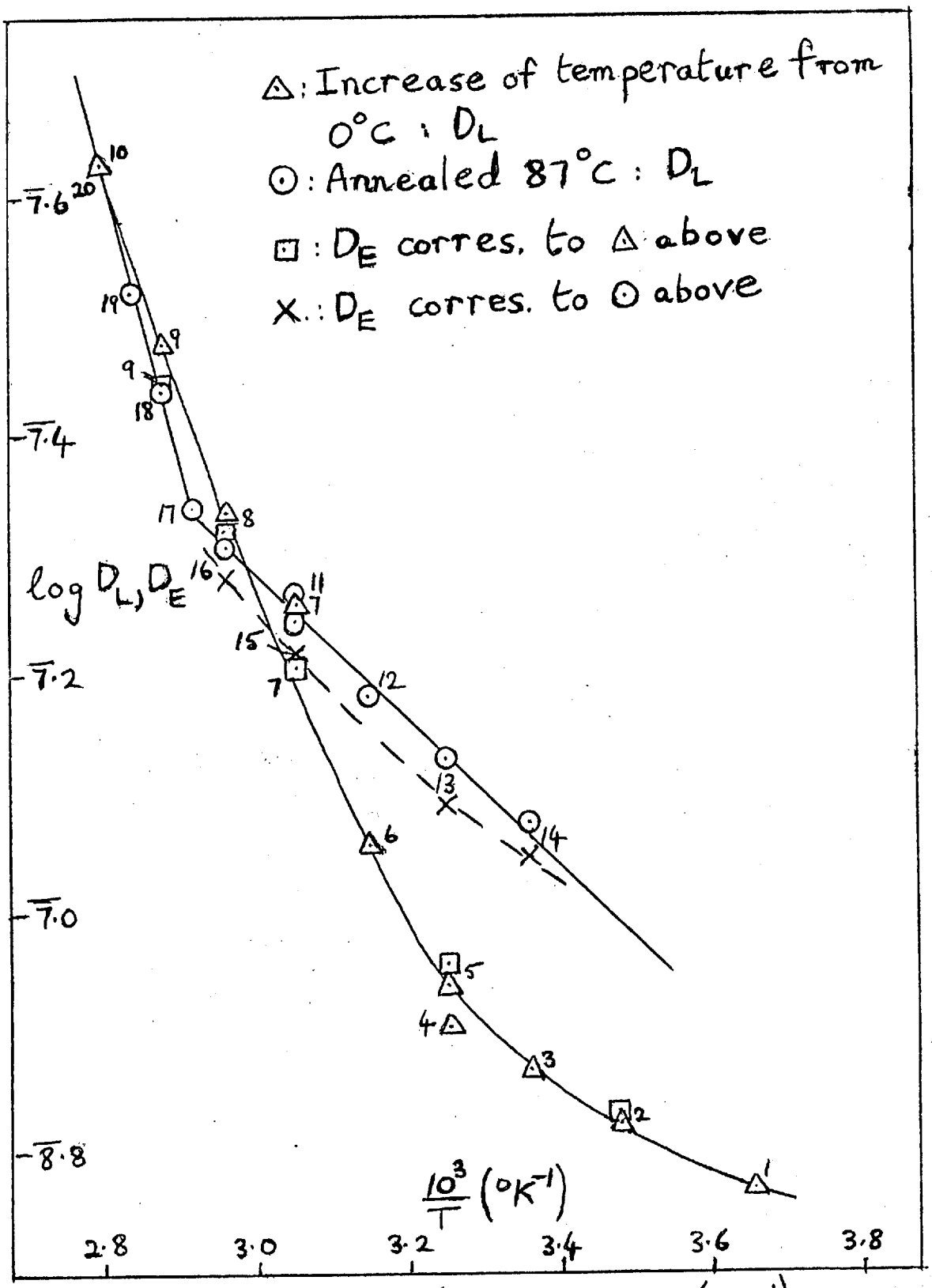


Fig. 4-5 Log. D_L and log. D_E vs. $\frac{1}{T}$ $(°K^{-1})$ for J1 : H_2

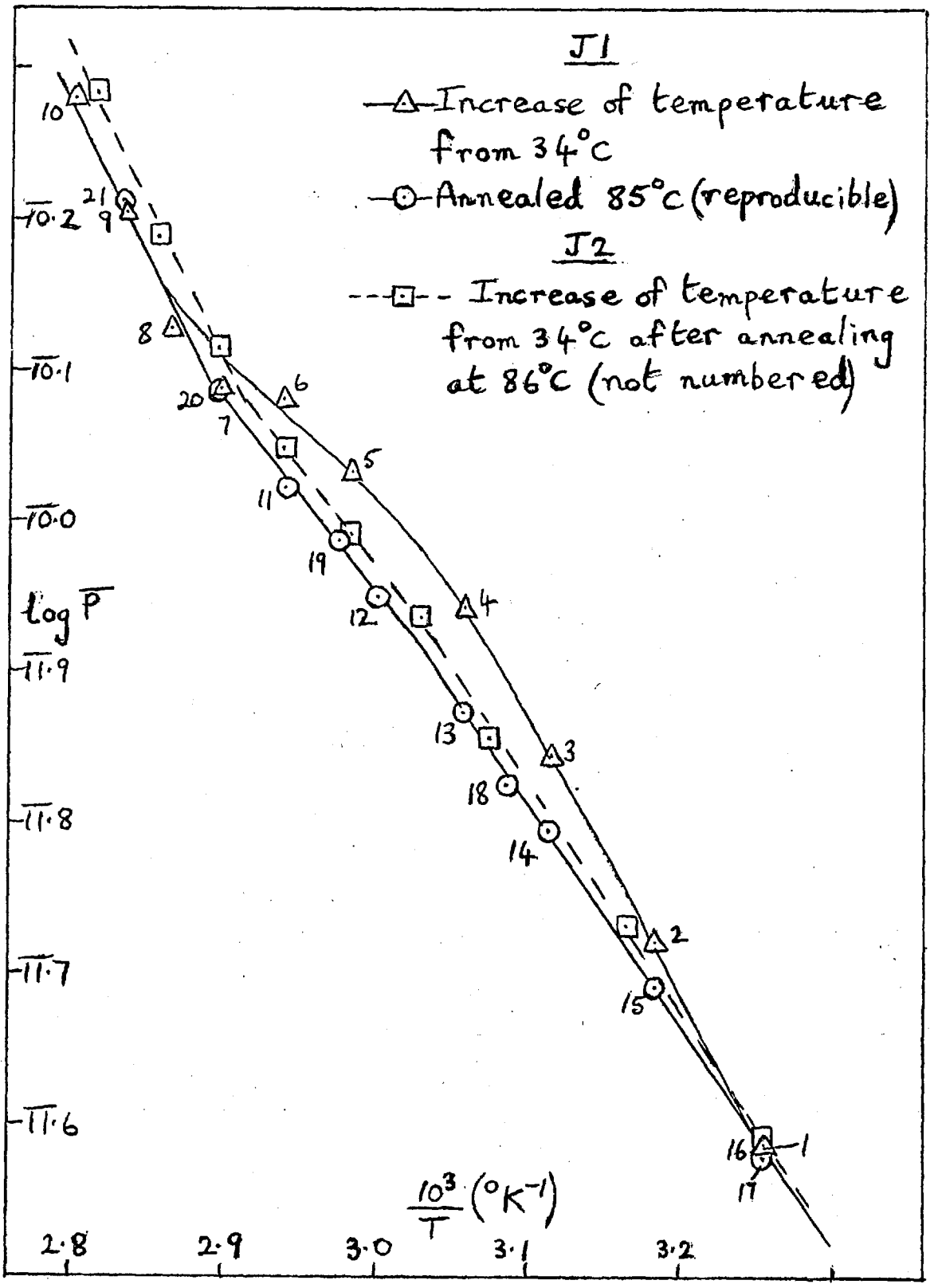


Fig. 4-6 Log. $\bar{P}$ vs. $\frac{1}{T}(^{\circ}K^{-1})$ for J1 and J2 : Ne gas

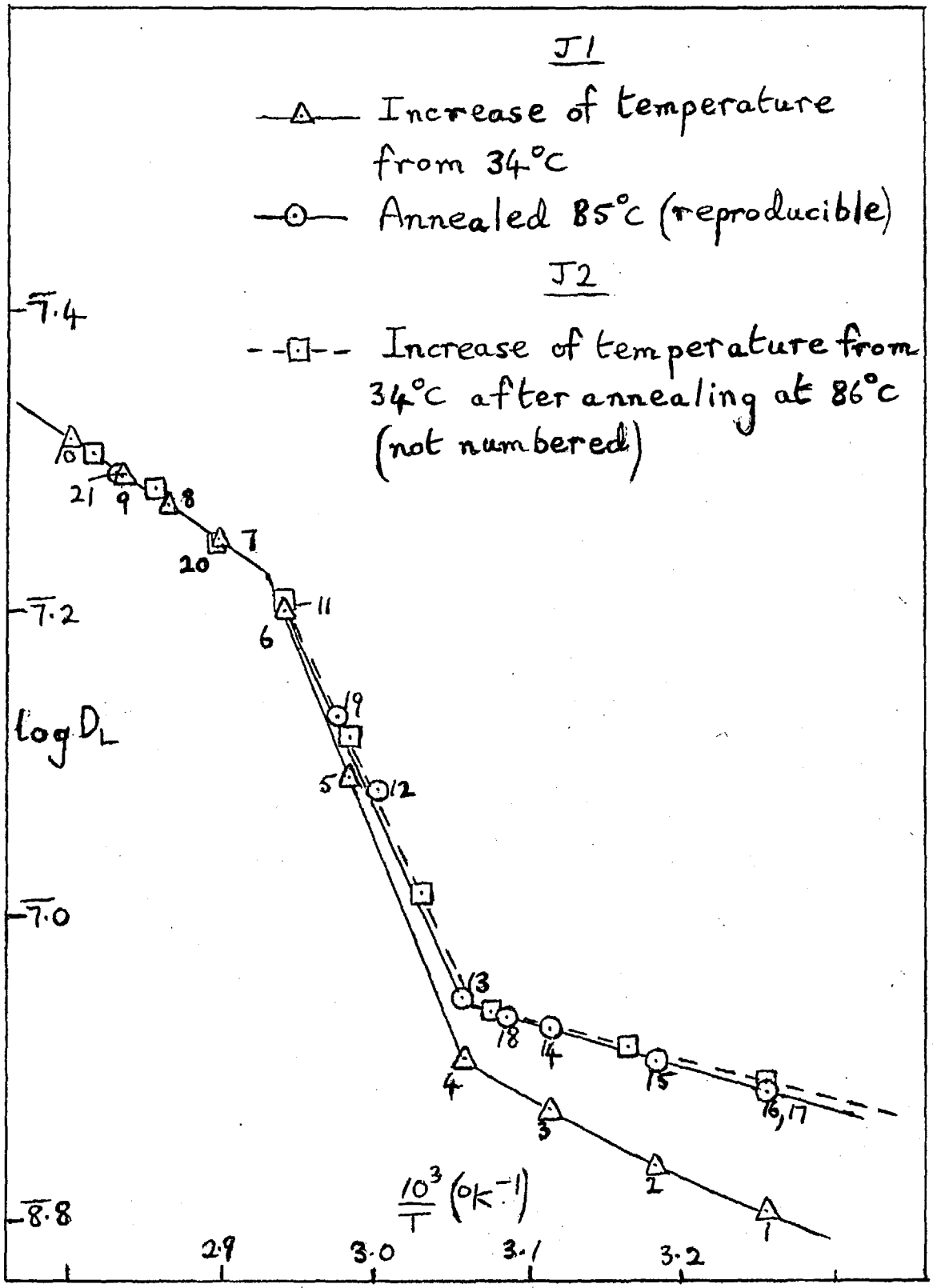


Fig. 4-7 Log D_L vs. $\frac{1}{T}$ ($^\circ K^{-1}$) for J1 and J2 : Ne gas

Runs 8-10 were then performed and the sample was carefully annealed at 87°C for 12 hours.

(2) On cooling slowly at 0.5°C/hour and repeating runs between 54.0 and 24.1°C (11 to 14), $\bar{P}$ was found to be considerably reduced (maximum reduction: 20%) and D_L increased by up to 30% above the original values. These shifts are well outside the range of experimental error. The repeat run 15 at 54.0°C showed a good degree of reproducibility with 11.

(3) The second series of $\bar{P}$ and D values from 69.0 to 84.0°C (17 to 20) showed reasonable agreement with the first group of runs 9-10.

Throughout this sequence of experiments the D_E values, although not as accurate as D_L, followed a similar pattern to the latter as shown in Fig.4-5.

The permeation results for neon in membrane J1 were determined in a similar way to hydrogen five weeks later, and are tabulated in Table 4-5 and graphed in Fig.4-6 and 4-7. The general similarity of the permeability graphs Fig.4-4 and 4-6 is apparent, although on close inspection it is possible to represent the reproducible runs 7-21 (runs 11-21 were determined after annealing at 85°C) by 3 straight lines and 2 intersections. Despite the anomalous nature of Fig.4-7, it is also noticeable

that the D_L values from runs 11-19 (reproducible within the time of the experiments, i.e. 3 weeks) are still above the values from the initial series 1-6.

So as to examine the behaviour of neon in greater detail, its permeation was observed through a second unplasticised membrane J2. This membrane was cut from the same sheet as J1 so as to minimise any differences between them, annealed at 86°C for 12 hours and cooled slowly to 34.1°C before commencing the experiments. The $\bar{P}$ values from the J2 membrane (see Table 4-6 and Fig.4-6) were found to lie 1 to 8% above the corresponding $\bar{P}$ values from the series 7-21 (reproducible for J1). The D_L values for J2 were, however, in reasonable agreement with the reproducible values (7-21) for J1 (see Fig.4-7).

The data indicate that, so far as the unplasticised polymer is concerned, the permeation of hydrogen and neon below about 70°C is governed by history - and time-dependent effects, which may be associated with the slow relaxation of polymer chains. On annealing a particular membrane above about 70°C, which corresponds to the glass transition region quoted in the literature[40,94,98,99,101,124,137] and cooling slowly below this temperature, it is possible to obtain reasonably reproducible permeation results at each experimental temperature. Each 'settled' state of

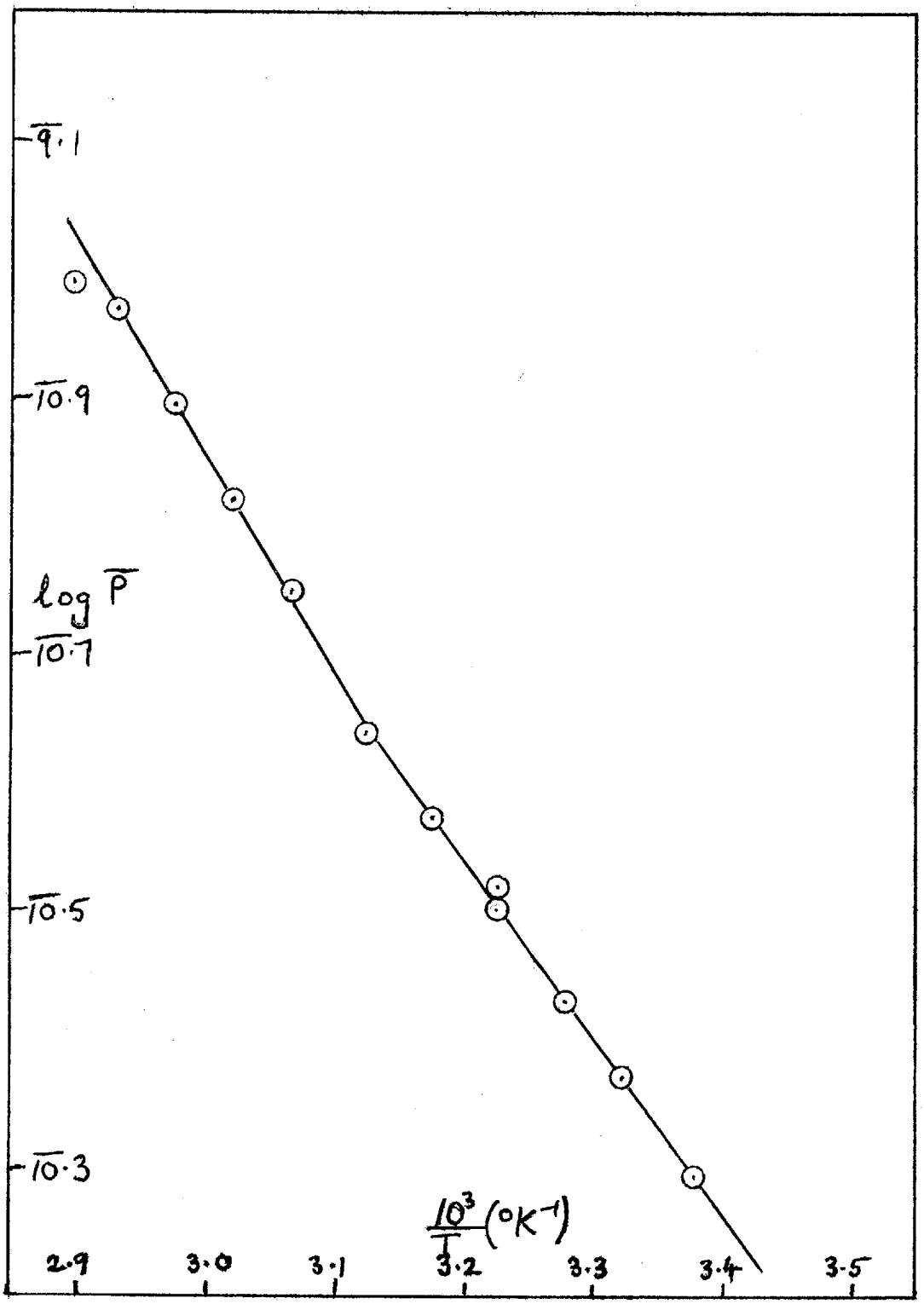


Fig. 4-8 Log $\bar{P}$ vs. $\frac{1}{T}(°K^{-1})$ for H : H_2

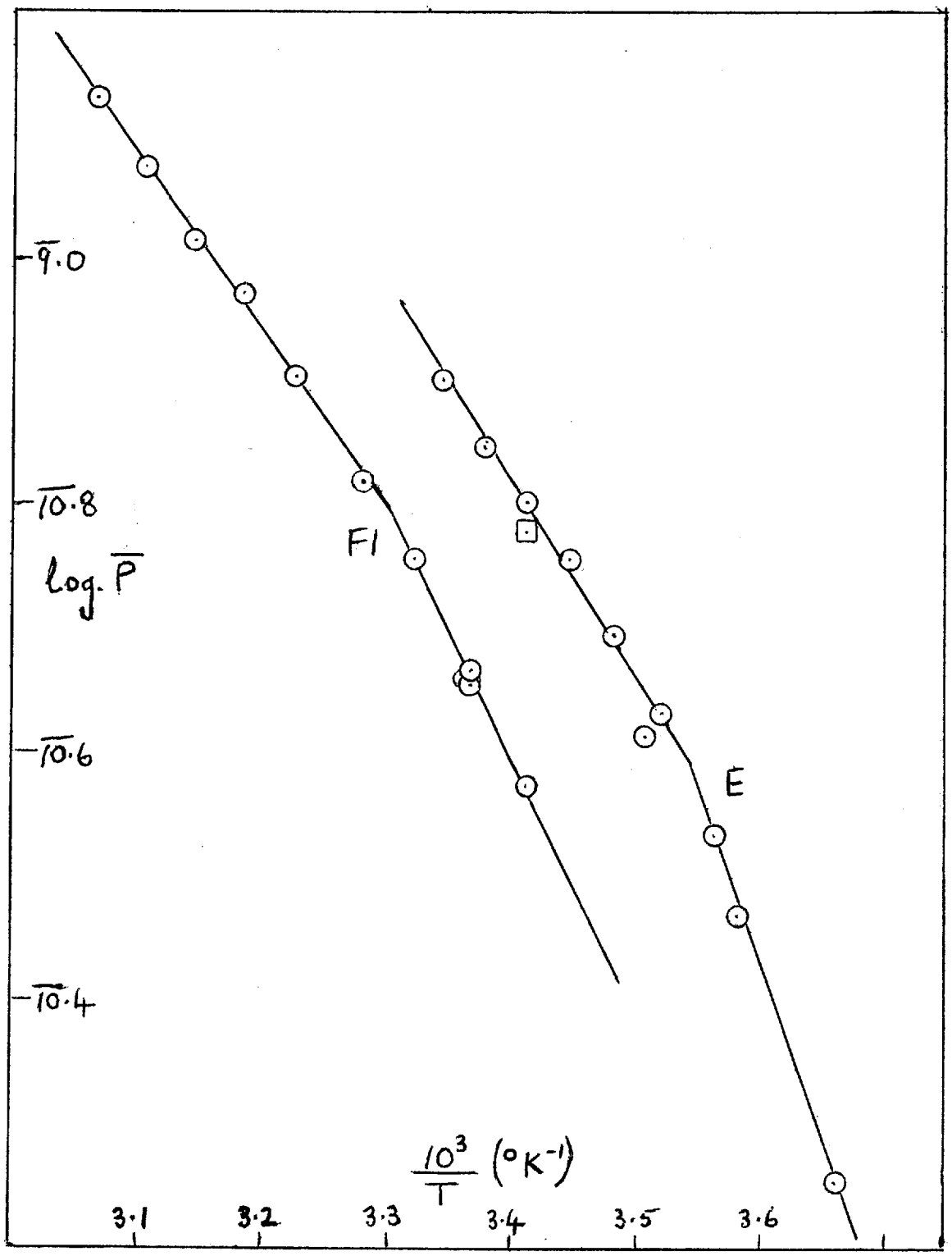


Fig. 4-9 Log $\bar{P}$ vs $\frac{1}{T}$ (°K^{-1}) for E and F1 : H_2 gas

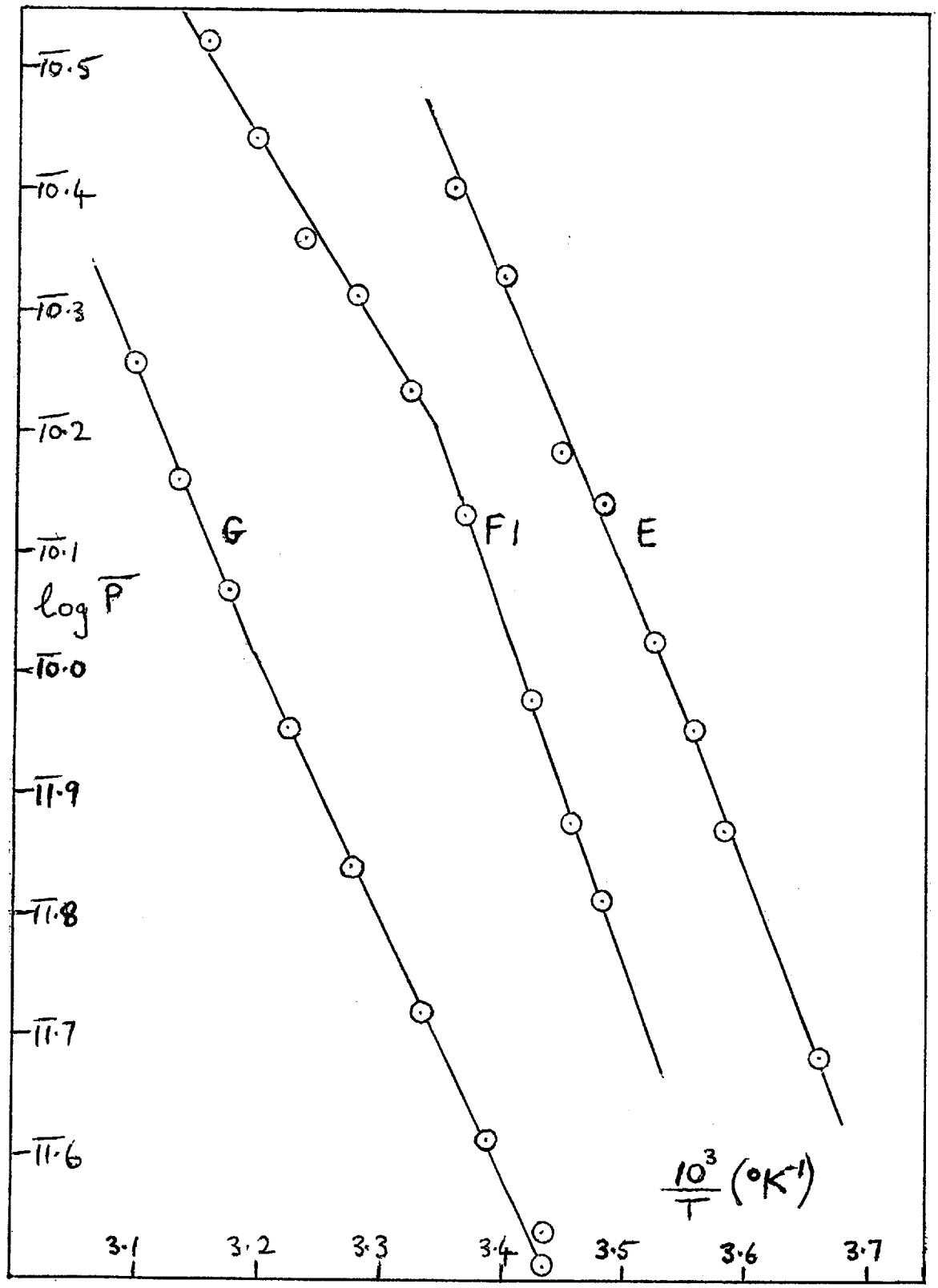


Fig. 4-10 Log. $\overline{P}$ vs. $\frac{1}{T}$ (°K^{-1}) for E, F1 and G : Ne gas

the polymer is, however, the most stable one realisable at the appropriate temperature, after the treatment given and within the time-scale of the experiments. In the rubbery region above T_g, where relaxation times are shorter, the polymer chains attain thermodynamic equilibrium quickly[59,94,98] and thus the permeation results for the probe molecules are reproducible.

(b) Plasticised polyvinyl chloride

Unlike the unplasticised material the permeability and diffusion coefficients of hydrogen and neon in the plasticised polymer membranes were reasonably reproducible over the appropriate ranges of temperature (see Fig.4-8 to 4-14). History- and time-dependent effects were also not apparent. For instance, the permeation of hydrogen through sample E at 20°C was measured one year after the initial experiments, and $\bar{P}$ and D_L were found to be in reasonable agreement with their original values (see point ⊡ in Fig.4-9 and 4-12). D_E values are also plotted in Fig.4-11 to 4-14. Particularly good agreement between D_L and D_E was obtained for neon permeation in membrane G (Fig.4-13).

Examination of Fig.4-8 to 4-14 also shows that in no case can the data for any one gas be represented by a single straight line. In general the experimental points

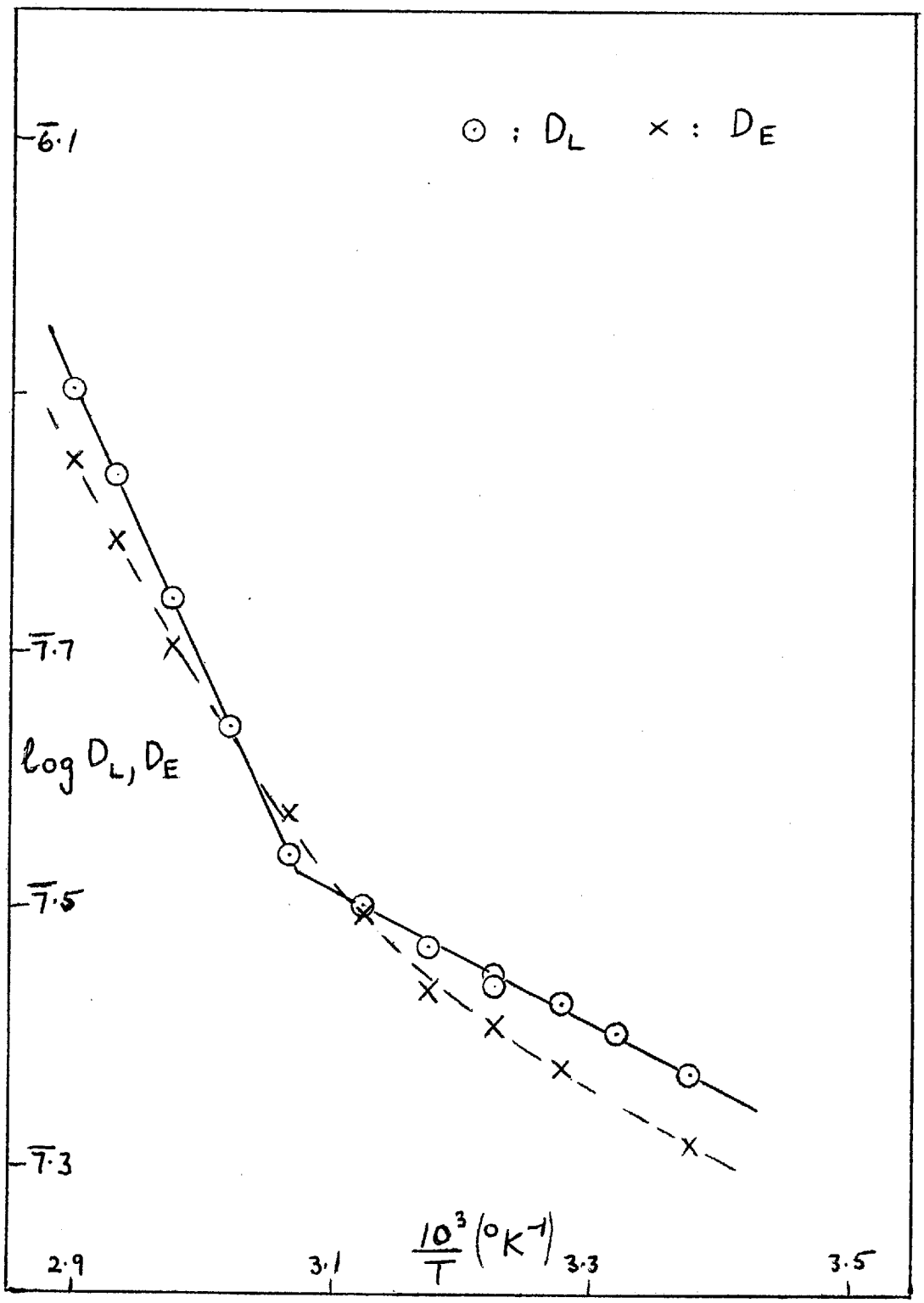


Fig. 4-11 Log. D_L, D_E vs. $\frac{1}{T}(°K^{-1})$ for H : H_2 gas

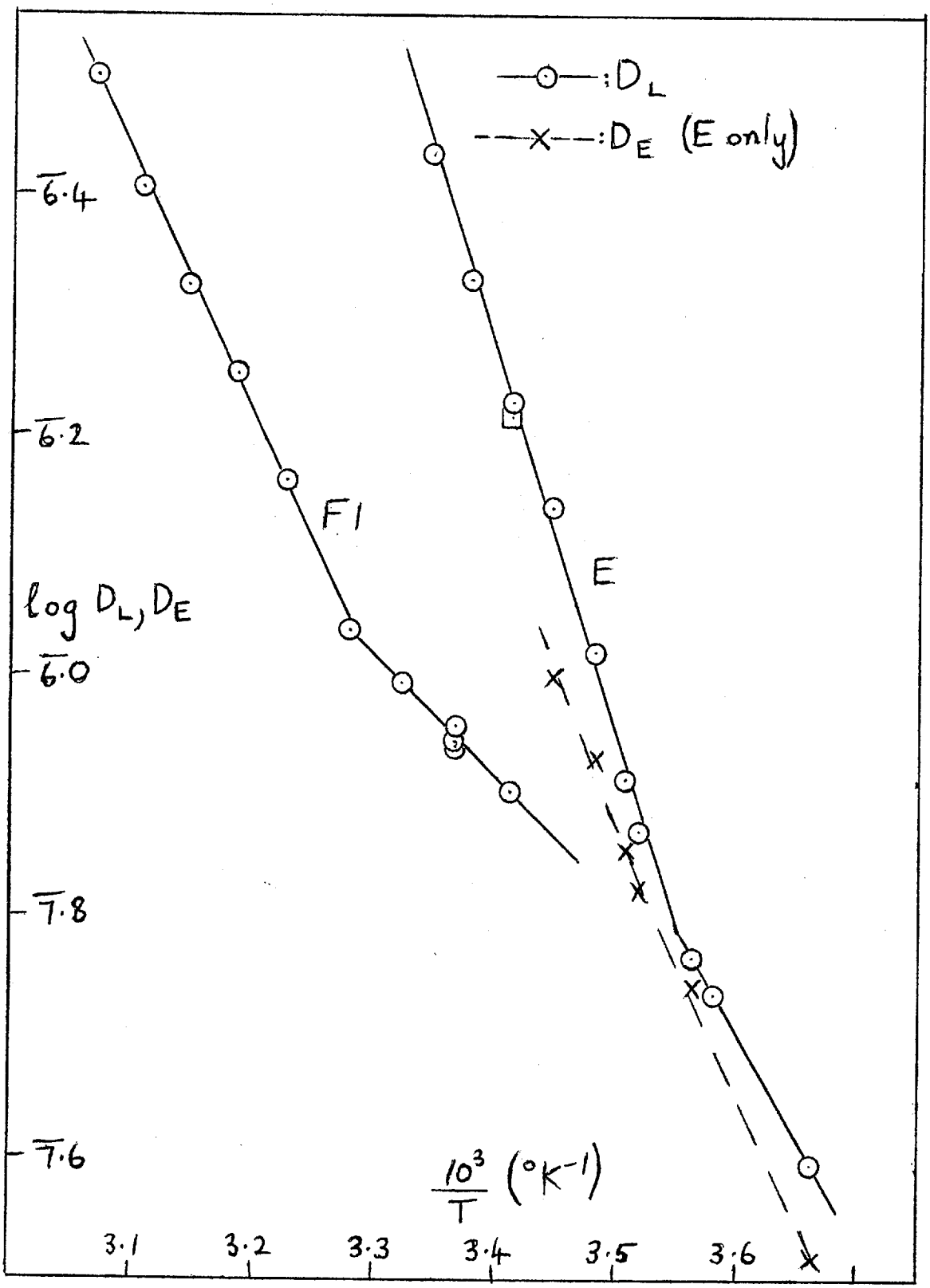


Fig. 4-12 Log. D_L, D_E vs. $\frac{1}{T}$ ($^\circ K^{-1}$) for E and F1 : H_2 gas

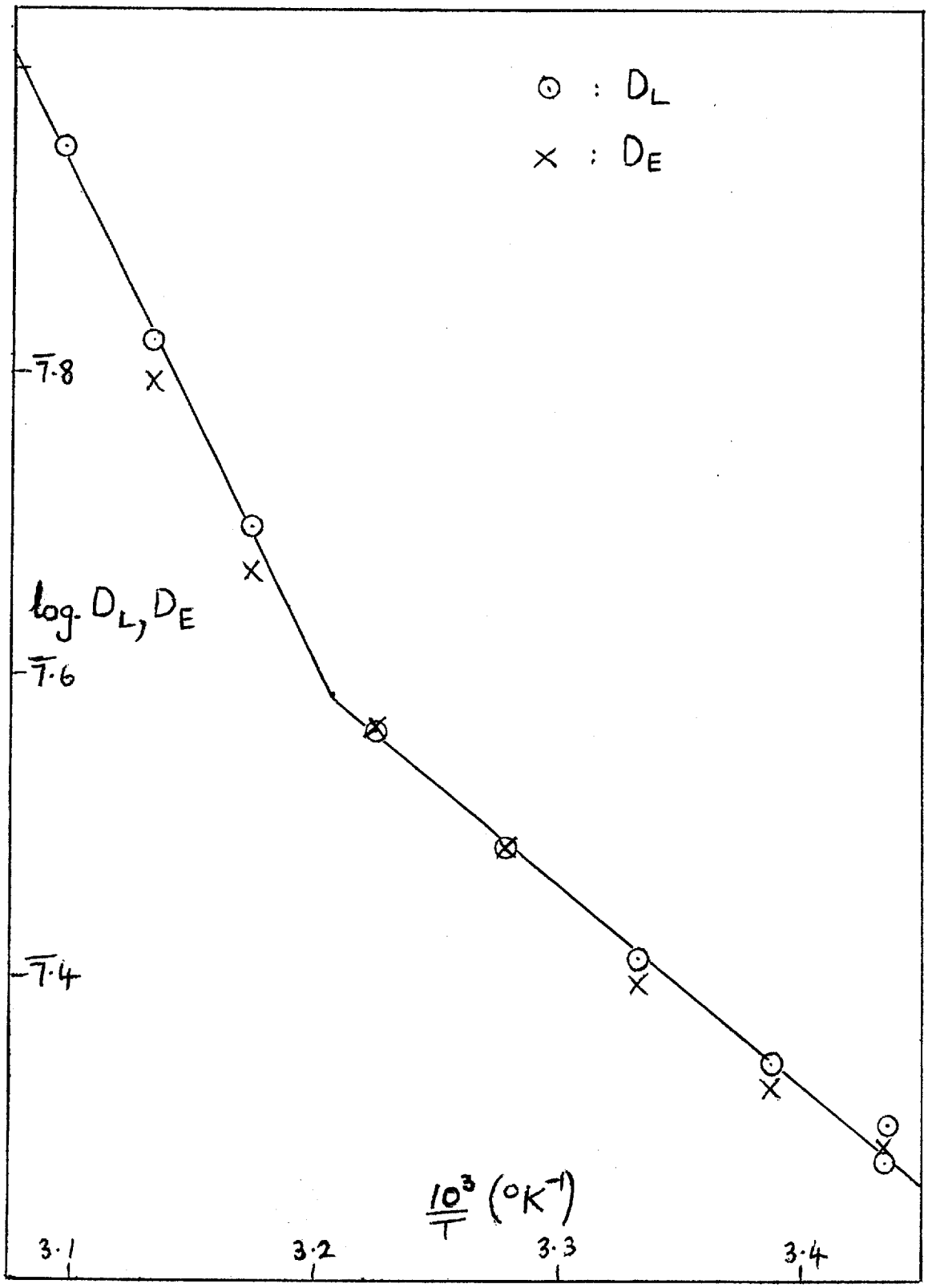


Fig. 4-13 Log. D_L, D_E vs. $\frac{1}{T}$ ($^oK^{-1}$) for G : Ne gas

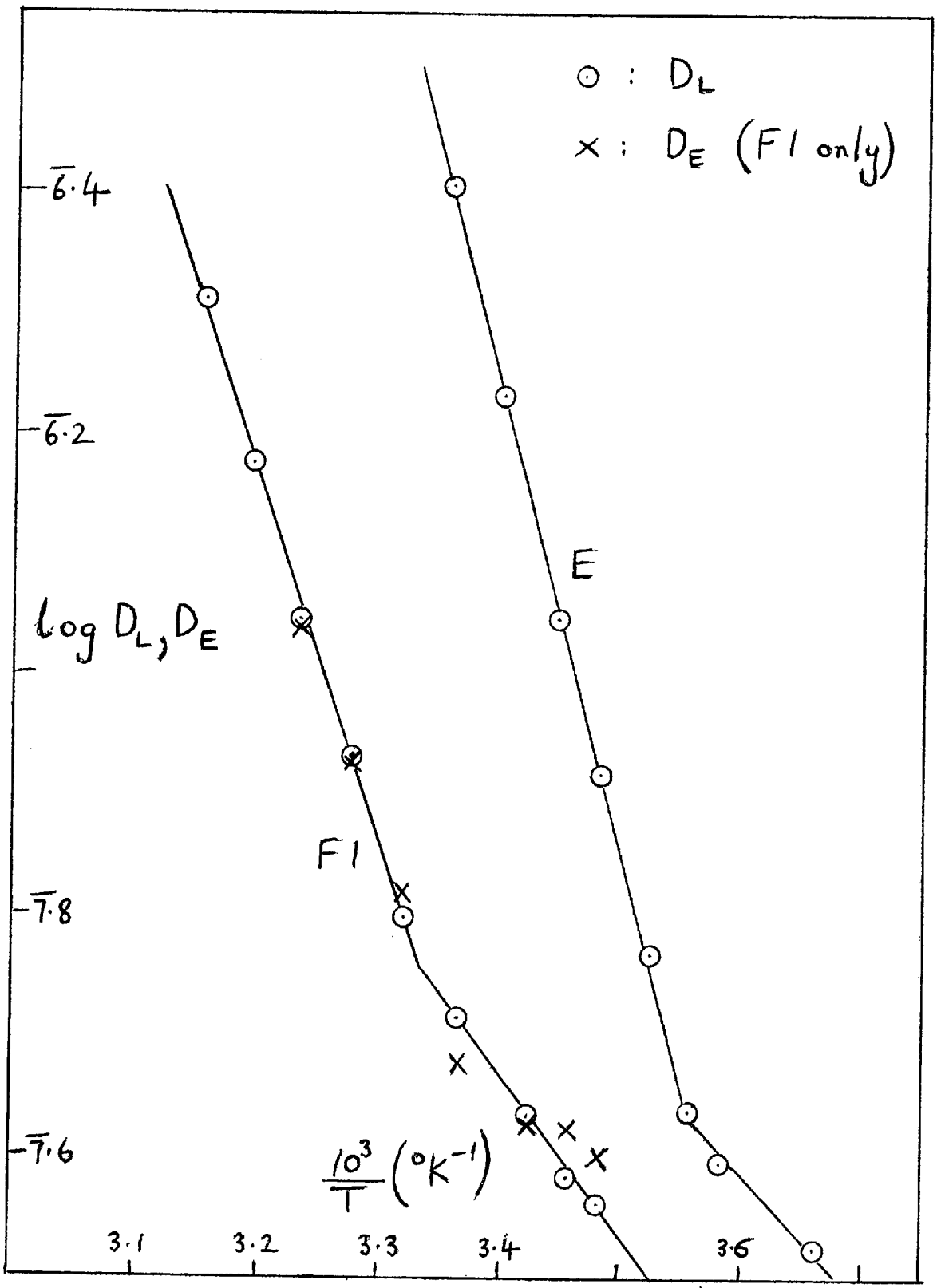


Fig. 4-14 Log. D_L, D_E vs. $\frac{1}{T}$ ($^\circ K^{-1}$) for E and F1 : Ne gas

representing $\bar{P}$ and D_L lie near two distinct straight lines with one intersection. The significance of this will be discussed in a later section.

4.2.2 Influence of plasticiser on the permeability and diffusion coefficients

Both the permeability and diffusion coefficients of hydrogen and neon at a given temperature are found to increase with increasing quantity of plasticiser in the polymer. Plots of $\log_{10} \bar{P}$ and $\log_{10} D_L$ vs. volume fraction v_1 of plasticiser are shown in Fig.4-15 and 4-16. The extrapolated values were calculated at the appropriate temperatures by means of a statistical treatment of the experimental data, and are shown in Fig.4-4 to Fig.4-14. It was assumed that no further polymer transition points were present apart from those determined experimentally. In the case of the unplasticised material only the reproducible experimental data was used in Fig.4-15 and Fig. 4-16. The data for hydrogen indicate a linear relationship between $\log_{10} \bar{P}$ and v_1 (Fig.4-15), although such a relationship is not demonstrable for neon owing to the scatter of the data. Indeed at $0^{\circ}C$, which is below the experimental intersection temperatures of all the membranes, a curve is observed for neon.

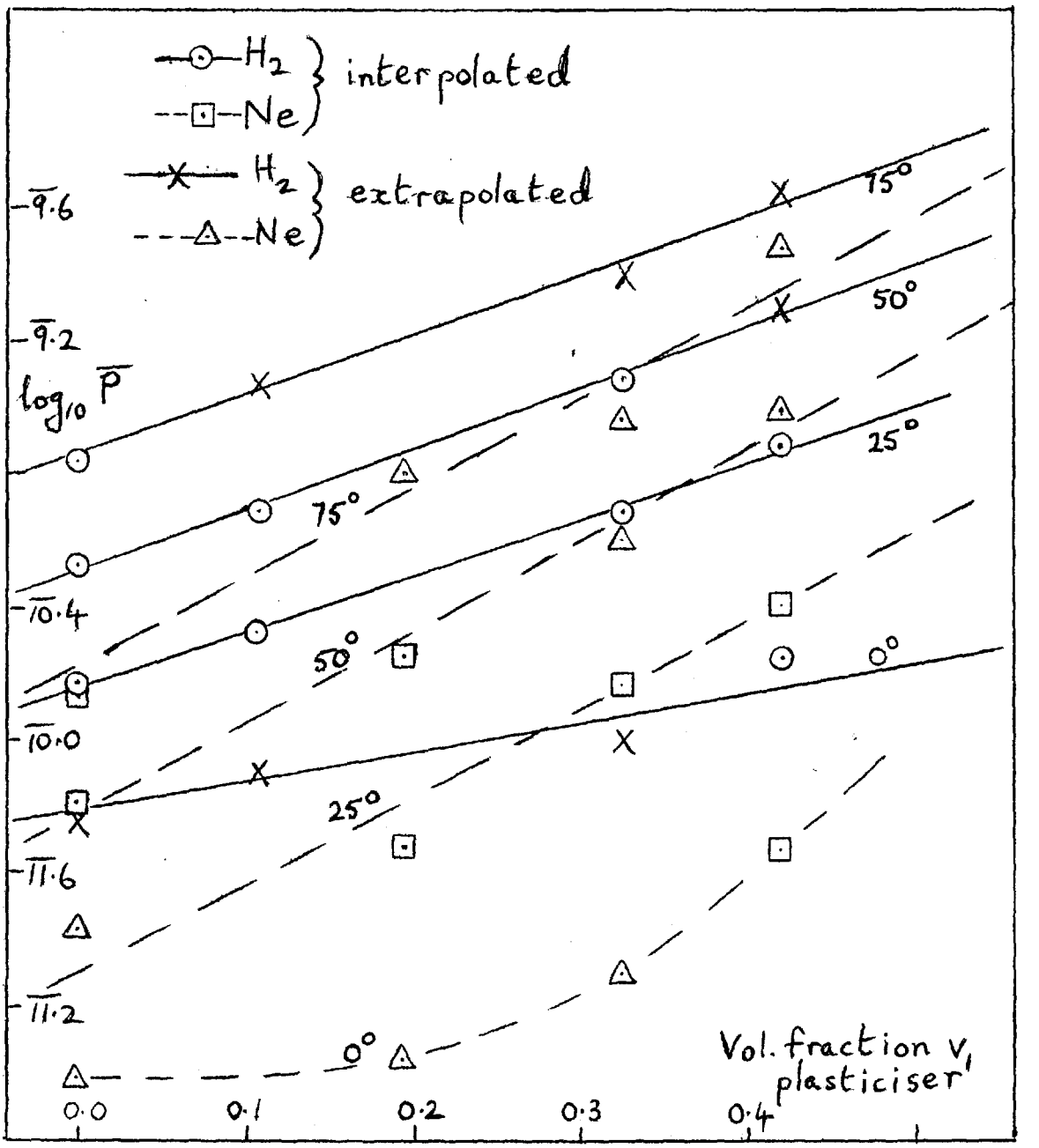


Fig. 4-15 Log $\bar{P}_H$ and $\bar{P}_{Ne}$ vs. vol. fraction v_1 of plasticiser

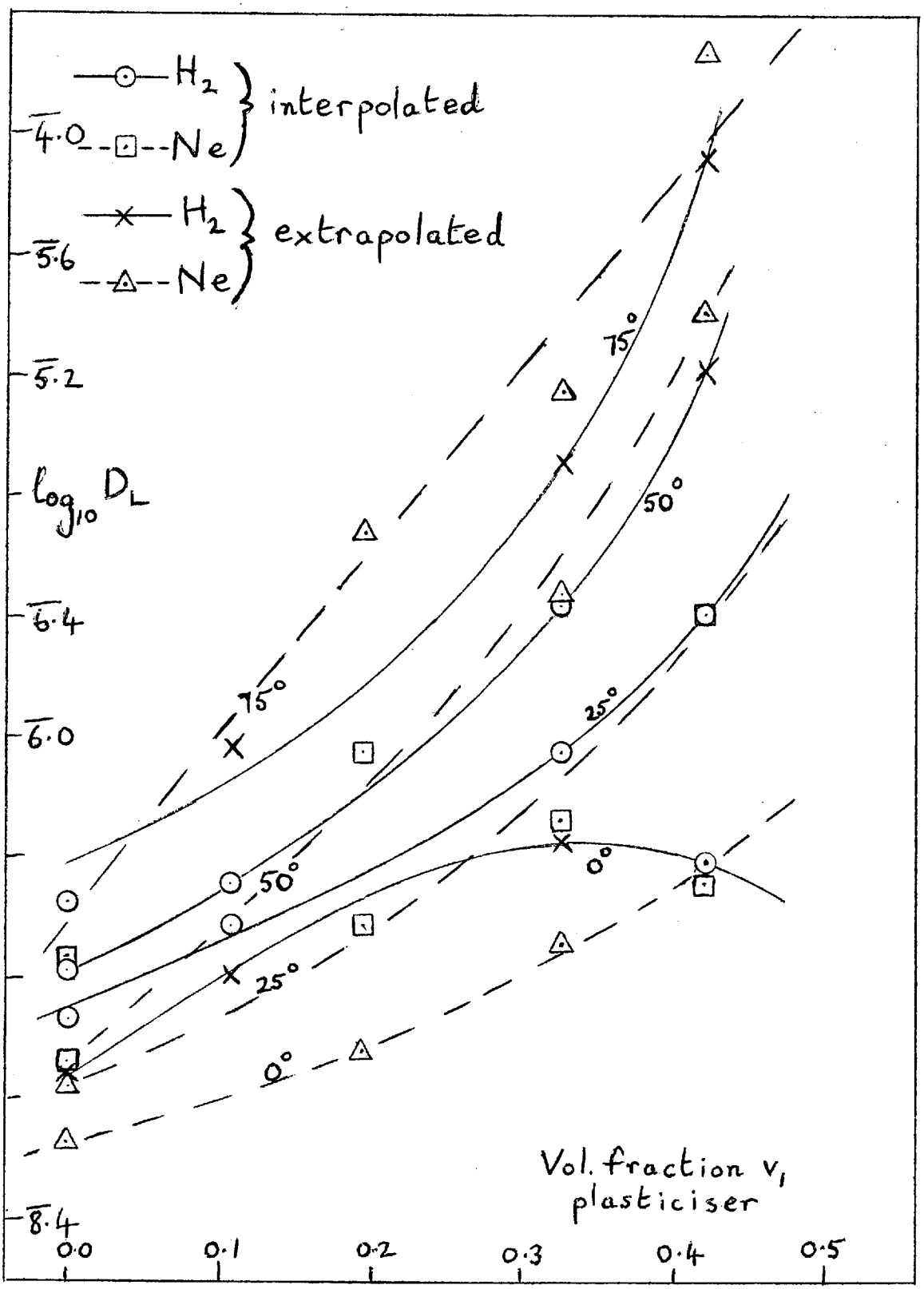


Fig. 4-16 Log. D_L of H_2 and Ne vs. volume fraction of plasticiser

From the work of Brubaker et al.,[23] there is also some indication of an exponential relationship between the permeability coefficient of carbon dioxide at a given temperature and the amount of dioctyl phthalate plasticiser contained in poly-vinyl chloride membranes. Hydrogen showed anomalous behaviour, however, as its permeability in the membrane containing the highest amount (16.7% by weight) of plasticiser was unexpectedly less than a membrane containing 4.8% plasticiser.[23]

Although the values of the diffusion coefficient increase rapidly with increasing plasticiser concentration in this work (see Fig.4-16), nevertheless, at 0°C hydrogen shows unusual behaviour. Comparison of the magnitudes of $\overline{P}$ for hydrogen and neon reveals that between 0°C and 75°C $\overline{P}(H_2) > \overline{P}(Ne)$. This order is in agreement with the permeabilities of these gases through natural rubber,[5,138] silicone rubber[48] and poly-vinyl acetate.[7] Brubaker[23] quotes $\overline{P}$ values for hydrogen in unplasticised poly-vinyl chloride in the range 3 to 4 x 10^{-10} between 20° and 40°C. This is in reasonable agreement with this work (see Table 4-1) considering that the membranes were obtained from different sources. Unplasticised poly-vinyl acetate[7] also shows a somewhat greater permeability to hydrogen and neon than poly-vinyl chloride. $\overline{P}$ for these gases in

poly-vinyl acetate lies within the range 10^{-10} - 10^{-9} for temperatures from 4^{o} to $44^{o}C$.

The sequence of the transient-state diffusion coefficients D_L for hydrogen and neon between 0^{o} and $50^{o}C$ is $D_L(H_2) > D_L(Ne)$ with some uncertainty of the placing above $50^{o}C$ (see Fig.4-16). This order is also in agreement with that found in other investigations.[5,7,48,138]

4.2.3 Separation of gases

Since polymeric membranes have a much higher permeability towards some gases than towards others, they should be quite effective as a means of gas separation. Aitken and Barrer[44] defined the separation factor S through permeation as $S = Q_1C_2/Q_2C_1$ where Q_1 and Q_2 are the volumes of species 1 and 2 permeated in time t, and C_1 and C_2 are the respective concentrations in the gas phase in contact with the ingoing side of the membrane. S can be estimated to a first approximation in the steady state from the ratio of the individual permeabilities, since, at least in the region where Henry's Law is valid and solubility rather small, interference effects are not likely to be large.

Values of permeability ratios for hydrogen and neon in poly-vinyl chloride are shown in Table 4-14 and compared with other membranes in Table 4-15. In general the

TABLE 4-14

Permeability ratios for hydrogen and neon in poly-vinyl chloride (PVC)

Vol. fraction TCP plasticiser v_2	Permeability ratio = $\overline{P}_H/\overline{P}_{Ne}$ †			
	0°C	25°C	50°C	75°C
0.0	6	5	5.1	5.1
0.107	8	5	4	4
0.194	8	5	4	3
0.325	5	3.3	3	3
0.419	3.7	3.0	2	2

†: $\overline{P}_H$, $\overline{P}_{Ne}$: permeability coefficients of hydrogen and neon determined by extrapolation and/or interpolation from Fig.4-15.

TABLE 4-15

Permeability ratios for hydrogen and neon in various membranes at the temperatures indicated

Membrane	T°C	$\overline{P}_H/\overline{P}_{Ne}$
Unplasticised PVC	50	5.1
Plasticised PVC (v_1 = 0.419)	25	3.0
Filled silicone rubber sheet¤	0	2.4_2
Filled silicone rubber sheet¤	-37	2.4_1
Filled silicone rubber tube¤	0	2.3_6
Filled silicone rubber tube¤	-78	3.2_0
Poly-vinyl acetate†	10	3.5
Poly-vinyl acetate†	40	3.7
'Vycor' glass/	400	2.8
'Vycor' glass/	450	3.6

¤ from ref.48 † from ref.7

/ from ref.111

separation factor decreases for increasing plasticiser concentration and increasing temperature. Leaving absolute rates out of consideration the most suitable poly-vinyl chloride medium for separating hydrogen and neon is an unplasticised membrane at a low temperature. The separation factor for the two gases is also somewhat higher for poly-vinyl chloride as compared with other systems (see Table 4-15). However, the permeability of silicone rubber to hydrogen and neon is more than one hundred times larger than those of poly-vinyl chloride. The low permeability in poly-vinyl chloride would therefore be a disadvantage in large scale separation by the steady-state method, as it would involve the use of extremely thin membranes of large surface area.

4.2.4 Intersection temperatures

Examination of Figs.4-4, 4-5 and 4-8 to 4-14 shows that in general the reproducible experimental data of $\log_{10} \bar{P}$ and $\log D_L$ lie near two straight lines with one intersection. For the system unplasticised poly-vinyl chloride and neon, however, the reproducible data apparently lie near three straight lines with two intersections (see Fig.4-6 and 4-7). As there are no transitions in the gases, the temperature of these intersections must reflect changes in the polymer medium. The

intersection temperatures are assembled in Tables 4-16 and 4-17.

TABLE 4-16

Intersection temperatures T_1°C in plasticised poly-vinyl chloride

Sheet	Volume fraction plasti-ciser v_1	Average T_1(°C) for hydrogen	Average T_1(°C) for neon	Average T_1(°C) for hydrogen and neon
H	0.107	53	-	[53]
G	0.194	-	39	[39]
F1	0.325	30	26	28
E	0.419	9	8	9

TABLE 4-17

Intersection temperatures T_1°C and T_2°C in unplasticised poly-vinyl chloride

Sheet	Gas	Average upper inter-section temp. T_1(°C)	Average lower inter-section temp. T_2(°C)
J1	H_2	70	-
J1	Ne	70	54
J2	Ne	69	54

It is of interest that the intersections are revealed not only by the kinetic process of diffusion but also by the property of solubility which will be discussed in section 4-3. The intersection temperature in Table 4-16 falls with increasing concentration of plasticiser and may be identified with the glass transition revealed in polymer plasticiser systems by various experimental techniques.[59,74,94,98,139,140] The upper intersection temperature T_1 for the unplasticised polymer is the same for hydrogen and neon, but a lower intersection point T_2 was observed for neon. As already mentioned the upper temperature T_1 for the unplasticised polymer corresponds with the normally observed glass transition temperature for which values of between 70 and 85°C have been reported.[40,94,98,99,101,124,137]

Simple linear correlations between the transition temperatures and the volume or weight fraction of plasticiser in polymers have been noted[74,142] but have lacked a satisfactory theoretical basis. The expression for the glass transition temperature of a polymer-diluent system according to the free volume theory is given by eq.(2.81). Heydemann et al.[98] determined the thermal expansion of unplasticised poly-vinyl chloride over the glass transition region and the effect of pressure

so that it can be taken that $\Delta \alpha_2 = 3.8 \times 10^{-4} deg^{-1}$. For the tricresyl phosphate plasticiser one can assume from data given by Mellan[73] that the value of $\alpha_1 = 5 \times 10^{-4} deg^{-1}$ is a fair approximation. The glass temperature of tricresyl phosphate T_{g_1} is also quoted by Boyer and Spencer[142] as $-50^{\circ}C$ and this value was used here.

The data for the experimental intersection temperature T_1 vs. volume fraction plasticiser are illustrated in Fig.4-17. The curve represents the theoretical relationship (2.81) with values of $\Delta \alpha_2, \alpha_1$ and T_{g_1} as indicated. The remarkably accurate representation of the experimental data by the expression (2.81) points to the applicability of the free volume approach to segmental mobility in poly-vinyl chloride. Kelley and Beuche[139] assumed the value of α_1 to be of the order $10^{-3} deg^{-1}$ for all his diluents, but in this work the value $\alpha_1 = 5 \times 10^{-4} deg^{-1}$ would appear to be more satisfactory for tricresyl phosphate plasticiser.[73]

The presence of a secondary transition temperature T_2 for neon in the unplasticised polymer is difficult to understand because of its apparent non-existence in the other systems. Heydemann et al.[98] during specific volume measurements with polyvinyl chloride found that the secondary transition below T_g is not experimentally

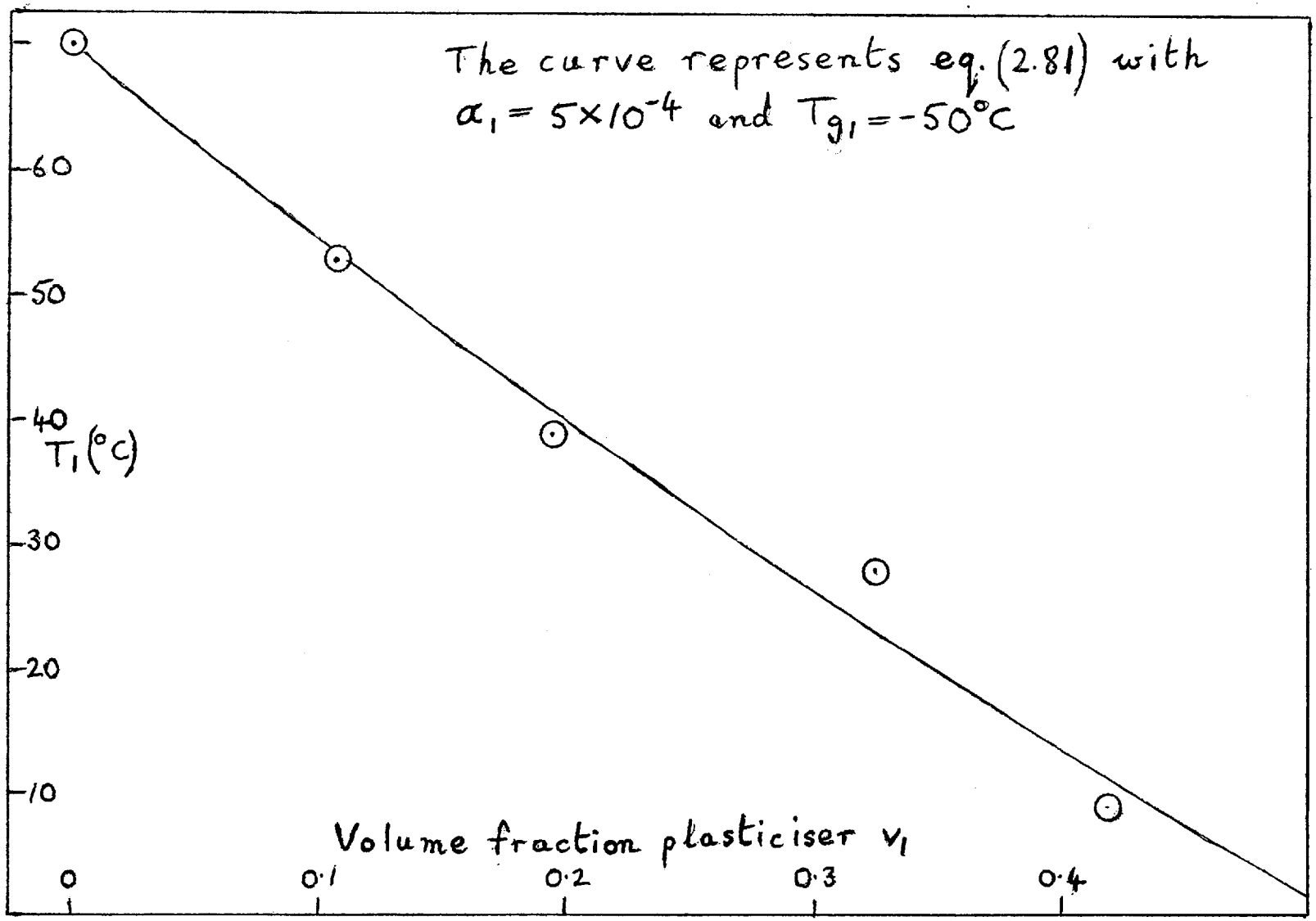


Fig. 4-17 Intersection temperature T_1 (°C) vs. vol. fraction v_1

observable with samples containing relatively high proportions of dioctyl phthalate plasticiser. They concluded that if the transition is caused by the same molecular process it is obviously hindered by the plasticiser molecules. However the type of molecular process is not completely elucidated yet. Evidence was also obtained by Meares[7,8,59] that the glass-rubber transition for polyvinyl acetate occurred over a short range of temperature and was completed at the normally recorded glass temperature.

4.2.5 Temperature coefficients of permeation and diffusion

The reproducible data for log $\bar{P}$ and log D_L shown in Figs.4-4 to 4-14 give a virtually linear relationship with $\frac{1}{T}$, whether above or below the intersection temperatures. It follows, therefore, that eq.(1.1) and eq.(1.3) are both obeyed within the temperature range investigated. Values of the apparent activation energy for permeation E_p and diffusion E_D together with the corresponding values of P_o and D_o are shown in Tables 4-18 to 4-23. The experimental temperature range is also indicated for each membrane. In accordance with eq.(1.1) and eq.(1.3) E_p and E_D have been determined from the slopes, and P_o and D_o from the intercepts on the ordinate of the linear

TABLE 4-18

The apparent energy of activation for permeation of hydrogen in cal.mole^{-1}

Sheet	Volume fraction plasticiser v_1	Mean intersection temp. T_1 (°C)	E_p below T_1	P_o below T_1	E_p above T_1	P_o above T_1	Experimental temp. range (°C)
J1	0.0	70	6350	6.55×10^{-6}	7680	4.65×10^{-5}	24-84
H	0.107	53	6290	8.61×10^{-6}	7380	4.92×10^{-5}	23-72
F1	0.325	28	9060	2.13×10^{-3}	6560	3.38×10^{-5}	20-53
E	0.419	9	12690	2.61	6400	3.71×10^{-5}	0-26

TABLE 4-19

The apparent energy of activation for diffusion of hydrogen in cal.mole^{-1}

Sheet	Volume fraction plasticiser v_1	Mean intersection temp. T_1 (°C)	E_D below T_1	D_o below T_1	E_D above T_1	D_o above T_1	Experimental temp. range (°C)
J1	0.0	70	2700	1.14×10^{-5}	10700	1.50	24-84
H	0.107	53	2270	1.13×10^{-5}	10020	1.80	23-72
F1	0.325	28	4530	1.92×10^{-3}	9700	9.93	20-53
E	0.419	9	7950	9.18×10^{-1}	14290	7.80×10^{4}	0-26

TABLE 4-20

The apparent energy of activation for permeation of neon in the plasticised sheets in cal.mole^{-1}

Sheet	Volume fraction plasticiser v_1	Mean intersection temp. T_1(°C)	E_p below T_1	P_o below T_1	E_p above T_1	P_o above T_1	Experimental temp. range (°C)
G	0.194	39	9280	3.08×10^{-4}	11390	9.08×10^{-3}	18-50
F1	0.325	28	12790	3.55×10^{-1}	7730	6.97×10^{-5}	14-44
E	0.419	9	11620	9.66×10^{-2}	10300	9.18×10^{-3}	0-25

TABLE 4-21

The apparent energy of activation for permeation of neon in the unplasticised sheets J1 and J2 in cal.mole^{-1}

Sheet	Upper intersection temp. T_1(°C)	Lower intersection temp. T_2(°C)	E_p below T_2	P_o below T_2	E_p above T_1	P_o above T_1	Experimental temp. range (°C)
J1	70	54	6660	2.09×10^{-6}	9190	7.85×10^{-5}	34-84
J2	69	54	6710	2.34×10^{-6}	9420	1.19×10^{-4}	34-82

TABLE 4-22

The apparent energy of activation for diffusion of neon in the plasticised sheets in $cal.mole^{-1}$

Sheet	Volume fraction plasticiser v_1	Mean intersection temp. T_1 (°C)	E_D below T_1	D_o below T_1	E_D above T_1	D_o above T_1	Experimental temp. range (°C)
G	0.194	39	5860	4.83×10^{-3}	15240	1.79×10^{4}	18-50
F1	0.325	28	6270	2.11×10^{-2}	13880	7.41×10^{3}	14-44
E	0.419	9	4800	2.31×10^{-3}	17450	1.58×10^{7}	0-25

TABLE 4-23

The apparent energy of activation for diffusion of neon in the unplasticised sheets J1 and J2 in $cal.mole^{-1}$

Sheet	Upper intersection temp. T_1 (°C)	Lower intersection temp. T_2 (°C)	E_D below T_2	D_o below T_2	E_D above T_1	D_o above T_1	Experimental temp. range (°C)
J1	70	54	1370	7.15×10^{-7}	3130	1.70×10^{-5}	34-84
J2	69	54	1210	5.60×10^{-7}	3220	1.93×10^{-5}	34-82

plots illustrated in Figs.4-4 to 4-14. The slopes and intercepts were calculated statistically from the experimental data by the least squares method. (NOTE: Experimental data at 72°C for the hydrogen/membrane H system were not included in the least squares calculations). For the unplasticised polymer/neon system values of E_p and E_D are also not given for the interval 54°C to 70°C (see Fig.4-6 and 4-7). The constancy of the lower intersection temperature (discussed in section 4.2.4) seems to indicate a two phase structure, intermediate between the glass-like and rubber-like states, for the polymer in this region so that the Arrhenius equations are not applicable.[8,98]

A general feature of Tables 4-19, 4-22 and 4-23 is that E_D values below the intersection temperatures T_1 and T_2 are always less than those above T_1. Similar observations have been made for gases diffusing in polyvinyl acetate,[7,8] for vapours diffusing at very low concentrations in polyvinyl acetate, polystyrene and polymethyl methacrylate[11] and for water vapour and carbon dioxide diffusing in polyvinyl chloride-polyvinyl acetate copolymer films.[33,54] This behaviour was also predicted by Brandt[58] who believed that the change of activation energy for diffusion at the glass transition can be understood as a consequence of the change of thermal expansion at this

point. With the exception of the unplasticised polymer/neon system, the values of D_L below T_1 are always greater than would be expected from a linear extrapolation of the D_L values above T_1 (see Fig.4-5, 4-11 to 4-14). A resemblance between the shape of these log D_L vs. $\frac{1}{T}$ plots and the specific volume vs. temperature plots is apparent.[98]

For diffusion of gases in rubbers the activation energy for diffusion approaches the activation energy for viscous flow of the rubber.[45,48] The activation energy for self diffusion of unplasticised polyvinyl chloride has been calculated to be about 34 K.cal.mole^{-1} at 25°C.[143] Values of E_D below the intersection temperatures do not reach a quarter of this value so that the diffusion may not involve the movement of polymer segments of the size contributing to viscous flow. However, on passing above T_1 the activation energies E_D are at least twice as great as those below T_1, and the approach to the value quoted above is closer especially at the higher plasticiser concentrations. The activation energy for viscous flow might also be expected to be lower for plasticised polymer as compared to the unplasticised state, because the polymer facilitates the motions of polymer chain segments between different configurations.[59,74,143]

Notably with hydrogen the trend with increasing concentration of plasticiser is for E_D below the intersection temperatures to increase. Above the intersection temperatures a quasi-liquid state is considered to be present.[7,8,59,98] Apart from the anomalous behaviour of the unplasticised polymer/neon system, addition of plasticiser to the polymer appears to have little effect on E_D above T_1 except at the highest plasticiser content. E_D is considered to involve the work of separation of the surrounding medium in order to open up a passage through which the diffusing molecule can travel.[7,43] E_D is an important factor in determining the D_o value in the Arrhenius equation (1.3). The interpretation of D_o is discussed in the following section.

4.2.6 Interpretation of D_o

Values of D_o whether below the intersection temperatures T_1 and T_2 or above T_1 generally increase over a wide numerical range with increasing concentration of plasticiser (see Tables 4-19, 4-22 and 4-23). A comparably wide range of D_o values has also been obtained for diffusion of several gases in polyvinyl acetate over the glass transition region.[7,8] The magnitude of D_o according to the zone theory of activation may be considered as a measure of zone size. D_o depends, among other factors,

on E_D and the mean distance λ moved by the gas molecule in the unit diffusion process.

(a) Transition state theory

According to the transition state theory the expression for D_o is given by eq.(2.46). The values of the entropy of activation, $\Delta S^{\ddagger}$, associated with an Avogadro number of unit diffusion processes together with the corresponding heat $\Delta H^{\ddagger}$ and the free energy $\Delta G^{\ddagger}$ of activation are shown in Tables 4-24, 4-25 and 4-26. $\Delta S^{\ddagger}$ values were calculated from values of D_o above and below the intersection temperatures at conveniently chosen temperatures of 90°C and 0°C respectively using eq.(2.46). A value of $\lambda^2 = 10^{-15}(cm^2)$ was assumed for all the membranes. $\Delta H^{\ddagger}$ and $\Delta G^{\ddagger}$ can then be determined from eq.(2.45) and (2.38).

An interesting feature of Tables 4-24 to 4-26 is that $\Delta S^{\ddagger}$ for a given composition is consistently larger above the intersection temperatures than below them. $\Delta S^{\ddagger}$ is large and positive above T_1 (except for neon in unplasticised polymer) which, analogous to many elastomers,[6,43,44] indicates that an appreciable zone of activation is necessary in order for a unit diffusion process to take place. Below the intersection temperatures, it seems likely from the largely negative $\Delta S^{\ddagger}$ values that the gas diffusion process involves little disturbance in the polymer matrix

TABLE 4-24

Entropy, enthalpy and free energy of activation for diffusion of hydrogen according to the transition state theory (calculated at 273.16°K and 363.16°K)

Sheet	Volume fraction plasticiser v_1	Mean Intersection temp. T_1 (°C)	Below T_1			Above T_1		
			$\Delta S^{\ddagger}$ (e.u.)	$\Delta H^{\ddagger}$ (cal. $mole^{-1}$)	$\Delta G^{\ddagger}$ (cal. $mole^{-1}$)	$\Delta S^{\ddagger}$ (e.u.)	$\Delta H^{\ddagger}$ (cal. $mole^{-1}$)	$\Delta G^{\ddagger}$ (cal. $mole^{-1}$)
J1	0.0	70	-14.3	2160	6070	8.52	9980	6880
H	0.107	53	-14.4	1730	5650	8.89	9300	6070
F1	0.325	28	- 4.15	3990	5120	12.3	8980	4520
E	0.419	9	8.12	7410	5190	30.1	13570	2640

TABLE 4-25

Entropy, enthalpy and free energy of activation for diffusion of neon according to the transition state theory (calculated at 273.16°K and 363.16°K

Sheet	Volume fraction plasticiser v_1	Mean intersection temp. T_1(°C)	Below T_1			Above T_1		
			$\Delta S^{\ddagger}$ (e.u.)	$\Delta H^{\ddagger}$ (cal. mole^{-1})	$\Delta G^{\ddagger}$ (cal. mole^{-1})	$\Delta S^{\ddagger}$ (e.u.)	$\Delta H^{\ddagger}$ (cal. mole^{-1})	$\Delta G^{\ddagger}$ (cal. mole^{-1})
G	0.194	39	-2.31	5320	5950	27.2	14520	4650
F1	0.325	28	0.62	5730	5560	25.4	13160	3920
E	0.419	9	-3.78	4260	5290	40.7	16730	1960

TABLE 4-26

Entropy, enthalpy and free energy of activation for diffusion of neon according to the transition state theory (calculated at 273.16°K and 363.16°K)

Sheet	Upper intersection temp. T_1(°C)	Lower intersection temp. T_2(°C)	Below T_2			Above T_1		
			$\Delta S^{\ddagger}$ (e.u.)	$\Delta H^{\ddagger}$ (cal. mole^{-1})	$\Delta G^{\ddagger}$ (cal. mole^{-1})	$\Delta S^{\ddagger}$ (e.u.)	$\Delta H^{\ddagger}$ (cal. mole^{-1})	$\Delta G^{\ddagger}$ (cal. mole^{-1})
J1	70	54	-19.8	830	6250	-14.1	2410	7530
J2	69	54	-20.3	670	6220	-13.9	2500	7530

surrounding the penetrant in the formation of the transition state.[2.7,48]

There is also a trend, notably with hydrogen diffusion, towards increasing entropy of activation with increasing plasticiser concentration whether above or below the transitions. The addition of plasticiser molecules appears to induce an increasing disturbance of the polymer segments around the gas probe molecule during transition state formation.[2,7]

A linear plot of $\Delta S^{\ddagger}$ against E_D or $\frac{E_D}{T}$ was predicted by Barrer[45,56] for a process in which the activation energy is shared between a number of degrees of freedom in a zone of activation. The resultant plots for hydrogen and neon diffusion in the regions above and below the transitions are shown in Figs.4-18 and 4-19 respectively. Above the intersection temperatures the line shown in Fig.4-18 may be represented by:

$$\Delta S^{\ddagger} = -26.6 + 1.37 \frac{E_D}{T}$$

and below the intersections the equation (see Fig.4-19) is:

$$\Delta S^{\ddagger} = -24.9 + 1.15 \frac{E_D}{T}$$

The slopes of corresponding equations for various gases

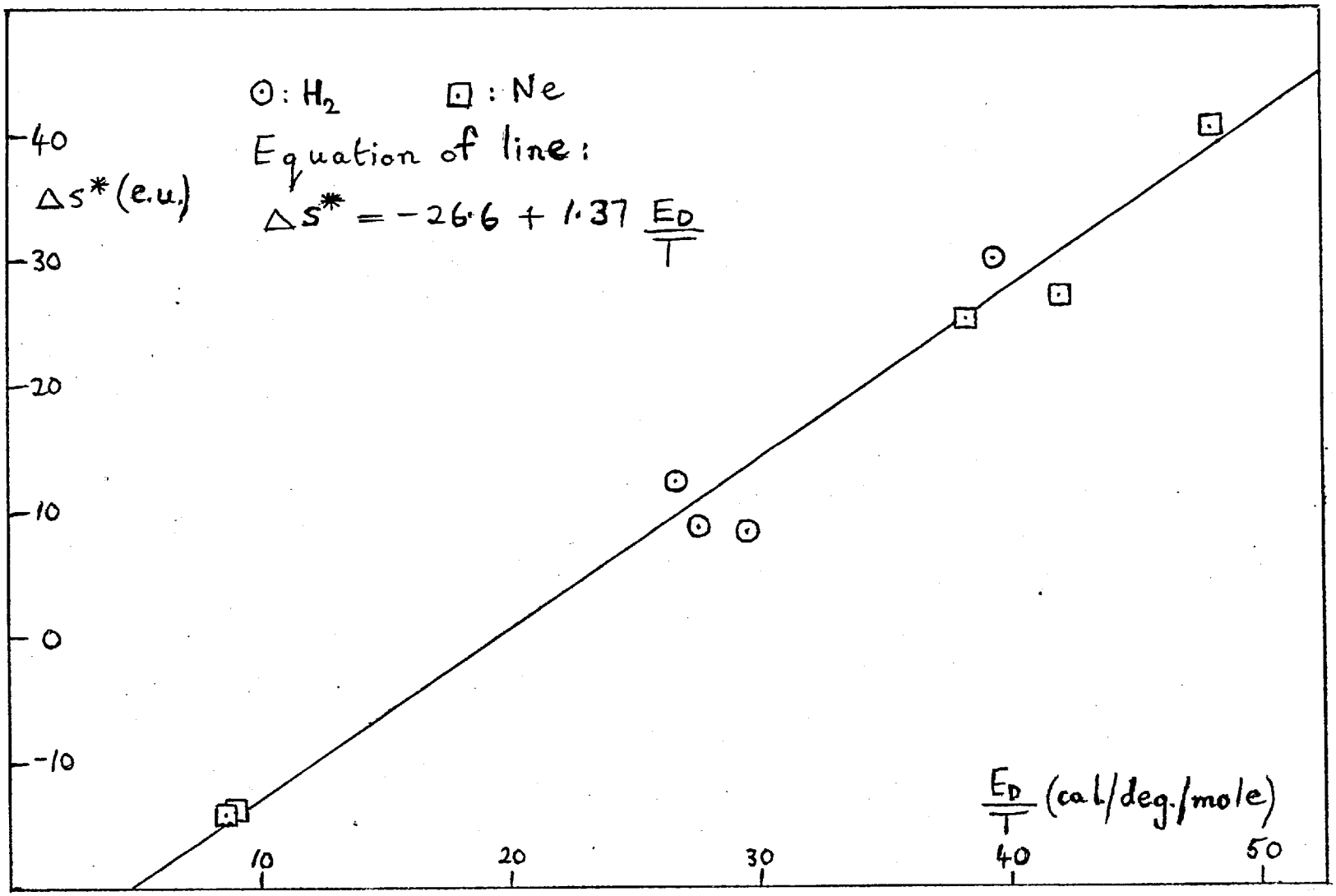


Fig 4-18 Plot of Δs^* vs. $\frac{E_D}{T}$ above the intersection temperatures T (calculated T for $T = 363.16°K$)

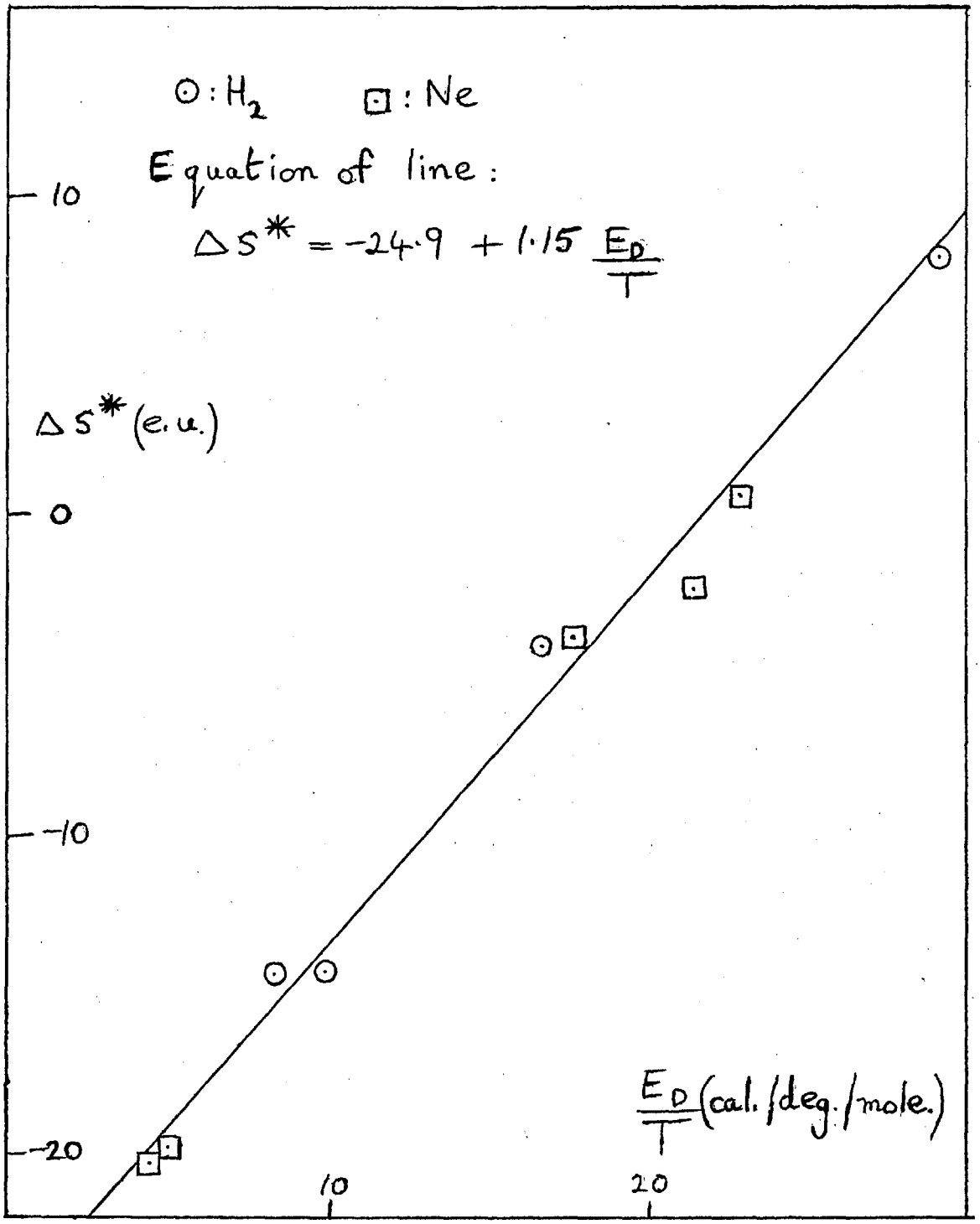


Fig. 4-19 Plot of ΔS^* vs. $\frac{E_D}{T}$ below the intersection temperatures T_1 and T_2 (calculated for $T = 273.16^\circ K$)

diffusing in silicone and natural rubbers[43,48] and in polyvinyl acetate[7] above its glass transition region were in the range 0.5 to 0.7. The significance of these and other functional relationships will be discussed in section 4.2.7.

(b) Zone theory

Attempts were made to deduce the number of degrees of freedom f among which the total activation energy is shared in any zone by means of eq.(2.52) and the method explained therein. Values of $\nu = 2.5 \times 10^{12}(sec^{-1})$, $\lambda^2 = 10^{-15}(cm^2)$ and $p_f = \frac{1}{6}$ were assumed in the calculation of f. The values of f so obtained are shown in Table 4-27 where f is quoted at 273.16°K (corresponding to the region below T_1) and at 363.16°K (corresponding to the region above T_1).

TABLE 4-27

Number of degrees of freedom f sharing in the diffusion process

Sheet	Volume fraction plasticiser v_1	Gas	Mean intersection temp. T_1 (°C)	f	
				Below T_1	Above T_1
J1	0.0	H_2	70	-	17
H	0.107	H_2	53	-	24
F1	0.325	H_2	28	2	>100
E	0.419	H_2	9	15	>100
G	0.194	Ne	39	3	>100
F1	0.325	Ne	28	5	>100
E	0.419	Ne	9	3	>100

The value of f is very sensitive to the value of the product $p_f \nu \lambda^2$. An interpretation of the analogous problem of viscous flow[56] suggested values of p_f of about $\frac{1}{6}$ to about 10^{-3}. Also values of λ^2 from 10^{-15} to 10^{-13} (cm^2) have been proposed[7,43] so that the range in $p_f \nu \lambda^2$ may be appreciable. The dashes in Table 4-27 indicate that f is so small that the experimental value of log D_o fails to give a satisfactory value of f for the value of $p_f \nu \lambda^2$ assumed. Above T_1 the method incorporating eq.(2.52) could not be used for the satisfactory determination of f of magnitude greater than 100. Again there are indications that, above the transitions T_1, the gas diffusion process involves a considerable disturbance in the polymer matrix surrounding the probe molecule in the formation of the activated zone.[43] However, diffusion of a small gas atom or molecule below T_1 requires a much smaller number of chain segments to be loosened for a successful unit diffusion process to take place.[7,43,48]

4.2.7 Functional relationships

Linear relationships have been observed when $\Delta S^{\ddagger}$ or log D_o is plotted against E_D or $\frac{E_D}{T}$ for a number of diffusion systems.[3,6,7,43,56,57] The fulfillment of this condition, which is valid for viscous flow in many kinds of liquids and diffusion in elastomers, is evidence

for the existence of internal mobility in the system concerned. Barrer[56] pointed out, however, that the most general relationship is between log D_o and $\frac{E_D}{T}$ (see also section 1.2).

The validity of this relationship for T = 273.16°K is shown in Fig.4-20 (representing data for hydrogen and neon obtained in this work) and Fig.4-21 (representing data for permanent and inert gases in polyvinyl acetate[7,8] and for helium, neon and hydrogen diffusing in various elastomers[2,6,48]). The equations of the lines are respectively:

$\log D_o = -6.78 + 0.21_3 \frac{E_D}{T}$ (Fig.4-20: polyvinyl chloride)

$\log D_o = -4.24 + 0.13_4 \frac{E_D}{T}$ (Fig.4-21: polyvinyl acetate, various elastomers)

In Fig.4-20 the wide range of both D_o and $\frac{E_D}{T}$ values for the polyvinyl chloride is apparent and the slope of the line shown is 0.21. This is in agreement with the predicted slope of 0.22 which is the maximum value to be expected only if the range in log D is negligible compared with that in $0.22 \frac{E_D}{T}$ (see section 1.2). This situation was also approached in some measurements of diffusion of paraffins in cross-linked rubbers made by Aitken and Barrer.[44]

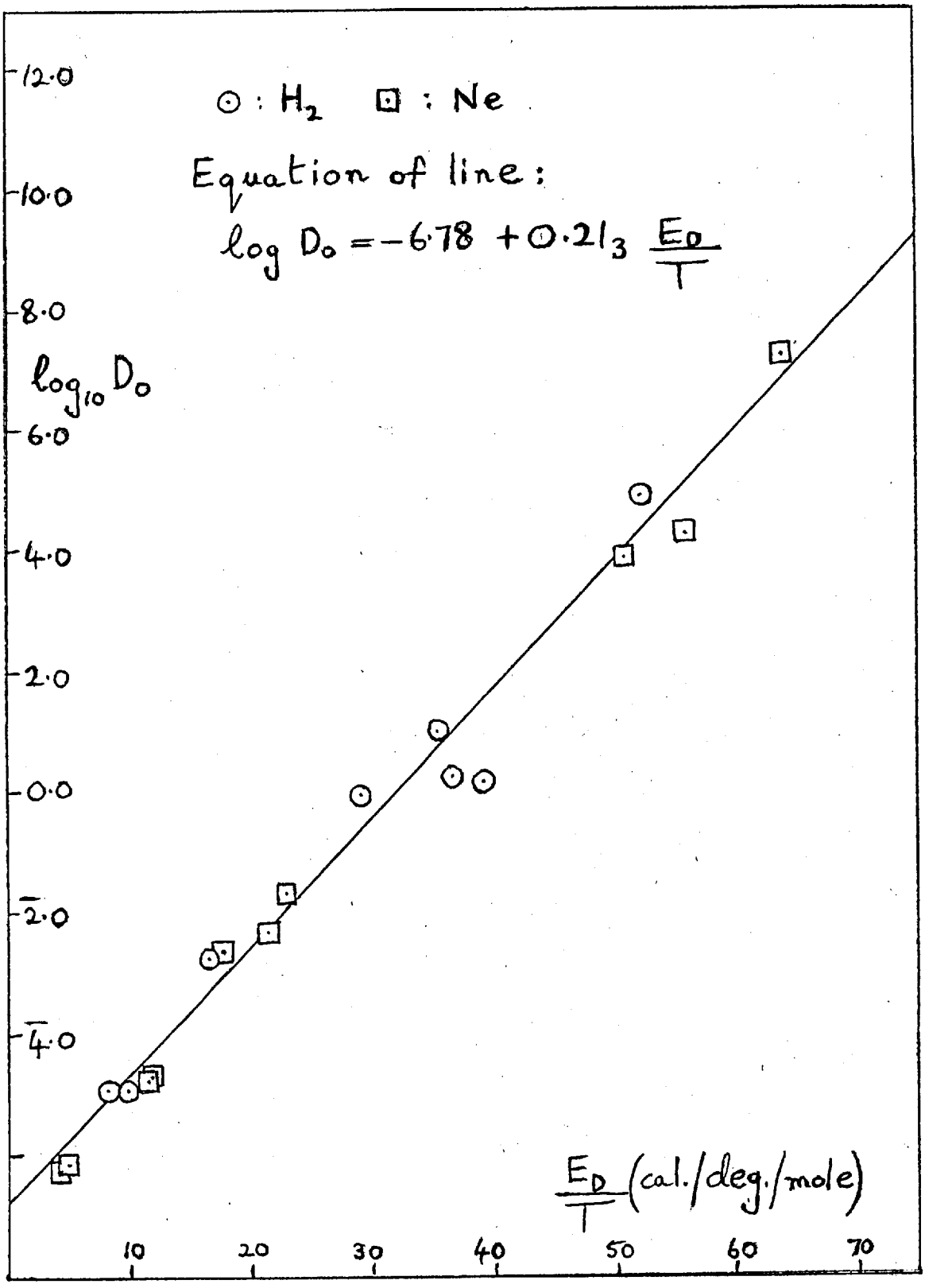


Fig. 4-20 $\text{Log}_{10} D_o$ vs. $\frac{E_D}{T}$ for polyvinyl chloride at $T = 273.16°K$

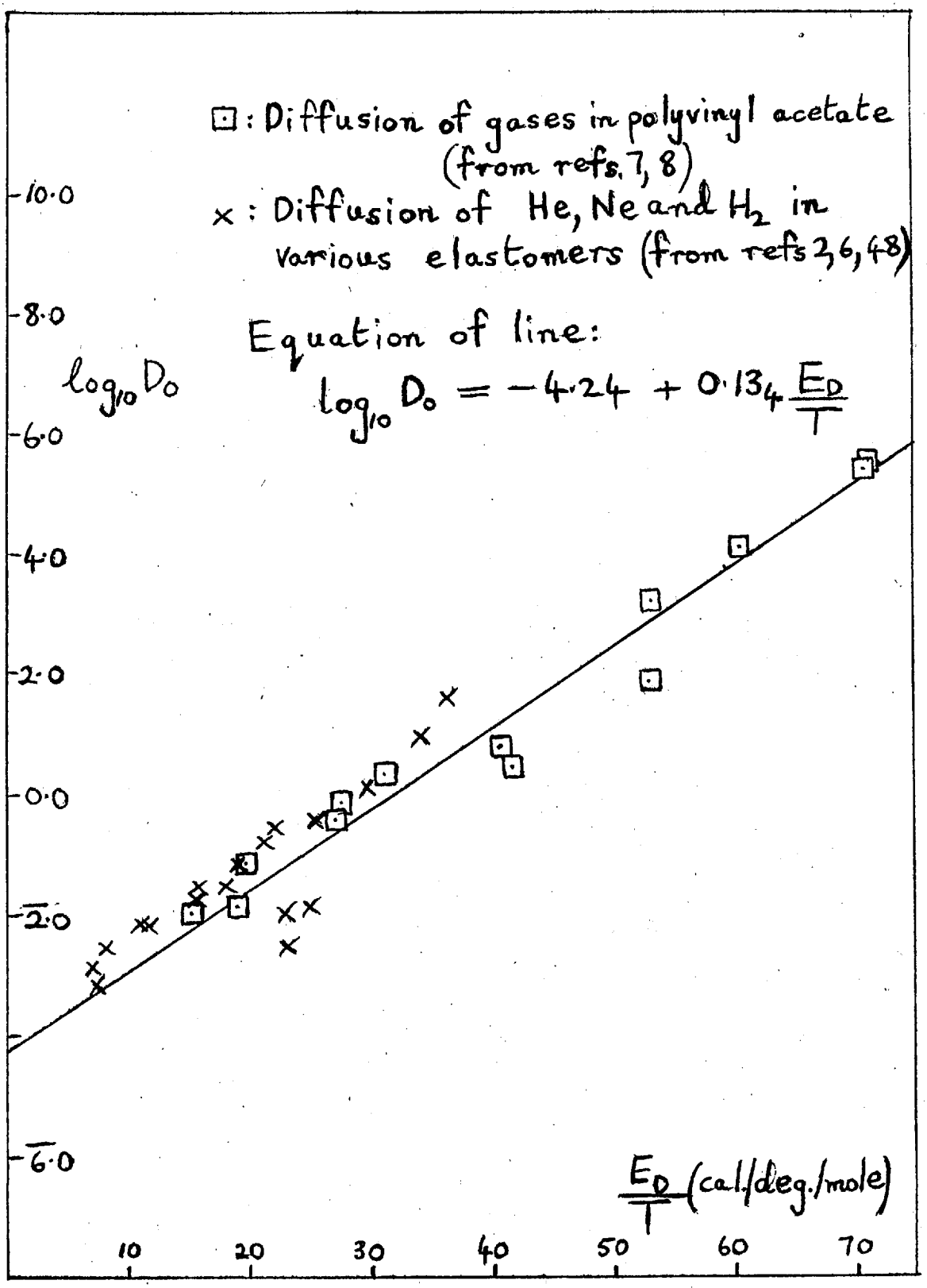


Fig. 4-21 : $\text{Log}_{10} D_o$ vs. $\frac{E_D}{T}$ for several gas-polymer systems ($T = 273.16°K$)

For gaseous diffusion in numerous elastomers and self-diffusion in liquids exhibiting a wide range of D_o values it was found that[48]:

$$\log D_o = -4.20 + 0.13_6 \frac{E_D}{T}$$

Gaseous diffusion data over the glass transition region of polyvinyl acetate, whose behaviour might be expected to show some resemblance to polyvinyl chloride, is included in Fig.4-21. The equation deduced from Fig.4-21 bears, however, a close resemblance to the above equation[48] for elastomers and liquids.

Seeing that D_o and $\Delta S^{\ddagger}$ are connected by eq.(2.46) from the transition state theory, the linear relationships demonstrated in section 4.2.6(a) between $\Delta S^{\ddagger}$ and $\frac{E_D}{T}$ are therefore a natural consequence of the log D_o vs. $\frac{E_D}{T}$ relationship. Thus, while D_o is a measure of the zone size according to the zone theory, the magnitude of $\Delta S^{\ddagger}$ provides a comparable measure of the degree of disturbance in terms of the transition state theory.

4.3 Equilibrium Phenomena

4.3.1 The solubility coefficients

The apparent dynamic solubility coefficients σ_D and σ_E of hydrogen dissolving in unplasticised and plasticised polymer are listed in section 4.1.1 (Tables 4-1 to 4-4), and those for neon are presented in section 4.1.2 (Tables 4-5 to 4-9). These tables also include data of $\bar{P}$ and D_L from which values of σ_D were deduced by means of eq.(2.9). σ_E was deduced by the early approximation analysis from the intercepts of plots of $\log (t_{\frac{1}{2}} \frac{dp_1}{dt})$ vs. $\frac{1}{t}$ followed by the use of eq.(2.15). Typical plots of $\log (t_{\frac{1}{2}} \frac{dp_1}{dt})$ vs. $\frac{1}{t}$ have been shown in Figs.4-1 to 4-3 and values of σ_E are given in Tables 4-1, 4-2 and 4-4 for hydrogen and Tables 4-7 to 4-8 for neon. Agreement between σ_D and σ_E was usually reasonably good although deviations were sometimes apparent, for example in the $J1/H_2$ system (Tables 4-1 and Fig.4-24). The accuracy of the determination of σ_E was largely dependent on the accuracy of the value of the intercept.

Static solubility coefficients, σ_s, of hydrogen and neon in unplasticised J3 and plasticised F2 polymer have also been measured over a suitable range of temperatures (see Tables 4-10A, 4-11A, 4-12A and 4-13A). These values of σ_s were deduced from the slopes of the plots

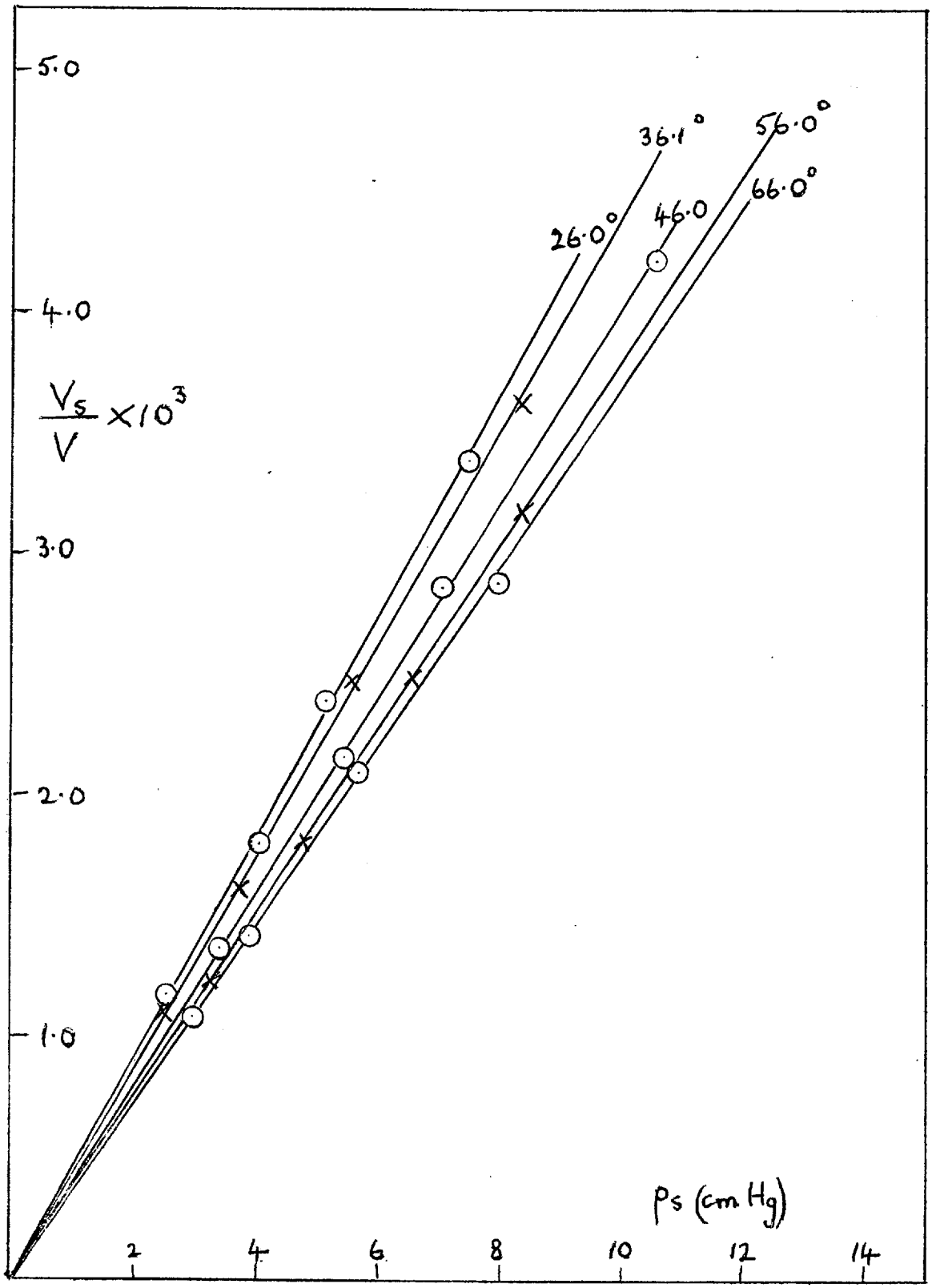


Fig. 4-22 Static solubility measurement for J3 : H_2

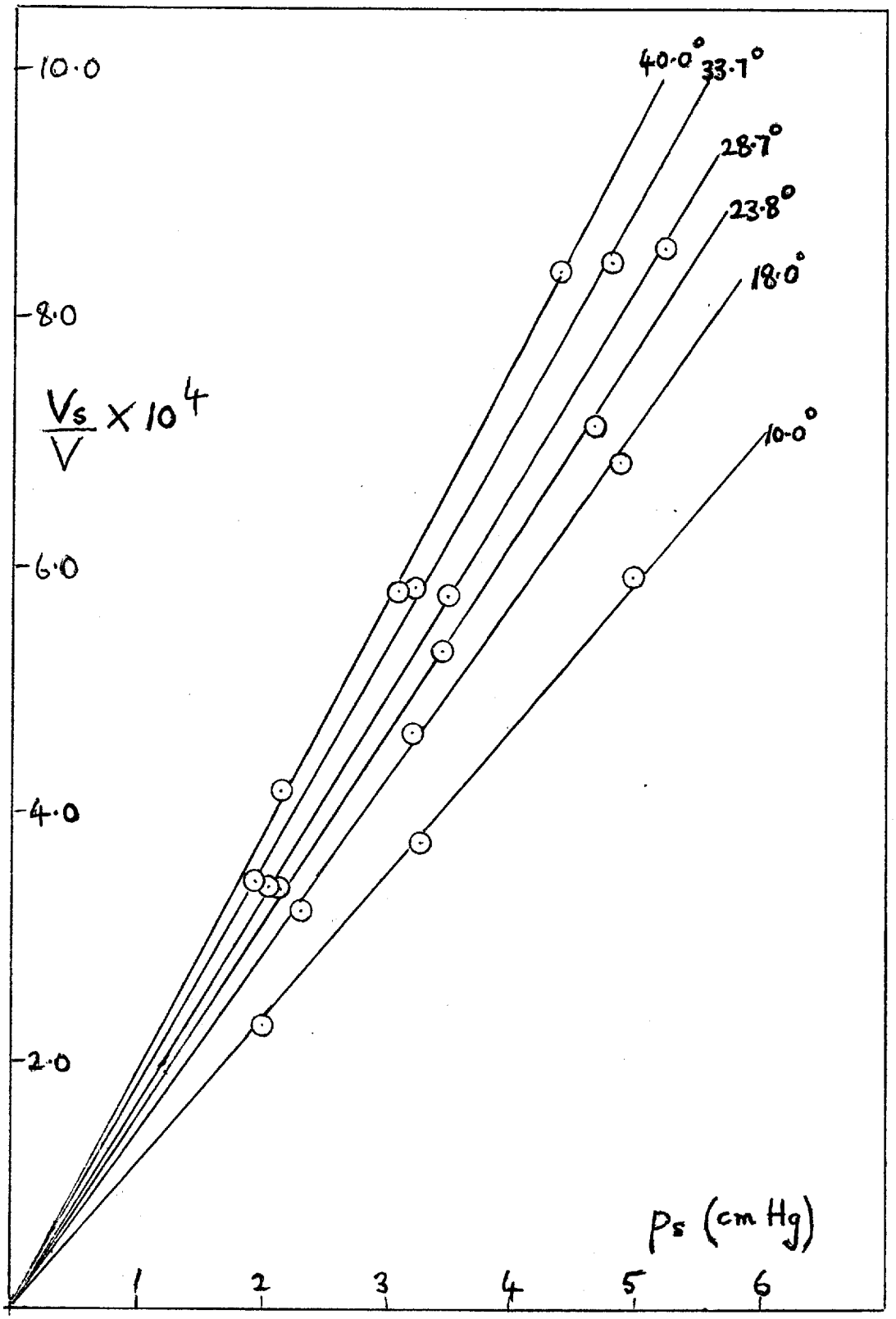


Fig. 4-23 Static solubility measurement for F2 : Ne

of $\frac{V_s}{V}$ against p_s of which two examples are shown in Figs.4-22 and 4-23. Experimental data of $\frac{V_s}{V}$ and p_s are given in Tables 4-10, 4-11, 4-12 and 4-13. Measurements were made at three or four pressures, p_s, at each thermostat temperature, and no departures from Henry's law were observed.

(a) Unplasticised polyvinyl chloride

The apparent dynamic solubility coefficients σ_D and σ_E in the unplasticised polymer J1 and J2 are given in Tables 4-1, 4-5 and 4-6 and their logarithms are plotted against $\frac{1}{T}$ ($^oK^{-1}$) in Figs.4-24 to 4-27. The history and time dependent effects, discussed in section 4.2.1(a), are also reflected in the value of σ_D and σ_E (see Figs. 4-24 and 4-26) where, as before, the numbers associated with the experimental runs performed on J1 represent the order in which they were determined. The 'settled' values of σ_D and σ_E (runs 11-20 in Fig.4-24 and runs 7-21 in Fig.4-26), largely determined after annealing at about 85°C, were reproducible within the time of the experiments. The reproducible σ_D and σ_E values were usually below those obtained from experiments (runs 1-7 in Fig.4-24 and runs 1-6 in Fig.4-26) conducted on the non-equilibrium state of the polymer below the glass transition T_1 of 70°C. The intersection temperatures T_1 and T_2 (see

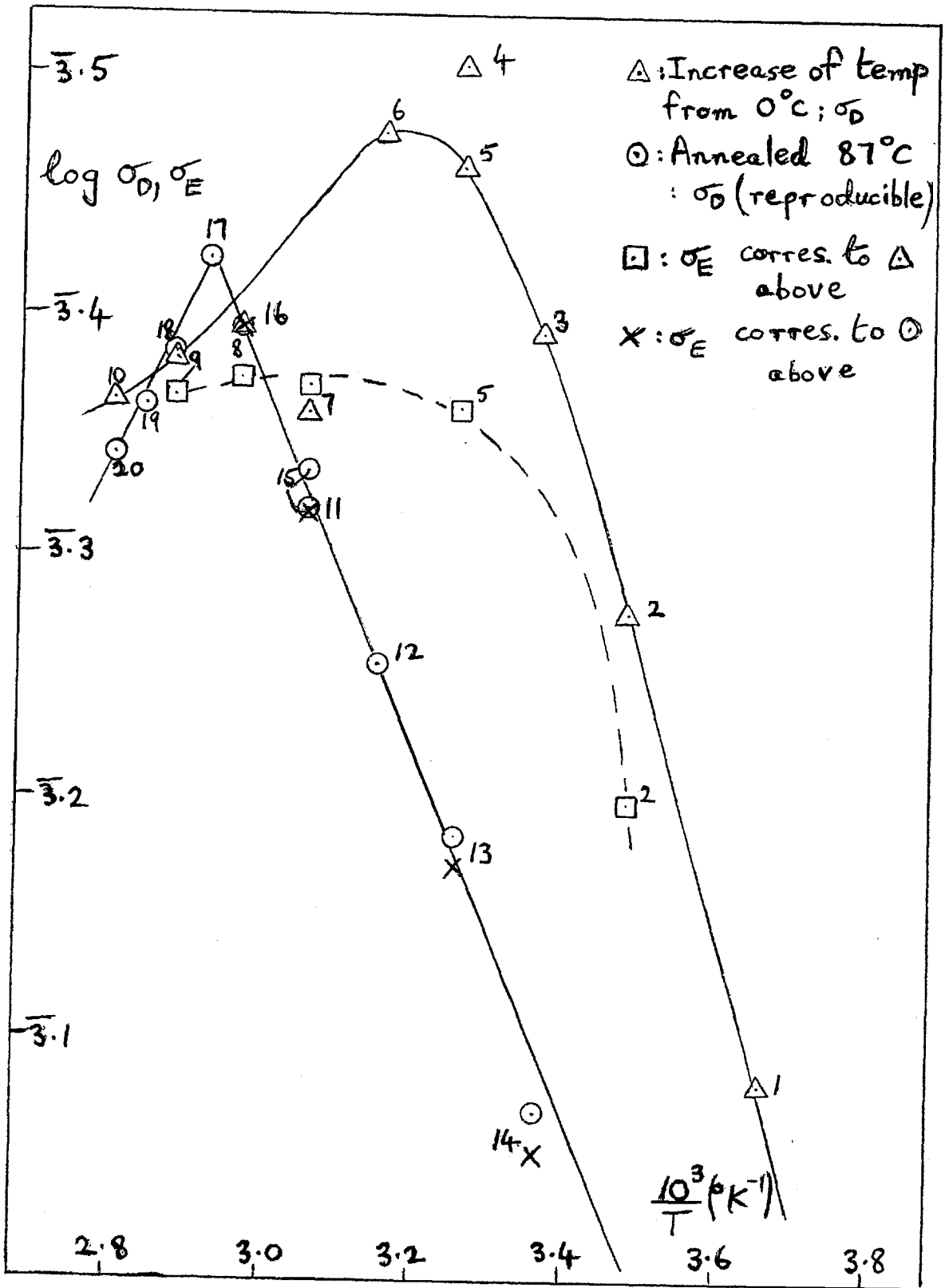


Fig. 4-24 Log. σ_D, σ_E vs. $\frac{1}{T}$ (°K^{-1}) for J1 : H_2 gas

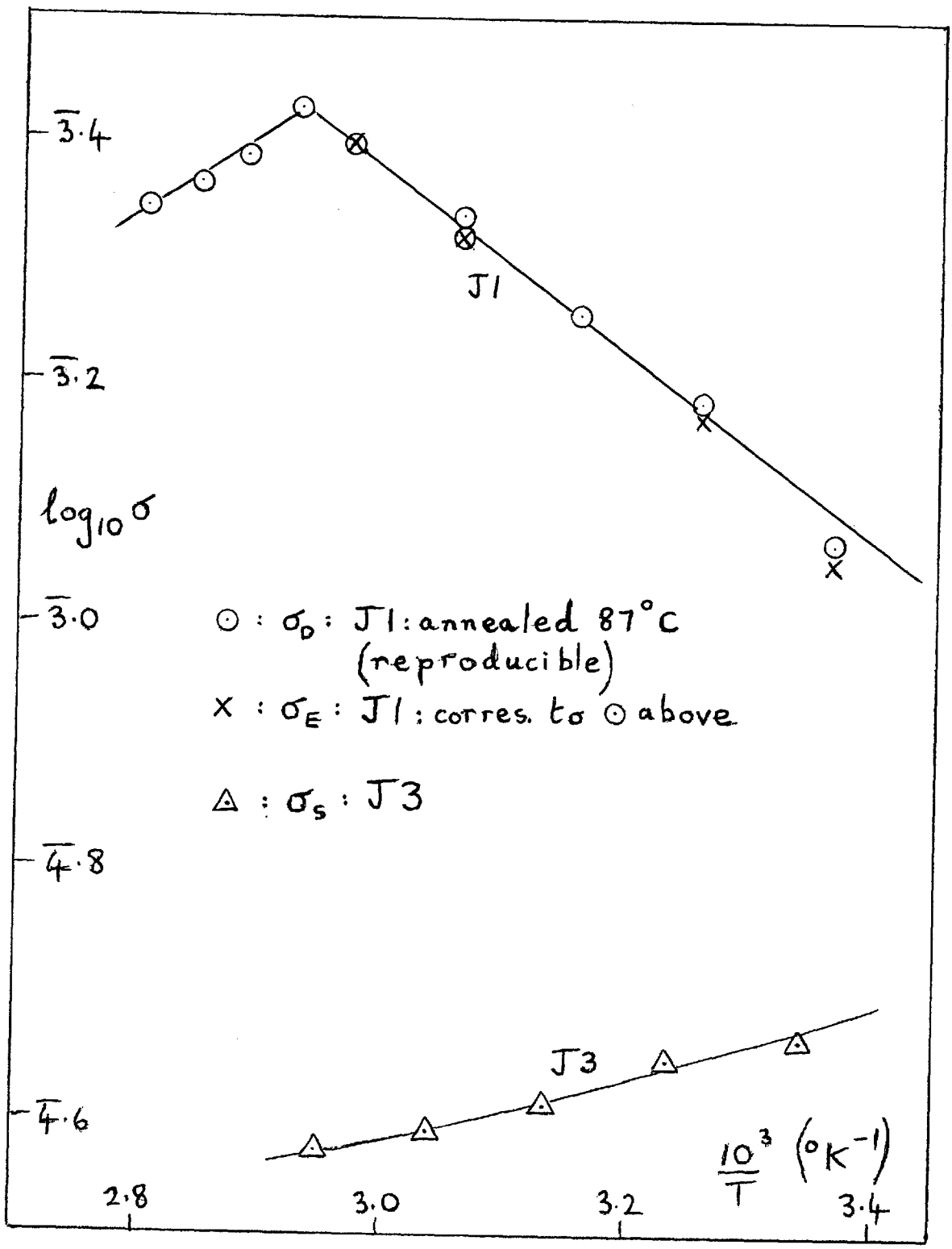


Fig. 4-25 $\text{Log}_{10}\sigma$ vs. $\frac{1}{T}$ for J1, J3 : H_2 gas

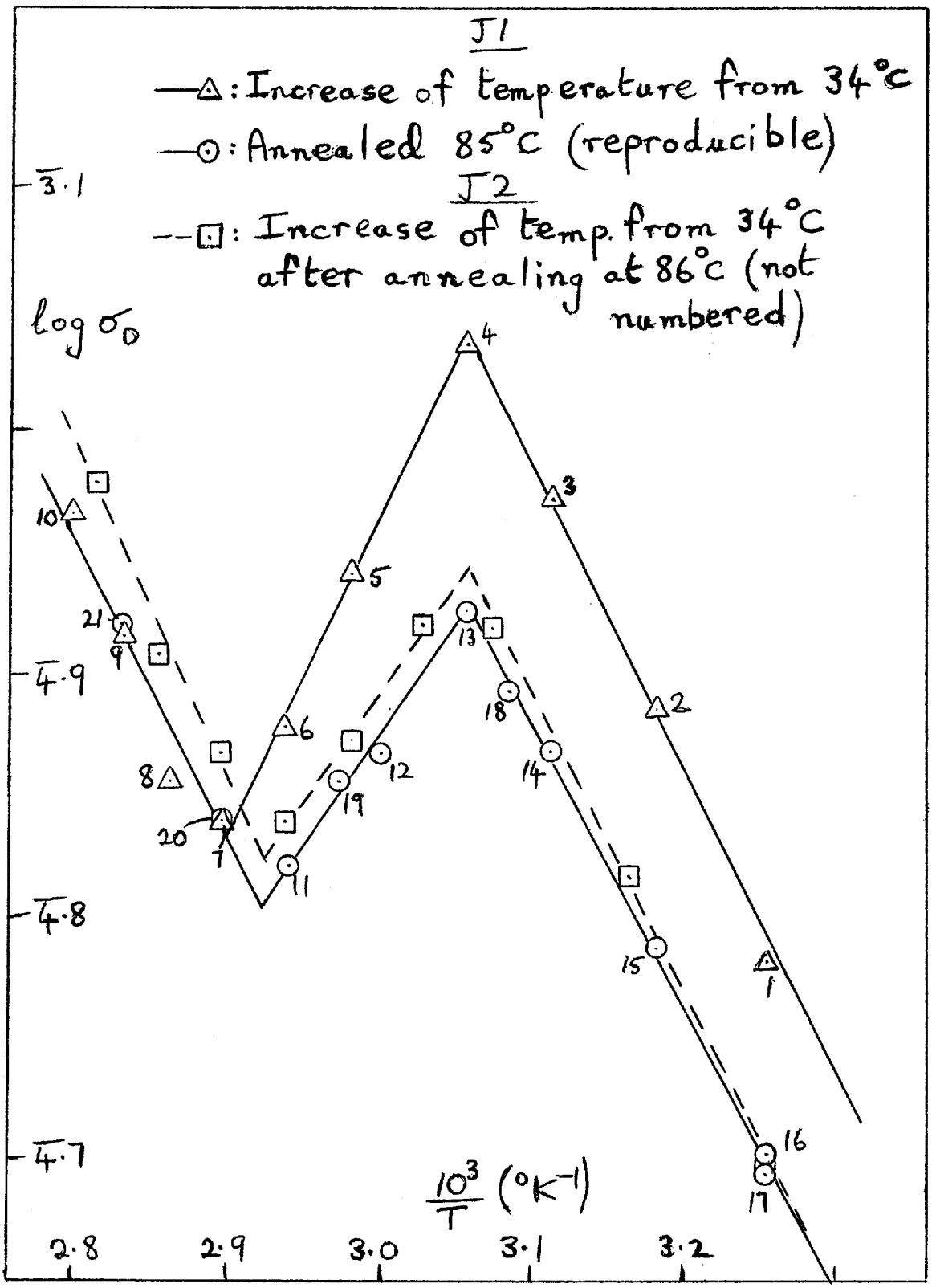


Fig. 4-26 Log. σ_D vs. $\frac{1}{T}$ (°K⁻¹) for J1 and J2 : Ne gas

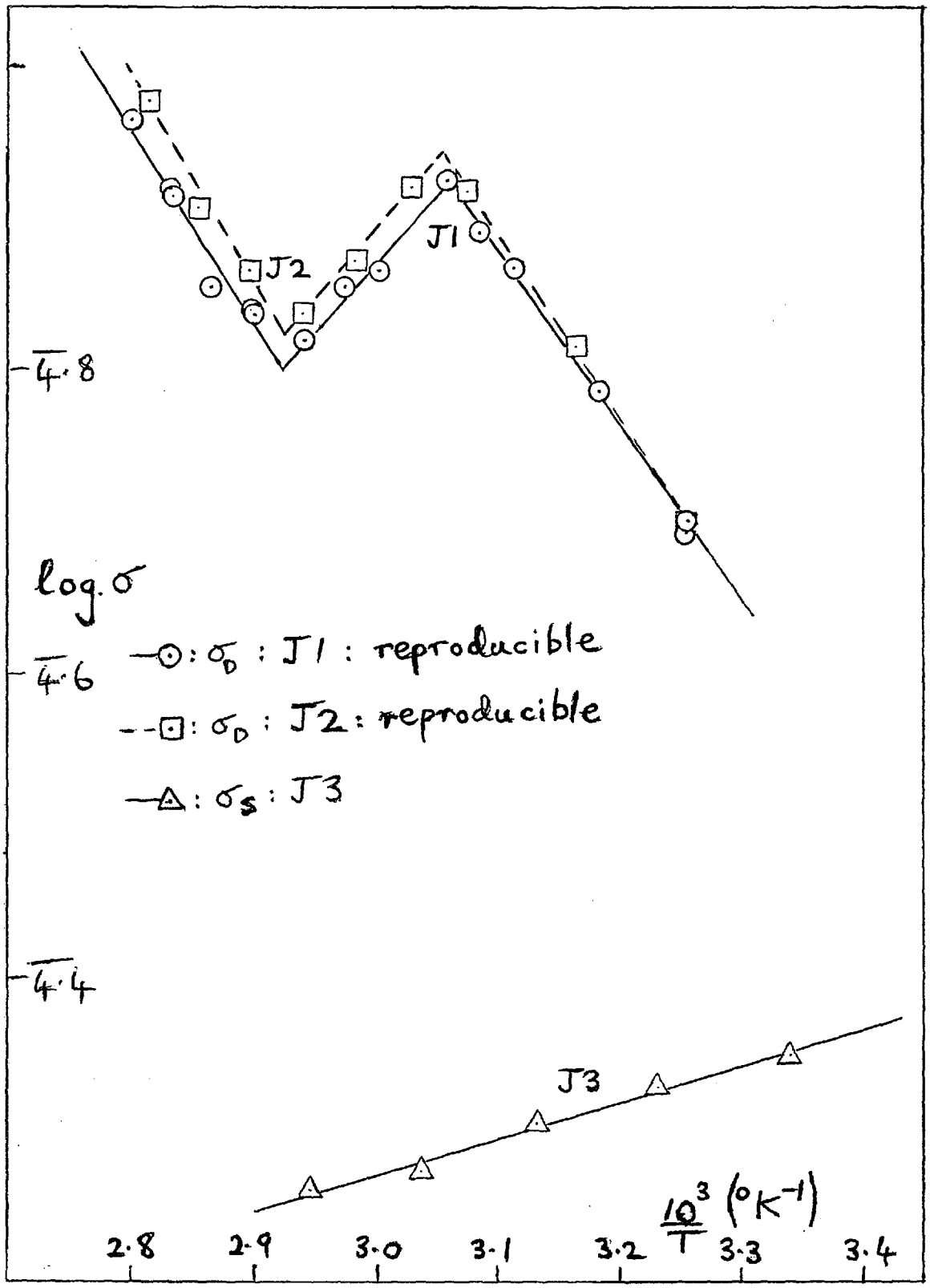


Fig. 4-27 Log. σ vs. $\frac{1}{T}$ ($^{\circ}K^{-1}$) for J1, J2 and J3 : Ne gas

section 4.2.4) are observed in plots of log σ_D vs. $\frac{1}{T}$ in the form of a maximum T_1 (see Fig.4-24) for the J1/H_2 reproducible data, and a maximum T_2 and a minimum T_1 (see Fig.4-26) for the J1, J2/Ne reproducible data. These correspond closely with the previously observed values of T_1 and T_2 from log $\bar{P}$ and log D_L vs. $\frac{1}{T}$ plots for these systems (see Figs.4-4 to 4-7 and section 4.2.4).

The anomalous behaviour of the temperature coefficients of σ_D (see section 4.3.3) brings into question the validity of the dynamic method employed in determining the correct values of the solubility coefficients. The dynamically derived solubility coefficients could be assumed to be correct only if the static and dynamic methods of solubility measurement yielded the same results. For this reason the static solubility coefficients σ_s of hydrogen and neon in an unplasticised sheet J3 were determined between 26°C and 66°C, corresponding to the region below the transition T_1 (70°C), and are listed in Tables 4-10A and 4-12A. The polymer sample J3 was taken from the same sheet as the permeation membranes J1 and J2 to minimise any differences between them and annealed at about 85°C under vacuum. Unfortunately σ_s in the temperature region above T_1 (70°C) could not be measured because mercury was liable to distil into the rest of the

apparatus from the reservoir R below the polymer sample (see Fig.3-4). Plots of log σ_s vs. $\frac{1}{T}$ are shown in Figs.4-25 and 4-27, where plots of the reproducible dynamic values of log σ for J1 and J2 are also presented for comparison.

By comparing the values of σ_s and σ_D given in Tables 4-10A and 4-12A, it is apparent that σ_D is 3 to 7 times greater than σ_s for hydrogen and 2-4 times greater for neon. Allowing for the greater inaccuracy of the dynamic values, σ_D, which arises from the interdependence of $\overline{P}$ and D_L, values of σ_D are significantly above the equilibrium values σ_s. σ_D may therefore be regarded only as an apparent dynamic solubility coefficient. σ_s and σ_D values for the solution of H_2, He and Ne in unplasticised polyvinyl acetate were found to be in agreement within experimental error above the transition T_g[9]. Below T_g, however, σ_s was significantly greater than σ_D and it was inferred from this that gas molecules, sorbed into regions of minimum density, contribute only a little to the diffusion flux.[7,9] This relation between the solubility coefficients is, however, the reverse of that found in this work.

(b) Plasticised polyvinyl chloride

The apparent dynamic solubility coefficients σ_D and σ_E for the plasticised sheets are given in Table 4-2 to

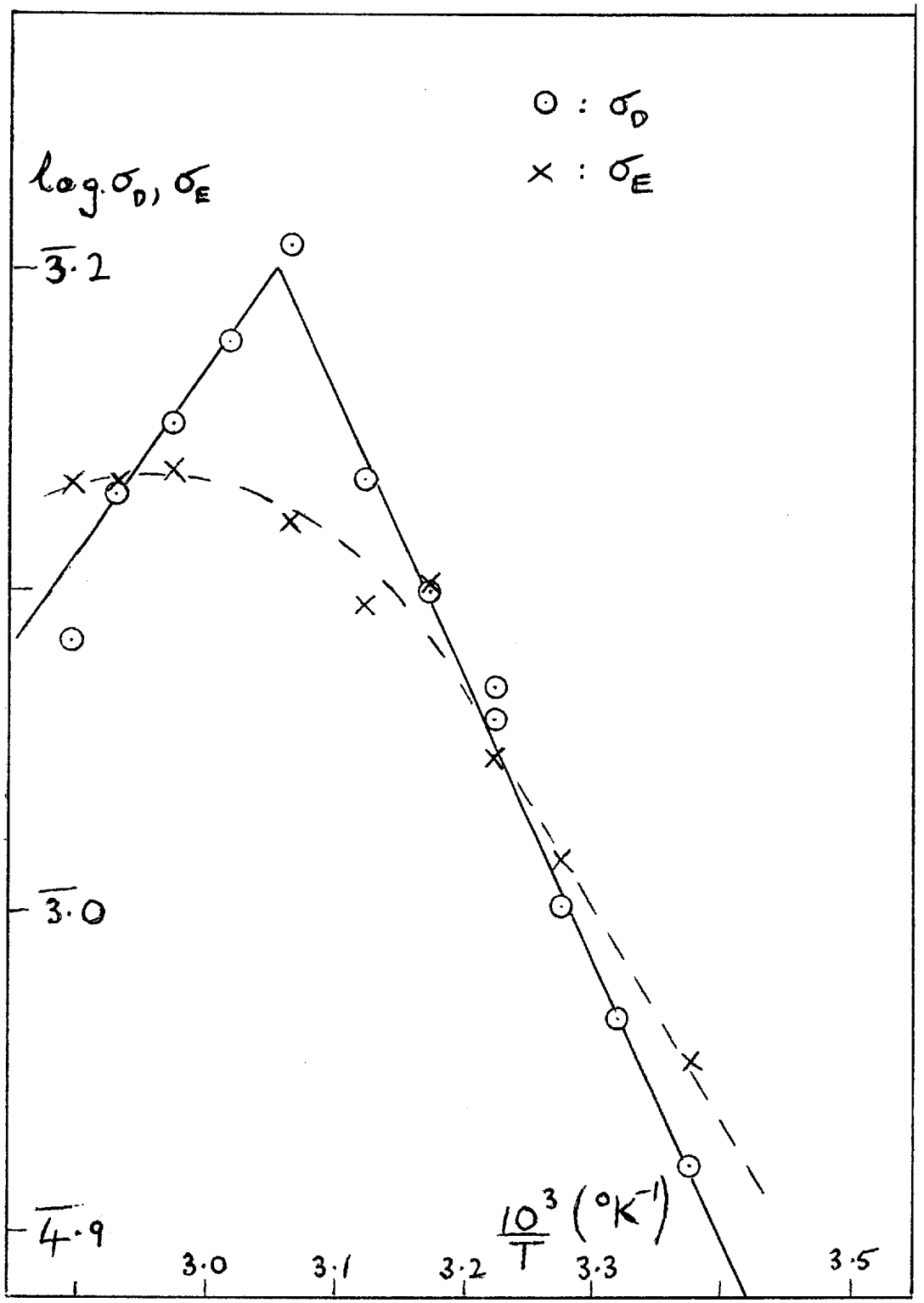


Fig. 4-28 Log. σ_D, σ_E vs. $\frac{1}{T}$ for H: H_2 gas

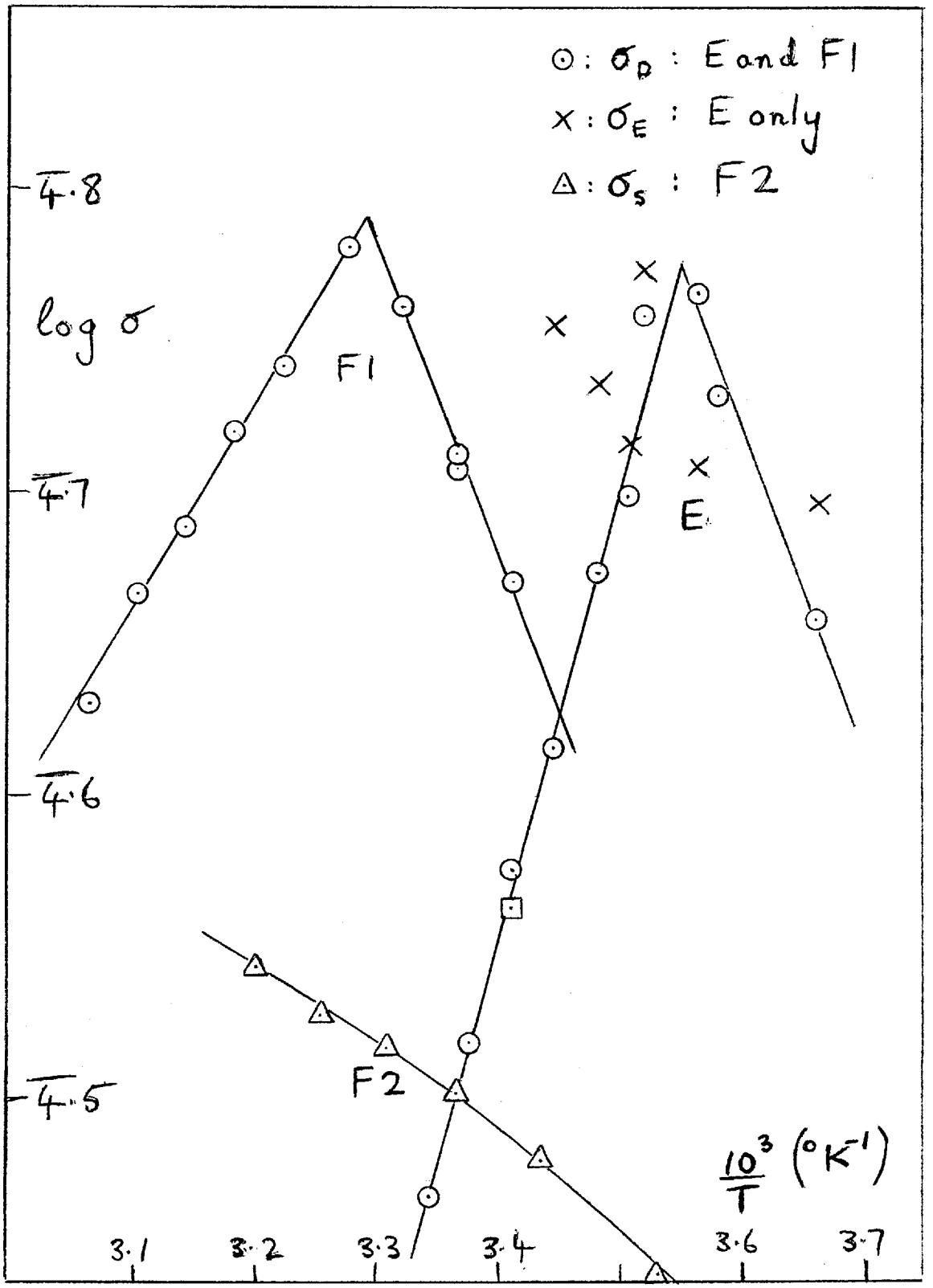


Fig. 4-29 Log σ vs. $\frac{1}{T}$ for E, F1 and F2 : H_2 gas

4-4 for hydrogen and Tables 4-7 to 4-9 for neon. Plots of $\log_{10}\sigma_D$ and σ_E vs. $\frac{1}{T}$ are shown in Figs.4-28 to 4-31. As already discussed in section 4.2.1(b) $\overline{P}$ and D_L were neither history nor time dependent so that it follows that σ_D, being the ratio of these two coefficients, was also reproducible. The plots of log σ_D vs. $\frac{1}{T}$ all showed a distinct maximum corresponding to the intersection temperatures T_1, previously observed in the other diffusion properties (see Figs.4-8 to 4-14 and section 4.2.4). Agreement between σ_D and σ_E was particularly good for the G/Ne system (Fig.4-30) although a smooth curve of log σ_E was perceptible in the region of T_1 for the sheet H/H_2 system (Fig.4-28).

For a plasticised sheet F2, values of $\log_{10}\sigma_s$, taken from Tables 4-11A and 4-13A, are also shown in Figs.4-29 and 4-31. F2 was taken from the same sheet which had been used for the permeation membrane F1. Comparing the absolute magnitudes of σ_D and σ_s for F2 in Tables 4-11A and 4-13A, it can be seen that σ_s is 50-80% of the value of σ_D for hydrogen and 60-100% for neon. This is more satisfactory agreement than was obtained for the unplasticised polymer. Neon appears to give slightly better agreement than hydrogen between σ_D and σ_s in both compositions J3 and F2. A noticeable feature of Figs.

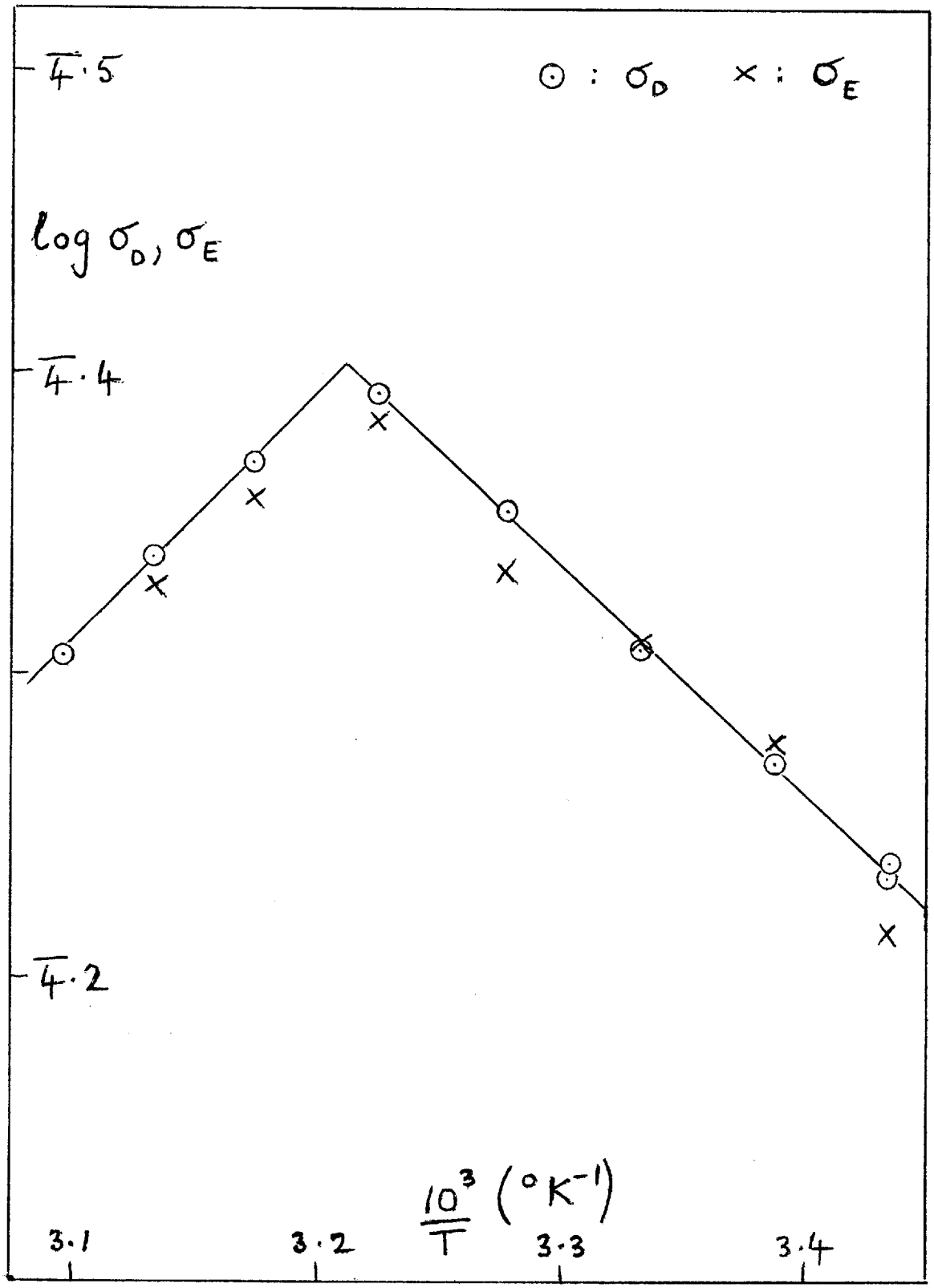


Fig. 4-30 Log σ_D, σ_E vs. $\frac{1}{T}$ for G : Ne gas

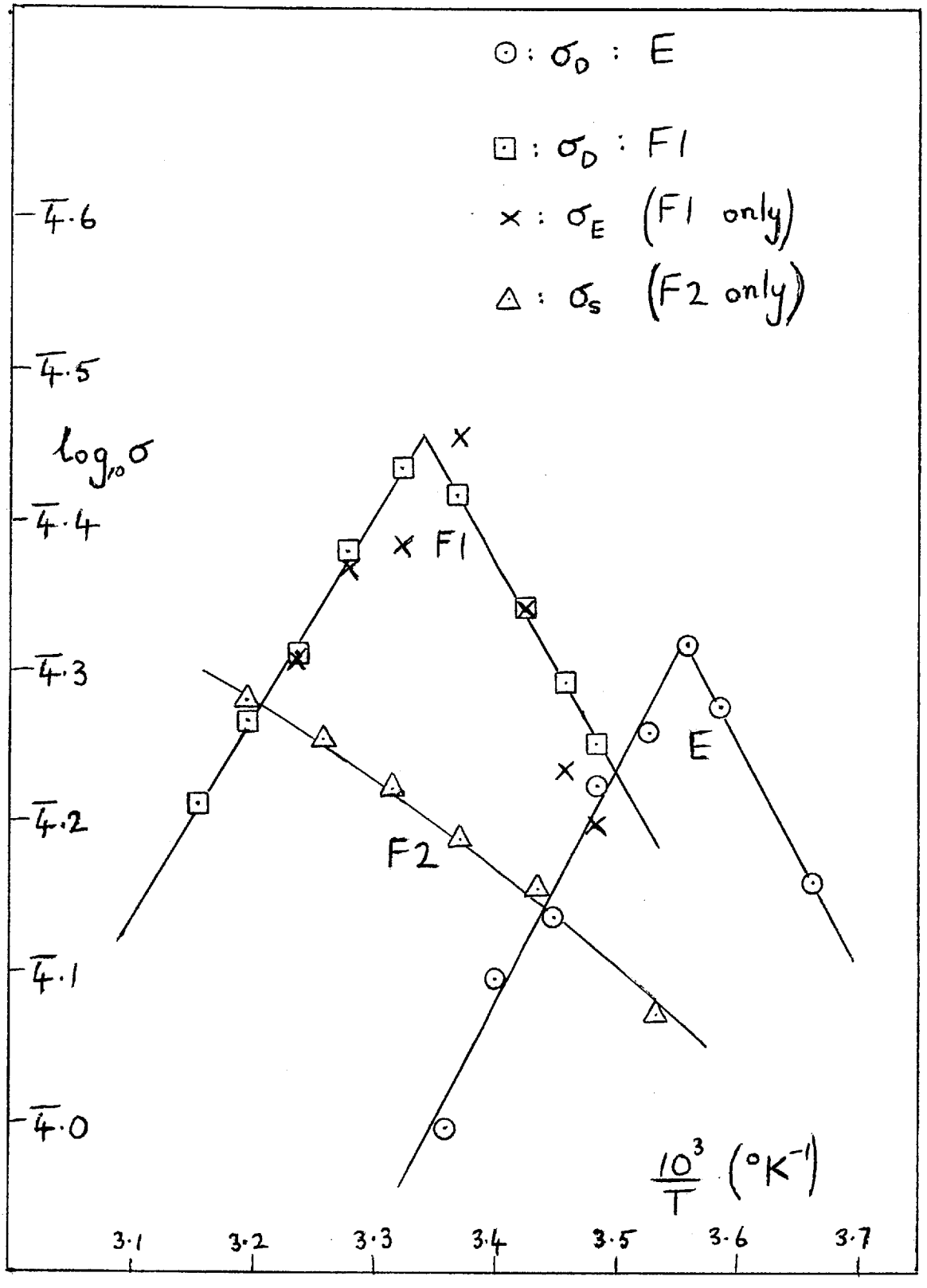


Fig. 4-31 Log σ vs. $\frac{1}{T}$ for E, F1 and F2 : Ne gas

4-29 and 4-31 is that the log σ_s vs. $\frac{1}{T}$ plots do not show a discontinuity at the intersection temperature T_1 for composition F, previously observed in the dynamic properties $\bar{P}$, D_L and σ_D (see Figs.4-9, 4-10, 4-12, 4-14, 4-29 and 4-31). The log σ_s values appear to lie on a curve which is slightly concave towards the $\frac{1}{T}$ axis. Once again the discrepancies between σ_D and σ_s lead to the conclusion that σ_D for the plasticised samples cannot be correct.

The magnitudes of σ_D and σ_s for plasticised and unplasticised polyvinyl chloride (see Figs.4-24 to 4-31) are in the order $\sigma_D(Ne) < \sigma_D(H_2)$ and $\sigma_s(Ne) < \sigma_s(H_2)$. This is in agreement with the solubilities of these gases in silicone rubber[48] and in polyvinyl acetate.[7,9]

4.3.2 Influence of plasticiser on the steady-state coefficients

For both neon and hydrogen, the values of the static solubility coefficient σ_s for the unplasticised polymer are larger than for the plasticised polymer at the lower temperatures (see Figs.4-25, 4-27, 4-29 and 4-31). σ_s values for a given gas appear to approach one another at the higher temperatures.

Tricresyl phosphate plasticiser in polyvinyl chloride could be non-uniformly distributed due to evaporation

of plasticiser from external surfaces of the polymer[103-108] The discrepancy between σ_D and σ_s might then arise from a non-uniform distribution of plasticiser because the diffusion coefficient of H_2 and Ne would then depend on x. Barrer[145] has considered the steady-state distribution of concentration across a membrane when $D = D_o [1 + f(x)]$. For the boundary conditions given in section 2.1.2 the rate, R, at which gas emerges from a unit area of the outgoing surface of the membrane is given by[145]:

$$R = \frac{D_o (C_2 - C_1)}{\int_o^{\ell} \frac{dx}{1 + f(x)}} \qquad (4.1)$$

When $f(x) = 0$, $D = D_o$ = constant and eq.(4.1) reduces to:

$$R = D \cdot \frac{C_2 - C_1}{\ell} \qquad (4.2)$$

which is the form obtained in eq.(2.5) for constant D. Values of the transient-state diffusion coefficient D_L were calculated from $L = \frac{\ell^2}{6D_L}$ (eq.2.10) also on the assumption that D is independent of x. If, however, $D = D_o [1 + f(x)]$ then the method of Frisch[153] gives[154]:

$$L = \frac{\int_0^{\ell}[1 + f(x)]^{-1} \int_x^{\ell} \int_x^{\ell}[1 + f(x)]^{-1}\, dx\, dx\, dx}{D_0 \int_0^{\ell}[1 + f(x)]^{-1}\, dx} \qquad (4.3)$$

and so a difference should arise between the diffusion coefficient D_s calculated from σ_s using $D_s = \frac{\bar{P}}{\sigma_s}$ (eq.2.9) and the diffusion coefficient D_L from eq. (2.10). Although a difference between D_s and D_L is observed for H_2 and Ne, (D_s being greater than D_L) the greater discrepancy is obtained for the unplasticised polymer (see Tables 4-10A, 4-11A, 4-12A and 4-13A). If $D_s = D_o [1 + f(x)]$ because of a non-uniform distribution of plasticiser, the difference between D_s and D_L would be expected only for the plasticised sheet F2. Therefore dependence of plasticiser concentration on x is not the factor contributing to the discrepancy between D_s and D_L and hence between the dynamic and static coefficients σ_D and σ_s. x dependence of D (if it is the cause of the discrepancy) exerts a greater effect in unplasticised polymer. Oxidation of surface layers has been noted in the case of rubber as a cause of such dependence.[117] Time dependence of D through slow relaxations could be an alternative explanation of the behaviour that has been observed, but seems ruled out by the reproducibility of the measurements of D in 'settled' membranes of the PVC.

4.3.3 Temperature dependence of the solubility coefficients

(a) Heat of solution

The plots of log σ_D vs. $\frac{1}{T}$ of H_2 and Ne in both unplasticised and plasticised polymer have been shown in Figs.4-24 to 4-31. Within the limit of experimental error, the reproducible data are virtually linear above and below the intersection temperatures T_1 and T_2. On calculating apparent heats of solution from the slopes according to eq.(1.4), a large positive value is obtained below T_1 (or T_2 for the J1, J2/Ne system), which changes to a large negative value above T_1 (except for the J1, J2/Ne system which exhibits a positive apparent heat above T_1). The heats of solution of permanent gases such as hydrogen, neon and helium in the majority of polymers[1,3,5,7,48,59,64] fall within the range of 1 to 2 K.cal.mole^{-1}. As the apparent heats of solution calculated from σ_D fall within the range of -7 to 7 K.cal.mole^{-1}, the temperature dependence of σ_D is obviously anomalous and its thermodynamic interpretation would not be meaningful. Nevertheless the values of σ_D for the plasticised and also the unplasticised polymer (after 'annealing') were reproducible even after a period of some weeks.

A knowledge of the equilibrium state of the dissolved gas molecules is important in understanding the diffusion process and the static solubility coefficient σ_s can be analysed in thermodynamic terms. Plots of log σ_s vs. $\frac{1}{T}$ for sheets of unplasticised (J3) and plasticised (F2) polymer have been shown in Figs.4-25, 4-27, 4-29 and 4-31. From the solubility expressed by eq.(1.4), the heats of solution ($\Delta \overline{H}^o$) and the constant σ_o were deduced from the statistical slopes and intercepts of these plots and are presented in Table 4-28.

TABLE 4-28

Heats of solution $\Delta \overline{H}^o$ and σ_o in unplasticised polymer J3 (26° to 66°C) and plasticised polymer F2 (10° to 40°C)

Sheet	J3		F2	
Gas	H_2	Ne	H_2	Ne
$\Delta \overline{H}^o$ (cal.mole^{-1})	-1170	-1080	1370	2770
$\sigma_o \times 10^4$	0.65	0.36	32	166

Below the glass transition T_1 (previously recorded as 70°C for unplasticised polymer in section 4.2.4) both hydrogen and neon exhibit negative values of $\Delta \overline{H}^o$ (heat

evolved) in the unplasticised polymer J3 corresponding with solubility coefficients σ_s of these gases which decrease with increasing temperature. Similar behaviour has been reported for hydrogen and neon in polyvinyl acetate[7,9] and for hydrogen in polyethylene terephthalate[65] below their glass transition temperatures. The negative heats support the suggestion that a polymer below this transition temperature contains more than the equilibrium number of 'holes' for a liquid of similar cohesive density at the same temperature.[7] The heat of solution is the sum of the work required (endothermic contribution) to create a hole to accommodate the solute particle and the interaction energy (exothermic contribution) between this particle and the surrounding polymer.[7,59] If dissolved gas molecules are accommodated in holes already present in the bulk polymer structure, then the gas molecule in a hole is in a potential minimum of depth determined by the dispersion interaction between it and the surrounding polymer.[7,18,59]

For the plasticised sample F2 hydrogen and neon both show positive heats of solution $\Delta \bar{H}^{o}$ (heat absorbed) so that σ_s increases with increasing temperature (see Figs.4-29 and 4-31). The transition temperature T_1

(deduced from the temperature dependence of $\bar{P}$, D_L and σ_D of F1 as being about 28°C) is no longer apparent in the plots of log σ_s vs. $\frac{1}{T}$. Plots of log σ_s vs. $\frac{1}{T}$ for hydrogen, neon and helium in polyvinyl acetate[9] and hydrogen in polyethylene terephthalate[65] showed, however, a discontinuity at or near the glass transition temperature. Kumins and Roteman[54] found that log D vs. $\frac{1}{T}$ plots, for H_2, He and Ne in polyvinyl chloride-polyvinyl acetate copolymer, did not show any discontinuities at the temperatures where dilatometric studies indicated second order transitions. Unfortunately solubility coefficients were not recorded there.[54] The plasticised polymer probably consists of a liquid-like distribution of holes and matter perhaps with some rotational freedom of the polymer segments, especially above the glass transition temperature. From the previous discussion, the positive $\Delta\bar{H}^o$ values indicate that the gas molecules dissolving now have to create their own space by separation of the segments of surrounding polymer chains.

(b) Free energy and entropy of solution

For a gas dissolving to give a solution obeying Henry's law, the standard partial molar free energy ($\Delta\bar{G}^o$), heat ($\Delta\bar{H}^o$) and entropy ($\Delta\bar{S}^o$) of solution may

be expressed as:

$$\Delta \overline{G}^{o} = -RT \ln \sigma_s^{\ast} \qquad (4.4)$$

$$\Delta \overline{H}^{o} = RT^2 \frac{\partial \ln \sigma_s^{\ast}}{\partial T} \qquad (4.5)$$

and

$$\Delta \overline{S}^{o} = R \ln \sigma_s^{\ast} + RT \frac{\partial \ln \sigma_s^{\ast}}{\partial T} \qquad (4.6)$$

Eqs.(4.4), (4.5) and (4.6) are of course related by:

$$\Delta \overline{G}^{o} = \Delta \overline{H}^{o} - T\Delta \overline{S}^{o} \qquad (4.7)$$

The Bunsen solubility coefficient $\sigma_s^{\ast}$ is obtained from the present data by multiplying σ_s by 76. The chosen standard states were, for the gas phase, a pressure of 76 cm and the experimental temperature and for the solution phase, a sorbed gas concentration of 1 cm^3 at NTP per cm^3 of the plasticised or unplasticised polymer. Values of $\Delta \overline{G}^{o}$ and $\Delta \overline{S}^{o}$ so calculated at $T = 303.16^{o}K$ are tabulated in Table 4-29. Corresponding data for $\Delta \overline{H}^{o}$ have previously been recorded in Table 4-28.

TABLE 4-29

Free energy $\Delta\bar{G}^{o}$ and entropy $\Delta\bar{S}^{o}$ of solution at 303.16°K

	J3		F2	
Gas	$\Delta\bar{G}^{o}$	$\Delta\bar{S}^{o}$	$\Delta\bar{G}^{o}$	$\Delta\bar{S}^{o}$
H_2	2030	-10.6	2220	**-2.79**
Ne	2470	-11.7	2620	0.50

The observed values of $\Delta\bar{G}^{o}$, $\Delta\bar{H}^{o}$ and $\Delta\bar{S}^{o}$ in J3 and F2 and those in normal hydrocarbons are shown in Tables 4-28 to 4-30 for comparison.

TABLE 4-30

Bunsen solubility coefficients, free energies and entropies of solution at 25°C of gases in hydrocarbons

Gas	Solvent	$\sigma^{x}x10^{2}(25^{o})$	$\Delta\bar{G}^{o}$	$\Delta\bar{H}^{o}$	$\Delta\bar{S}^{o}$
H_2	Nonane	$^{x}8.64$	1450	580	-2.92
Ne	Heptane	$^{+}5.29$	1740	1220	-1.76
Ne	Octane	$^{+}4.91$	1790	1530	-0.88

^{x} Data of Thomsen et al.[147]

$^{+}$ Data of Clever et al.[146]

The collected data in Table 4-30 were calculated from papers by Clever et al.[146] and Thomsen et al.[147] Values of $\Delta \overline{H}^{o}$ are observed to be distinctly positive for F2 and the hydrocarbons, and the values of $\Delta \overline{S}^{o}$ are of the same order of magnitude in both cases.

The interstitial mechanism of solution in J3 (also discussed in sections 4.3.3(a) and 4.3.4) corresponds more closely with Langmuir's isotherm, where localised sorption occurs in intra-polymer pre-existing 'holes', than with the usual polymer-penetrant formula for entropy of dilution given in eq.(2.59).

The process of solution of a gas may be considered as made up of the condensation of the gas followed by some form of mixing of the condensed gas with the polymer.[5,43,44] The entropy of dilution of the liquefied gas is given by:

$$\Delta \overline{S}_1 = \overline{S}_s - \widetilde{S}_L \qquad (4.8)$$

where $\overline{S}_s$ and $\widetilde{S}_L$ denote, respectively, the partial molar and molar entropies of the liquid in the polymer and as pure liquid. With a similar form for $\widetilde{S}_L$, the entropy $\overline{S}_s$ may be written as:

$$\overline{S}_s = \overline{S}_c + \overline{S}_{th} \qquad (4.9)$$

where subscripts 'c' and 'th' denote, respectively,

'configurational' and 'thermal'. If molecules of penetrant are placed only in pre-existing 'holes', one penetrant molecule per hole, then the configurational entropy is given by

$$\overline{S}_c = R \ln \left(\frac{1 - \theta}{\theta}\right) \qquad (4.10)$$

where θ denotes the fraction of sites filled. $\overline{S}_c$ is positive for $0 < \theta < 0.5$ and negative for $0.5 < \theta < 1.0$. Large negative values of $\Delta \overline{S}^o$ are found for J3 (see Table 4.29) and some form of 'hole filling' would appear to make an important contribution in the solution process. In addition to the dominant process of filling 'holes', there must also be the alternative process of sorption by mixing of penetrant with polymer by a substitutional mechanism, as embodied in the lattice treatment.[18] The lattice theory requires positive values of $\Delta \overline{S}_1$, and corresponds more closely to the behaviour of penetrant molecules in F2 rather than in J3.

4.3.4 Comparison between the theoretical and observed heats of dilution

As already noted the process of solution of gas in a polymer may be considered as made up of condensation followed by some process of mixing of the condensed gas

with polymer. Therefore the standard heat $\Delta \bar{H}^{o}$ may be expressed as:

$$\Delta \bar{H}^{o} = \Delta \bar{H}_1 - \lambda_1 \qquad (4.11)$$

where λ_1 is the molar heat of vaporisation and $\Delta \bar{H}_1$ is the partial molar heat of mixing of the liquefied penetrant with an infinite volume of polymer-penetrant mixture, in which the liquid and mixture are in their standard states. This value of ΔH_1 evaluated from the observed value of $\Delta \bar{H}^{o}$, can be compared with the theoretical $\Delta \bar{H}_1$ given by Hildebrand's equation (eq.2.74). Assuming $v_2 = 1$, the solubility parameter δ_2 of pure polyvinyl chloride is given by Small[150] as $\delta_2 = (\frac{E_2}{V_2})^{\frac{1}{2}} = 9.6$.

The results are tabulated in Table 4-31. A wide deviation is particularly noticed for J3, but the agreement for the F2/H_2 system appears to be reasonable. According to the proposed solution mechanism for J3, $\Delta \bar{H}_1$ will not be given by Hildebrand's equation (eq.2.74) which is for a substitutional not an interstitial type of mixing. Since in the latter case the interstices are pre-existing 'holes' no work need be expended in making them. The solute molecules in the 'holes' react exothermally with their surroundings and, since the latent heat of condensation is also exothermal, the

TABLE 4-31

Comparison between the theoretical and observed heats of dilution

Gas	E_1 or λ_1 ($cal.mole^{-1}$)	V_1 (cm^3)	$(\frac{E_1}{V_1})^{\frac{1}{2}} = \delta_1$	$\Delta\bar{H}^o$ ($cal.mole^{-1}$)		$\Delta\bar{H}_1$ ($cal.mole^{-1}$)		
				J3	F2	$(\delta_1-\delta_2)^2 V_1 v_2^2$ eq.(2.74)	$\Delta\bar{H}^o+\lambda_1$ eq.(4.10) J3	$\Delta\bar{H}^o+\lambda_1$ eq.(4.10) F2
H_2	217.7	28.8	2.75(2.5*)	-1170	1370	1470	-950	1590
Ne	414	16.72	4.976	-1080	2770	360	-670	3180

NOTE:

E_1 or λ_1 is the latent heat of vaporisation of liq.gas at n.b.p. Neon data from Cook[148] and hydrogen data from ref.149.

V_1 is the molar volume of liq.gas calculated from V_1 = atomic (or molecular weight)/ density of liq.gas at n.b.p.

$(\frac{E_1}{V_1})^{\frac{1}{2}} = \delta_1$ is the solubility parameter of the gas: * represents data from ref.5.

$\Delta\bar{H}^o$ is the observed heat of solution.

$\Delta\bar{H}_1$ is the heat of dilution of the liquid gas with the polymer/plasticiser mixture. Theoretical data in column 7 and experimental data in cols. 8 and 9.

overall heat of solution is exothermal. In F2 on the other hand the situation is dominated by the expenditure of energy in making 'holes'. Hildebrand's substitutional mechanism is applicable; and $\Delta \bar{H}_1$ should be zero or positive corresponding to endothermal dilution.

Hydrogen and neon are at the temperature of the experiments which is far above their critical temperatures making the hypothetical condensation process physically unreal; hence, E_1 has been obtained for a much lower temperature, the n.b.p. The solubility parameters δ_1 of the gases, calculated at the n.b.p., decrease with increasing temperature owing to decreasing E_1 and increasing V_1. A lower value of E_1 would yield better agreement between the calculated and experimental $\Delta \bar{H}_1$ values for F2, for which this treatment is particularly applicable. The solubility parameter δ_2 strictly refers to the pure polymer, but it has been necessary to use it for F2 as well.

4.3.5 Statistical treatment of the solubility of gases

Barrer[151] developed the theory of solubility of gases in polymers using the statistical thermodynamics of random mixing of monomer-polymer mixtures. As already considered, the sorption process in a polymer

can be considered to occur in two steps, namely, condensation of the gas (physically unnatural process) followed by some mechanism of mixing of the hypothetical condensed gas in the polymer. In the simplest case the heat of mixing was considered to be zero. At equilibrium the tendency of the sorbed molecules to dissolve is exactly counteracted by the tendency of the molecules to evaporate. Using Miller's expression[152] for the partial molar configurational free energy of mixing, $\Delta \bar{G}_1$, Barrer[151] obtained for the sorption isotherm of a freely rotating gas in a polymer:

$$\frac{v_1}{\left[1 - (1 - \frac{1}{x})\frac{2v_2}{z}\right]^{\frac{z}{2}} n_1} = K = \left(\frac{kT}{2\pi m}\right)^{\frac{3}{2}} \cdot \frac{1}{\nu^3} \cdot \exp\left(\frac{X}{RT}\right) \qquad (4.12)$$

where v_1 and v_2 = volume fractions of the gas and polymer molecules respectively.

x = number of segments in the number average molecular weight polymer molecule.

z = co-ordination number of lattice site.

n_1 = number of molecules per cm^3.

K = solubility constant.

m = mass of the gas molecule.

ν = mean vibration frequency for the gas molecule in the polymer matrix.

χ = the least energy required to remove a mole of gas from the mixture (corresponding to the assumed lattice structure) to the gas phase.

If ΔU is defined by:

$$\frac{\partial \ln K}{\partial T} = \frac{\Delta U}{RT^2} \qquad (4.13)$$

we find by comparing eq.(4.13) with the logarithm of the r.h.s. of eq. (4.12) that:

$$X = -\Delta U + \frac{3}{2} RT \qquad (4.14)$$

From eq.(4.12) and (4.14) it follows that:

$$\frac{v_1}{[1 - (1 - \frac{1}{x})\frac{2v_2}{z}]^{\frac{z}{2}} n_1} = K = (\frac{kT}{2\pi m})^{\frac{3}{2}} \frac{1}{\nu^3} \exp(\frac{-\Delta U + \frac{3}{2} RT}{RT}) \qquad (4.15)$$

At low pressures of gas, where Henry's Law is obeyed for gas-polymer systems, the solution is usually very dilute so that $v_1 << 1$ and $v_2 \longrightarrow 1$. In the case of large x, eq.(4.15) becomes:

$$\frac{v_1}{(1 - \frac{2v_2}{z})^{\frac{z}{2}} n_1} = K = (\frac{kT}{2\pi m})^{\frac{3}{2}} \frac{1}{\nu^3} \exp(\frac{-\Delta U + \frac{3}{2} RT}{RT}) \qquad (4.16)$$

For the condition of constant pressure, substitution of $p = n_1 kT$ and $\Delta U = \Delta H + RT$ in eq.(4.16) gives:

$$\frac{v_1}{(1 - \frac{2v_2}{z})^{\frac{z}{2}} p} = K = \frac{1}{kT}(\frac{kT}{2\pi m})^{\frac{3}{2}} \cdot \frac{1}{\nu^3} \cdot \exp(\frac{-\Delta H + \frac{1}{2}RT}{RT}) \qquad (4.17)$$

Since ν is not known independently, the best test of the isotherm (eq.4.17) is to determine the value of ν for which the experimental and calculated v_1 agree. The calculated values of ν which give agreement with observed solubilities for z = 4 and z = 6 at T = 303.16°K are shown in Table 4-32.

TABLE 4-32

Test of isotherm (eq.4.17) for hydrogen and neon in polyvinyl chloride

Sheet	Gas	$v_1 \times 10^7$	ν (sec^{-1}) z = 4	ν (sec^{-1}) z = 6
J3	H_2	5.84	4.51×10^{10}	4.77×10^{10}
	Ne	1.64	2.06×10^{10}	2.18×10^{10}
F2	H_2	4.27	1.23×10^{10}	1.30×10^{10}
	Ne	1.27	0.27×10^{10}	0.28×10^{10}

TABLE 4-32 (continued)

NOTE:

ν has been calculated from eq.(4.17) where the volume fraction of the sorbate is deduced from

$$v_1 = \frac{76\ \sigma_s(^{\circ}C)\ \text{x mol.vol.}}{22{,}400}$$ (see Table 4-31 for values of mol.vol.)

$p = 76$ cm Hg; $T = 303.16^{\circ}K$; $v_2 = 1$; $k = 1.04 \times 10^{-20}$

ΔH is the heat of solution and is equivalent to $\Delta \overline{H}^{o}$ given in Table 4-28.

Eq.(4.12) is for the mechanism of solution by substitutional mixing and therefore applicable only to F2. For membrane J3 if molecules occupy only pre-existing 'holes' in the polymer, an alternative form of eq.(4.12), given by:

$$\frac{\theta}{(1-\theta)n_1} = K = \left(\frac{kT}{2\pi m}\right)^{\frac{3}{2}} \cdot \frac{1}{\nu^3} \cdot \exp\left(\frac{X}{RT}\right) \qquad (4.18)$$

should from previous results come nearer to being correct. θ is the fraction of 'holes' occupied by the penetrant molecules and is unknown here.

From the small differences between the ν values for a given system, one can see that the term $(1 - \frac{2v_2}{z})^{\frac{z}{2}}$ does not vary very greatly for values of z between 4 and 6. As already noted by other workers [43,48,151] the values of ν decrease with increase of molecular or atomic mass (from H to Ne). For elastomers[43,48,151] the mean vibration frequency is found to correspond to the infra-red region ($\sim 10^{12}$ sec^{-1}) but ν in this rigid polymer is of the order $10^9 - 10^{10}$ sec^{-1} for both F2 and J3. As gas is probably sorbed by the plasticiser in F2 as well as by the polymer, the assumption that x is large is probably not applicable to this composition.

REFERENCES

1. Barrer, R.M., Trans.Faraday Soc., 1939, 35, 628.
2. Barrer, R.M., J.Phys.Chem., 1957, 61, 178 and references cited.
3. Van Amerongen, G.J., J.Appl.Phys., 1946 17, 972.
4. Van Amerongen, G.J., Rubber Chem.and Technol. 1947 20, 479.
5. Van Amerongen, G.J., J.Polymer Sci. 1950 5, 307.
6. Van Amerongen, G.J., Rubber Chem.and Technol. 1964 37, 1065.
7. Meares, P., J.Amer.Chem.Soc. 1954 76, 3415.
8. Meares, P., Trans.Faraday Soc. 1957 53, 101.
9. Meares, P., Trans.Faraday Soc. 1958 54, 40.
10. Meares, P., J.Appl.Polymer Sci. 1965 9, 917.
11. Zhurkov, S.N., Ryskin G.Y., Zh.Tekh.Fiz. 1954 24, 797.
12. Ryskin, G.Y., Zh.Tekh.Fiz. 1955 25, 458.
13. Brandt, W.W., J.Polymer Sci. 1959 41, 403,415.
14. Brandt, W.W., Anyas, G.A., J.Appl.Polymer Sci. 1963 7, 1919.
15. Michaels, A.S., Parker, Jr., R.B., J.Polymer Sci. 1959 41, 53, 415.

16. Michaels, A.S., Bixler, H.J., J.Polymer Sci. 1961 50, 393.

17. Michaels, A.S., Bixler, H.J., J.Polymer Sci. 1961 50, 413.

18. Michaels, A.S., Vieth, W.R., Barrie, J.A., J.Appl. Phys. 1963 34, 1,13.

19. Barrer, R.M., Barrie, J.A., Raman, N.I., Polymer, 1962 3, 595, 605.

20. Barrer, R.M., Barrie, J.A., Rogers, M.G., J.Polymer Sci. 1963 1, 2565.

21. Graham, T., Phil.Mag. 1866 32, 401.

22. Muller, T., Kolloid Z. 1942 100, 355.

23. Brubaker, D.W., Kammermeyer K., Ind.Eng.Chem., 1952 44, 1465.

24. Brubaker, D.W., Kammermeyer, K., Ind.Eng.Chem. 1953 45, 1148.

25. Reitlinger, S.A., Rubber Chem.and Technol. 1946 19, 385.

26. Morris, V.N., Ind.Eng.Chem. 1931 23, 837.

27. Adams, R.J., Buckler, E.J., Wanless, G.G., Proc. 2nd Rubber Technol.Conf. London 1948, p.34.

28. Simril, V.L., Herschberger, A., Mod.Plastics 1950 27, (10) 97; 1950 27, (11) 95.

29. Heilman, W., Tammela, V., Meyer, J.A., Stannett, V., Szwarc, M., Ind.Eng.Chem. 1956 48, 821.

30. Myers, A.W., Tammela, V., Stannett, V., Szwarc, M., Mod.Plastics 1960 37, (6) 139.

31. Meyers, A.W., Meyer, J.A., Rogers, C.E., Stannett, V., Szwarc,M., Tappi 1961 44, 58.

32. Major, C.J., Kammermeyer, K., Mod.Plastics, 1962 39, (11) 135.

33. Kumins, C.A., Rolle, C.J., Roteman, J., J.Phys.Chem. 1957, 61, 1290.

34. Long, F.A., Thompson, L.J., J.Polymer Sci. 1954 14, 321.

35. Doty, P.M., Aiken, W.H., Mark, H., Ind.Eng.Chem. 1946, 38, 788.

36. Doty, P.M., J.Chem.Phys. 1946, 14, 244.

37. Thomas, A.M., J.Appl.Chem. 1951, 1, 141.

38. Morgan, P.W., Ind.Eng.Chem. 1953, 45, 2296.

39. Lasoski, S.W., J.Appl.Polymer Sci. 1960, 4, 118.

40. Kanamaru, K., Sigiura, M., Kolloid Z. 1964, 194, 110.

41. Kanamaru, K., Sigiura, M., Kolloid Z. 1961, 178, 1.

42. Barrer, R.M., 'Diffusion in and through solids,' Cambridge, 1951.

43. Barrer, R.M., Skirrow, G., J.Polymer Sci. 1948 3, 549, 564.

44. Aitken, A., Barrer, R.M., Trans.Faraday Soc. 1955 51, 116.

45. Barrer, R.M., Trans.Faraday Soc. 1942, 38, 322.

46. Eyring, H., J.Chem.Phys. 1935, 3, 107.

47. Prager, S., Long, F.A., J.Amer.Chem.Soc. 1951, 73, 4072.

48. Chio, H.T., London University Thesis, 1964.

49. Barrer, R.M., Trans.Faraday Soc. 1940, 36, 645.

50. Barrer, R.M., Trans.Faraday Soc. 1939, 35, 644.

51. Carpenter, A.S., Twiss, D.F., Ind.Eng.Chem.(Anal.Ed.) 1940, 12, 99.

52. Van Amerongen, G.J., Rubber Chem.and Technol. 1955, 28, 821.

53. Melikhova, N.A., Reitlinger, S.A., Kuzina, N., Sov.Rubber Technol. 1959, 18, 344 (Eng.Trans.).

54. Kumins, C.A., Roteman, J., J.Polymer Sci., 1961, 55, 683, 699.

55. Long, F.A., Thompson, L.J., J.Polymer Sci. 1955, 15, 413.

56. Barrer, R.M., Trans.Faraday Soc., 1943, 39, 48, 59.

57. Barrer, R.M., Trans.Faraday Soc., 1943, 39, 237.

58. Brandt, W.W., J.Phys.Chem., 1959, 63, 1080.

59. Meares, P., Polymers, Structure and Bulk Properties, 1965.

60. Schulz, G.V., Gerrens, H.Z., Z.Phys.Chem. 1956, 7, 182.

61. Frisch, H.L., J.Phys.Chem., 1956, 60, 1177.

62. Lasoski, S.W., Cobbs, W.H., J.Polymer Sci., 1959, 36, 21.

63. Klute, C.H., J.Appl.Polymer Sci., 1959, 1, 340.

64. Jeschke, D., Stuart, H.A., Z.Naturforsch, 1961, 16a, 37.

65. Draisbach, H., Jeschke, D., Stuart, H.A., Z.Naturforsch., 1962, 17a, 447.

66. Barrie, J.A., Platt, B., J.Polymer Sci. 1961, 49, 479; 54, 261.

67. Landrock, A.H., Procter, B.E., Tappi, 1952, 35, 241.

68. Brown, W.E., Sauber, W.J., Mod.Plastics, 1959, 36, 107.

69. Stern, S.A., Garies, P.J., Sinclair, T.F., Mohr, P.H., J.Appl.Polymer Sci., 1963, 7, 2035.

70. Burk, R.E., Grummit, O. (eds.), 'The Chemistry of Large Molecules', 1943, Ch.7.

71. Natta, G., 'Advances in Catalysis', 1959, 11, 1.

72. Hodgkins, J.E., J.Org.Chem., 1958, 23, 1369.

73. Mellan, I., 'Industrial Plasticisers', 1963.

74. Mellan, I., 'The Behaviour of Plasticisers', 1961.

75. Schildknecht, C.E., 'Polymer Processes', 1956.

76. Gilbert, J.B., Kipling, J.J., McEnaney, B., Sherwood, J.N., Polymer, 1962, 3, 1.

77. Fuller, C.S., Chem.Rev., 1940, 26, 143.

78. Natta, G., Corradini, P., J.Polymer Sci., 1956, 20, 251.

79. Mammi, M., Nardi, V., Nature, 1963, 199, 247.

80. Krimm, S., Adv.in Polymer Sci., 1960 2, 51 and references cited.

81. Krimm, S., Enomoto, S., J.Polymer Sci., 1964, A2, 669.

82. Enomoto, S., Koguro, M., Ahasina, M., J.Polymer Sci. 1964, A2, 5355.

83. Krimm, S., Folt, V.L., Shipman, J.J., Berens, A.R., J.Polymer Sci. 1964, B2, 1009.

84. Germar, H., Hellwege, K.H., Johnsen, U., Makromol. Chem., 1963, 60, 106.

85. Germar, H., Kolloid Z., 1963, 193, 25.

86. Johnsen, U., J.Polymer Sci., 1961, 54, 56.

87. Tincher, W.C., J. Polymer Sci., 1962, 62, 5148.

88. Satoh, S., J.Polymer Sci., 1964, A2, 5221.

89. Bovey, F.A., Anderson, E.W., Douglass, D.C., Manson, J.A., J.Chem.Phys., 1963, 39, 1199.

90. Hellwege, K.H., Johnsen, U., Kockott, D., Kolloid Z., 1964, 194, 5.

91. Flory, P.J., Trans.Faraday Soc., 1955, 51, 848.

92. Cotman, J.D., Ann.N.Y.Acad.Sci., 1953, 57, 417.

93. George, M.H., Grisenthwaite, R.J., Hunter, R.F., Chem.and Ind., 1958, 1114.

94. Taylor, R.B., Tobolsky, A.V., J.Appl.Polymer Sci., 1964, 8, 1563.

95. Kovacs, A., Comptes rendus, 1956, 243, 50.

96. Martin, H., Muller, F.H., Kolloid Z., 1963, 191, 1.

97. Kockott, D., Kolloid Z., 1964, 198, 17.

98. Heydemann, P., Guicking, H.D., Kolloid Z., 1963, 193, 1,6.

99. Tobolsky, A.V., 'Properties and Structures of Polymers', 1960.

100. Woodward, A.E., Sauer, J.A., Adv.in Polymer Sci., 1958, 1, 114.

101. Nielsen, L.E., 'Mechanical Properties of High Polymers', 1962.

102. Slichter, W.P., Adv.in Polymer Sci., 1958, 1, 35 and references cited.

103. Liebhafsky, H.A., Marshall, A.L., Verhoek, F.H., Ind.Eng.Chem., 1942, 34, 704.

104. Small, P.A., J.Soc.Chem.Ind., 1947, 66, 17.

105. Knappe, W., Z.angew.Physik, 1954, 6, 97.

106. Heine, K., Hellwege, K.H., Knappe, W., Z.angew Physik, 1958, 10, 162.

107. Hellwege, K.H., Knappe, W., Lohe, P., Kolloid Z., 1961, 179, 40.

108. Luther, H., Meyer, H., Z.Elektrochem., 1960, 64, 681.

109. Daynes, H.A., Proc.Roy.Soc.(London), 1920, A97, 286.

110. Rogers, W.A., Buritz, R.S., Alpert, D., J.Appl.Phys., 1954, 25, 868.

111. Leiby, C.C., Chen, C.L., J.Appl.Phys., 1960, 31, 268.

112. Altemose, V.O., J.Appl.Phys., 1961, 32, 1309.

113. Hartley, G.S., Crank, J., Trans.Faraday Soc., 1949, 45, 801.

114. Carman, P.C., Stein, L.H., Trans.Faraday Soc., 1956, 52, 619.

115. Crank, J., 'The Mathematics of Diffusion', 1956.

116. Fujita, H., Advances in Polymer Sci., 1961, 3, 1 and references cited.

117. Barrie, J.A., Levine, J.D., Michaels, A.S., Wong, P., Trans.Faraday Soc., 1963, 59, 869.

118. Frisch, H.L., J.Phys.Chem., 1957, 61, 93.

119. Ash, R., Barrer, R.M., Palmer, D.G., Brit.J.Appl. Phys., 1965, 16, 873.

120. Denbigh, K., Raumann, G., Proc.Roy.Soc.(London), 1951, A210, 377, 518.

121. Glasstone, S., Laidler, K.J., Eyring, H., 'The Theory of Rate Processes', 1941.

122. Park, G.S., Trans.Faraday Soc., 1950, 46, 684.

123. Flory, P.J., J.Chem.Phys., 1942, 10, 51.

124. Flory, P.J., 'Principles of Polymer Chemistry', Cornell University Press, 1953.

125. Meyer, K.H., Z.physik.Chem., 1939, B.44, 383.

126. Huggins, M.L., J.Chem.Phys., 1942, 46, 151.

127. Huggins, M.L., J.Am.Chem.Soc., 1942, 64, 1712.

128. Huggins, M.L., Ann.N.Y.Acad.Sci., 1942, 41, 1.

129. Miller, A.R., Proc.Cambridge Phil.Soc., 1943, 39, 54, 131.

130. Guggenheim, E.A., Trans.Faraday Soc., 1948, 44, 1007.

131. Hildebrand, J.H., Scott, R.L., 'Solubility of Non-electrolytes', 1950.

132. Gee, G., I.R.I.Trans., 1943, 18, 266.

133. Flory, P.J., Rehner, J., J.Chem.Phys., 1943, 11, 521.

134. Flory, P.J., J.Chem.Phys., 1950, 18, 108.

135. Doty, P., Zable, H.S., J.Polymer Sci., 1946,1, 90.

136. Boyer, R.F., Spencer, R.S., J.Polymer Sci., 1948, 3, 97.

137. Dole, M., Kolloid Z., 1959, 165, 40.

138. Bearman, R.J., J.Phys.Chem., 1957, 61, 708.

139. Kelley, F.N., Bueche, F., J.Polymer Sci., 1961, 50, 549.

140. Jenckel, E., Heusch, R., Kolloid Z., 1953, 130, 89.

141. Williams, M.L., Landel, R.F., Ferry, J.D., J.Amer. Chem.Soc., 1955, 77, 3701.

142. Boyer, R.F., Spencer, R.S., J.Polymer Sci., 1947, 2, 157.

143. DiBenedetto, A.T., J.Polymer Sci., 1963, A1, 3459, 3477.

144. Jost 'Diffusion in solids, liquids and gases', 1952, Chap.1.

145. Barrer, R.M., Proc.Phys.Soc., 1946, 58, 321.

146. Clever, H.L., Battino, R., Saylor, J.H., Gross, P.M., J.Phys.Chem., 1957, 61, 1078.

147. Thomsen, E.S., Gjaldback, J.Chr., Acta Chem.Scand., 1963, 17, 127.

148. Cook, G.A., (Ed.) 'Argon, Helium and Rare Gases', Vol.I., Inter.Sci.Publ., 1961.

149. 'Handbook of Chemistry and Physics', 38th Ed., 1956-1957.

150. Small, P.A., J.Appl.Chem., 1953, 3, 71.

151. Barrer, R.M., Trans.Faraday Soc., 1947, 43, 3.

152. Miller, A.R., Proc.Camb.Phil.Soc., 1942, 38, 109.

153. Frisch, H.L., J.Phys.Chem., 1957, 61, 93.

154. Ash, R., Barrer, R.M., Palmer, D.G., in preparation.